AN ABSTRACT OF THE DISSERTATION OF

Xia Zeng for the degree of Doctor of Philosophy in Chemistry presented on July 12, 2007.
Title: Development, Validation and the Application of A Congener Specific Photodegradation Model for PBDEs

Abstract approved:

Staci L. Simonich Douglas F. Barofsky

The thermodynamic properties of 39 PBDEs have been calculated using Gaussian 03 on the B3LYP/6-31G(d)//B3LYP/6-31G(d) level. The PBDE congeners' enthalpies of formation increase with increasing number of bromines and show a strong dependence on the bromine substitution pattern. The effects of bromine substitution pattern have been quantitatively studied by GAM model based on the output of the theoretical calculations. Based on the GAM model, the enthalpies of formation of the 209 PBDE congeners were calculated. A photodegradation model was developed and validated to predict the products, and their relative concentrations, from the photodegradation of PBDEs. Photodegradation experiments were conducted for octa-BDE technical mixture and its individual components together with BDE-209, 184, 100, 99 and 47. Based on the results of the photodegradation experiments, as well as the model predictions, the photodegradation of PBDEs is a first order reaction and, further, the rate determining step is the stepwise loss of bromine. The predicted reaction time profiles of the photodegradation products correlate well with the experimental results. In addition, the

photodegradation results were compared with anaerobic biodegradation. The PBDE products measured in the anaerobic biodegradation were found to be the major products in the photodegradation experiments. The photodegradation experiments and the model predictions were also compared with zero-valent iron reduction of BDE-209, 100 and 47 from a previous study and the same products were found in both photo and Fe^0 degradation. Good correlation between 15 previously reported photodegradation rate constants of PBDE congeners and their calculated LUMO energies was found. This indicates that, similar to the Fe^0 reduction, debromination by UV light is caused by electron transfer. Furthermore, the rate constants for the three different degradation processes are controlled by C-Br bond dissociation energy. The model was proved to be predictive for the photodegradation of PBDEs and it should be predictive for anaerobic biodegradation and Fe^0 reduction of PBDEs.

© Copyright by Xia Zeng
July 12, 2007
All Rights Reserved

DEVELOPMENT, VALIDATION AND THE APPLICATION OF A CONGENER SPECIFIC PHOTODEGRADATION MODEL FOR PBDES

by
Xia Zeng

A DISSERTATION

submitted to

Oregon State University

in partial fulfillment of
the requirements for the
degree of

Doctor of Philosophy

Presented July 12, 2007
Commencement June 2008

Doctor of Philosophy dissertation of Xia Zeng presented on July 12, 2007.

APPROVED :

Co-Major Professor, representing Chemistry

Co-Major Professor, representing Chemistry

Chair of the Department of Chemistry

Dean of the Graduate School

I understand that my dissertation will become part of the permanent collection of Oregon State University libraries. My signature below authorizes release of my dissertation to any reader upon request.

Xia Zeng, Author

ACKNOWLEDGEMENTS

The author expresses heartfelt appreciation to Chun Li for her love and support. The author is very appreciative for his major professor, Dr. Staci L. Simonich and Dr. Douglas F. Barofsky for providing guidance, support, encouragement, and trust. In addition, the author is grateful to members in Dr. Simonich's group for support and encouragement. The author is also very thankful for support from his committee members as well as Dr. Max Deinzer, Kristin R. Robrock, Dr. Lisa Alvarez-Cohen and Dr. Peter Korytár. Finally, the author would like to thank the National Institute of Environmental Health Sciences for funding and Harris Fellowship for summer support.

CONTRIBUTION OF AUTHORS

Dr. Staci L. Simonich and Dr. Douglas F. Barofsky provided leadership in all aspects of this dissertation. Dr. Peter K. Freeman, Dr. Yury V. Vasil'ev, Dr. Valery G. Voinov provided suggestions in interpreting results, and edited chapter 2. Dr. Peter Korytár provided additional PBDE standards in helping identify products in chapter 3. Kristin R. Robrock and Dr. Lisa Alvarez-Cohen provided suggestion in interpreting results, and edited chapter 3. Kristin R. Robrock also identified some of the PBDE photodegradation products.

TABLE OF CONTENTS

TABLE OF CONTENTS (Continued)

LIST OF FIGURES

LIST OF FIGURES (Continued)

LIST OF FIGURES (Continued)

LIST OF TABLES

DEVELOPMENT, VALIDATION AND THE APPLICATION OF A CONGENER SPECIFIC PHOTODEGRADATION MODEL FOR PBDES

CHAPTER 1. INTRODUCTION

Goal

The goal of this doctoral research and thesis has been to study the photodegradation of polybrominated diphenyl ethers (PBDEs) and to build a model to explain and predict the PBDE degradation products and their relative abundance.

Structures and Uses of PBDEs

PBDEs are a flame retardant sub-family of the brominated flame-retardant group. The family of PBDEs consists of 209 different structures, which are called congeners. A PBDE congener consists of two phenyl rings connected by an ether bond with the hydrogens on the phenyl ring substituted by various numbers of bromines (Figure 1.1). The chemical formula of a PBDE can be written as $C_{12}H_{10-a}Br_aO$ (a = 1-10 = x + y) (x and y are number of bromines on the phenyl rings as shown in Figure 1.1).

PBDE congeners are numbered from 1 to 209 (Appendix A) using the same IUPAC scheme used for polychlorinated biphenyls (PCBs), where the 2-monoBDE is named BDE-1 and the fully brominated PBDE congener is named BDE-209 (*1*). The 209 PBDE congeners are cataloged into ten homologous groups based on their degree of bromination, namely, mono, di, tri, tetra, penta, hexa, hepta, octa, nona, and deca-BDEs.

PBDE flame retardants are widely used as additives to reduce the risk of fire, particularly in items that are susceptible to igniting in fire situations, such as furniture and textiles, or in which fires may start, like electrical devices. In the event of a fire involving

these products, PBDEs slow the ignition and the rate of fire growth, allowing more time for people to extinguish or escape the fire. The use of brominated flame retardants in household materials saved thousands of lives and resulted in a 20% reduction in fire deaths between 1990 and 2000. (*2*)

There are three commercially available technical PBDE products: penta, octa, and deca-BDEs. Penta and octa-BDEs are mixtures of several congeners (*3*) and the compositions of these two commercial products vary with manufacturer and with the year in which they were produced (See Table 1.1 for an example) (*6*). The penta-BDE products are primarily comprised of tetra-BDEs (especially BDE-47) and penta-BDEs (especially BDE-99 and BDE-100), along with smaller quantities of hexa-BDEs (BDE-153 and BDE-154). The commercial octa-BDE mixture is primarily comprised of hepta-BDEs (mainly BDE-183) and octa-BDEs (BDE-197, BDE-203 and BDE-196), along with small quantities of hexa-BDEs and nona-BDEs. The commercial deca-BDE product is comprised almost entirely of BDE-209, and contains small quantities of nona-BDEs (*4*) (*5*).

The commercial penta-BDE products are mainly used in textiles and polyurethane foam in furniture, mattresses, carpet padding, and automobile seats. The commercial octa-BDE products are used in polycarbonate, thermostats and acrylonitrile-butadiene-styrene (ABS) plastic that is used in certain electric and electronic devices. Deca-BDE products are used in most types of synthetic materials such as polyester used for printed circuit boards and in certain types of flame-retardant textiles. (*4*)

The global annual production of penta, octa and deca-BDE commercial products in 1990 was estimated to be 4000, 6000 and 30 000 metric tons, respectively (*7*) The majority of the three commercial products is deca-BDE product, which constitutes 82% of the total global PBDE market (*8*). After their introduction during the 1960s, consumption of PBDEs continued to increase over the years, reaching 67,125 metric tons in 1999. In this particular year, 8,290 tons penta-BDE products were consumed in North America, about 98% of the global penta-BDE demand (*8*). In 2001, the total global demand for PBDEs was 67,000 tons, including 7,500 tons of the penta-BDE product (*9*).

PBDE in the Environment

PBDEs are important in preventing fire and saving lives. However, they are found to slowly migrate to and bioaccumulate in the environment. Although the pathways of PBDEs into the environment are not fully understood, it is widely believed that their presence in the nature world is due to leaching from a wide range of plastics, electronic equipment and textiles, industrial facilities that produce PBDEs, consumer manufacturing facilities that use PBDE in a wide range of consumer products, as well as disposal and recycling of PBDE containing products (*4*). PBDEs were first detected in the environment in 1979 (*10*) and in biota in the 1980s (*11*). Recent monitoring of PBDEs suggests that several PBDE congeners, especially BDE-47, 99 and 100, are ubiquitous in biotic and abiotic matrices including air, sewage sludge, sediment, wildlife, and human tissues (*12-16*). BDE-209 is not thought to be a likely candidate for airborne transport; the finding of BDE-209 in arctic biota, however, suggests the possibility of long-range distribution (*17*). Studies of biota in Baltic Sea, Arctic, aquatic ecosystems along northern

California, and British Columbia indicates that the PBDE concentrations increase with the tropic level (*4*) (*18*). Some data has shown that PBDE concentrations are higher in the European Arctic than in the North American Arctic (*17*,*19*). But other data suggests that people from North America are exposed to more PBDE contamination than those in Europe (*5*).

A meta-analysis of the published PBDE concentration data reported in a recent review (*5*) indicates that PBDEs have migrated in large quantities from industrial products to the environment and to people and, furthermore, that their concentrations have increased exponentially in the last 20 years. For example, in human blood, milk, and tissues, total PBDE levels have increased by a factor of ~100 during the last 30 years; this is a doubling time of ~5 years. Another astonishing fact from this review is that herring gull eggs from the Great Lakes region have PBDE concentrations as high as ~7,000 ng/g lipid and that these levels have doubled every ~3 years.

Toxicology of PBDEs

It has been established that PBDEs, which share toxicity with the structurally related PCBs, polychlorinated dibenzofurans (PCDFs), and polychlorinated dibenzo-p-dioxins (PCDDs), may negatively affect processes of hormonal regulation in living organisms; therefore they are classified as so-called environmental endocrine disruptors (EEDs). Numerous experiments in rodents have proven thyroid hormone homeostasis disruption in the serum and plasma of individuals exposed to various doses of PBDEs, such as pentaBDE technical mixture, octaBDE technical mixture, and decaBDE technical mixture (*20*) (*21*). Possible adverse effects on hormonal regulation involving sex steroid

hormones have also been examined. Among other PBDE congeners, BDE-100 (the most abundantly found PBDE congeners in the environment), BDE-75 and BDE-51 showed the strongest tendency to bind to estrogen receptors (ER) (*22*), thus competing with the natural ER ligand estradiol to produce estrogenic or anti-estrogenic effects. Embryonic exposure to BDE-47 resulted in the development of morphological, cardiac and neural deficits that impair survivorship for zebra fish larvae (*23*). Spermatogenesis disorders in male rodents were observed when exposed to BDE-99 even at very low doses (*24*). Besides the above toxic effects, neonatal exposure to some PBDE congeners impairs spontaneous behavior, learning and memory in exposed mice (*25*). Limited toxicological studies have been done and little is known about the toxicological effects of PBDE exposure.

Regulatory Status of PBDEs

Because of their potential toxicity (*26*,*27*), use of penta-BDE and octa-BDE commercial products was banned in Europe in 2004 (*28*) and voluntarily phased out in the U.S. (*29*). Penta-BDE and octa-BDE products are also officially banned in several states in the U.S., including California, Washington and Oregon (*2*) due to their toxicity and high abundance found in the environment. Currently, there is no restriction in the production of deca-BDE product in the world.

With the continued use of the deca-BDE commercial products, large quantities of PBDEs are still being released into the environment. BDE-209, the major ingredient of deca-BDE technical mixture, has been reported to photodegrade under UV and natural sunlight to give lower PBDEs, including the banned penta and octa-BDEs (*30*,*31*). This

finding has led to a need for a model to explain and predict the products of the photodegradation of PBDEs and their relative abundances.

Thermodynamic Properties of PBDEs

It is important to know the physiochemical properties of PBDEs in order to explore the mechanisms by which PBDEs transform in the environment. PBDEs are highly lipophilic and chemically stable (*32-34*). Similar to the other polyhalogenated aromatic compounds, such as polychlorinated biphenyls (PCBs), polychlorodibenzo-*p*-dioxins (PCDDs), polychlorodibenzofurans (PCDFs), and polybromodibenzo-*p*-dioxins (PBDDs), the physical, chemical, and biological properties of PBDE congeners strongly depend on the halogen substitution pattern.(*35,36*) Although extensive studies have been conducted to measure the presence of PBDEs in the environment, their vapor pressures (*37*), and their octanol-air partition coefficients (*38*), none have been conducted to measure their thermodynamic properties. Therefore, theoretical calculations are of interest for estimating the thermodynamic properties of PBDEs.

Density Functional Theory (DFT) calculations have been performed on PBDDs (*39*), PCDDs (*36*) and PCDFs (*40*). As part of this research, the thermodynamic properties of 39 PBDE congeners were calculated using DFT calculations in Gaussian 03 and a Group Additivity Method (GAM) was developed (*41*). This approach made it possible in this research to predict the stability of all 209 PBDE congeners using the GAM model and develop a photodegradation model to predict the relative abundances of their photodegradation products.

Photodegradation of PBDEs

Until recently, few published studies were available regarding the biotic and abiotic transformation of PBDEs. Photodegradation may be one of the major abiotic transformation reactions of PBDEs in the environment. Some investigations on the photodegradation of PBDEs by both artificial and natural sunlight have been reported (*30,31,42,43*). BDE-209 and 14 other PBDE congeners were shown to undergo first order photodegradation reactions and stepwise loss of bromine (*30*). Bezares-Cruz et al. studied the degradation of BDE-209 by direct solar irradiation, and proposed a reaction pathway for BDE-209 photodegradation to BDE-47 (*31*). Their results indicated that BDE-209 dissolved in organic solvent photodegrades rapidly by natural sunlight, and they predicted that the photodegradation rate in natural waters could be attenuated. Others also reported that the rates for photodegradation of PBDEs varied in different types of solutions (*44*) (*30*). Photodegradation of BDE-209 in different matrices under artificial and natural sunlight was also studied, with the reaction time profile for products in homologous groups (*42*). It was found that the patterns for the photodegradation products of BDE-209 were similar in the different matrices or under different light conditions; however, the debromination rates were strongly dependent on the matrix and the light condition (*42*). Time profiles for the photodegradation products of several tetra- to hexa-BDE congeners coated on a Solid Phase Micro Extraction (SPME) fiber and irradiated with simulated sunlight, were reported in a recent study (*43*). In these previous studies, the photochemical behaviors of PBDEs were not well understood and the identification and interpretation of products and reaction pathways were limited.

Biodegradation of PBDEs

Pervious research has shown that halogenated aromatics can be biodegraded by bacteria under aerobic conditions, involving hydroxylation and methoxylation together with aromatic ring cleavage (*45-47*). This may result in the formation of toxic halogenated aliphatic metabolites. In contrast, anaerobic biodegradation may only remove the halogen substituents, resulting in the formation of less hydrophobic compounds, and eventually, complete mineralization, (*48*). The octa-BDE technical mixture was reported to undergo stepwise debromination in *Dehalococcoides*-containing cultures and produce the more toxic congener BDE-154, BDE-99, BDE-49, and BDE-47 (*49*). BDE-209 was also reported to degrade to lower PBDEs in sewage sludge (*50,51*) and *Sulfurospirillum multivorans* culture (*49*).

A recent study reported that both photodegradation and anaerobic biodegradation of BDE-15 (4,4'-diBDE) followed the same degradation pathway and that the step-wise products were BDE-3 and diphenyl ether (*48*). Neither rearrangement of Br nor C-O and heterolytic bond cleavage were found in either reaction. This indicates that anaerobic microbial degradation and photodegradation for PBDEs may share the same reaction mechanism.

Reduction of PBDEs by Zero-valent Iron

Zero-valent iron metal (Fe^0) has been studied for remediation of polyhalogenated aromatic compounds. Kinetic data for the dehalogenation of PBDEs by Fe^0 is available and a first order reaction rate was found (*52*). A linear correlation between the rate constants for dehalogenation and the LUMO energies was reported for PBDEs (*53*) and

other halogenated compounds (*54*). A lower LUMO energy makes it easier to add an electron than to a high-lying LUMO. The heat of formation was also found to correlate well with the degradation constant (*53*). The energy gap between HOMO and LUMO was considered to be an indication of kinetic stability and was reported to correlate well with the chemical reactivity of electrophilic aromatic substitution (*55*). A small HOMO-LUMO gap indicates low stability, and thus, high reactivity of a compound.

Although the three different forms of PBDEs degradation, namely anaerobic, photodegradation, and Fe^0 reduction, have been recently studied, the mechanisms of these processes are not well understood. These previous studies reported stepwise debromination, first order reaction, and the same degradation products, indicating that there may be some connection between them. Based on the above discussion, a congener specific model was developed, validated, and applied to explain and predict these reactions.

References

(1) Ballschmiter, K.; Zell, M., Analysis of polychlorinated biphenyls (PCB) by glass capillary gas chromatography. Composition of technical Aroclor- and Clophen-PCB mixtures. *Fresenius' Zeitschrift fuer Analytische Chemie* **1980**, *302*, 20-31.

(2) Gouin, T.; Bocking, S.; Mackay, D., Policy by analogy: precautionary principle, science and polybrominated diphenyl ethers. *Int. J. Global Environmental Issues* **2005**, *5*, 54-67.

(3) Alaee, M.; Arias, P.; Sjodin, A.; Bergman, A., An overview of commercially used brominated flame retardants, their applications, their use patterns in different countries/regions and possible modes of release. *Environ Int* **2003**, *29*, 683-689

(4) de Wit, C. A., An overview of brominated flame retardants in the environment. *Chemosphere* **2002**, *46*, 583-624.

(5) Hites, R. A., Polybrominated Diphenyl Ethers in the Environment and in People: A Meta-Analysis of Concentrations. *Environ Sci Technol* **2004**, *38*, 945-956.

(6) La, A. G. M. J.; Hale, R. C.; Harvey, E., Detailed polybrominated diphenyl ether (PBDE) congener composition of the widely used penta-, octa-, and deca-PBDE technical flame-retardant mixtures. *Environ Sci Technol* **2006**, *40*, 6247-6254.

(7) Arias, P., Brominated diphenyloxides as flame retardants: bromine based chemicals. *Consultant Report to the OECD, Paris* **1992**.

(8) Hale, R. C.; La Guardia, M. J.; Harvey, E. P.; Gaylor, M. O.; Mainor, T. M.; Duff, W. H., Flame retardants: Persistent pollutants in land-applied sludges. *Nature (London, United Kingdom)* **2001**, *412*, 140-141.

(9) Bromine Science and environmental Forum. Total Market Demand 2003. available at www.bsef.com.

(10) Alaee, M.; Wenning, R. J., The significance of brominated flame retardants in the environment: current understanding, issues and challenges. *Chemosphere* **2002**, *46*, 579-582.

(11) Jansson, B.; Asplund, L.; Olsson, M., Brominated flame retardants - ubiquitous environmental pollutants? *Chemosphere* **1987**, *16*, 2343-2349.

(12) Dodder, N. G.; Strandberg, B.; Hites, R. A., Concentrations and Spatial Variations of Polybrominated Diphenyl Ethers and Several Organochlorine Compounds in Fishes from the Northeastern United States. *Environ Sci Technol* **2002**, *36*, 146-151.

(13) Strandberg, B.; Dodder, N. G.; Basu, I.; Hites, R. A., Concentrations and Spatial Variations of Polybrominated Diphenyl Ethers and Other Organohalogen Compounds in Great Lakes Air. *Environmental Science and Technology* **2001**, *35*, 1078-1083.

(14) Darnerud, P. O.; Eriksen, G. S.; Johannesson, T.; Larsen, P. B.; Viluksela, M., Polybrominated diphenyl ethers: Occurrence, dietary exposure, and toxicology. *Environmental Health Perspectives Supplements* **2001**, *109*, 49-68.

(15) Rahman, F.; Langford, K. H.; Scrimshaw, M. D.; Lester, J. N., Polybrominated diphenyl ether (PBDE) flame retardants. *Science of the Total Environment* **2001**, *275*, 1-17.

(16) Palm, A.; Cousins, I. T.; Mackay, D.; Tysklind, M.; Metcalfe, C.; Alaee, M., Assessing the environmental fate of chemicals of emerging concern: a case study of the polybrominated diphenyl ethers. *Environmental Pollution (Oxford, United Kingdom)* **2002**, *117*, 195-213.

(17) Ikonomou, M. G.; Rayne, S.; Addison, R. F., Exponential increases of the brominated flame retardants, polybrominated diphenyl ethers, in the Canadian Arctic from 1981 to 2000. *Environ Sci Technol* **2002**, *36*, 1886-1892.

(18) Ikonomou, M. G.; Fischer, M.; He, T.; Addison, R. F.; Smith, T., Congener patterns, spatial and temporal trends of polybrominated diphenyl ethers in biota samples from the Canadian west coast and the Northwest Territories. *Organohalogen Compounds* **2000**, *47*, 77-80.

(19) van Bavel, B.; Dam, M.; Tysklind, M.; Lindstroem, G., Levels of polybrominated diphenyl ethers in marine mammals. *Organohalogen Compounds* **2001**, *52*, 99-103.

(20) Zhou, T.; Ross, D. G.; DeVito, M. J.; Crofton, K. M., Effects of short-term in vivo exposure to polybrominated diphenyl ethers on thyroid hormones and hepatic enzyme activities in weanling rats. *Toxicol Sci* **2001**, *61*, 76-82.

(21) Zhou, T.; Taylor, M. M.; DeVito, M. J.; Crofton, K. M., Developmental exposure to brominated diphenyl ethers results in thyroid hormone disruption. *Toxicol Sci* **2002**, *66*, 105-116.

(22) Meerts, I. A.; Letcher, R. J.; Hoving, S.; Marsh, G.; Bergman, A.; Lemmen, J. G.; van der Burg, B.; Brouwer, A., In vitro estrogenicity of polybrominated diphenyl ethers, hydroxylated PDBEs, and polybrominated bisphenol A compounds. *Environ Health Perspect* **2001**, *109*, 399-407.

(23) Lema, S. C.; Schultz, I. R.; Scholz, N. L.; Incardona, J. P.; Swanson, P., Neural defects and cardiac arrhythmia in fish larvae following embryonic exposure to 2,2',4,4'-tetrabromodiphenyl ether (PBDE 47). *Aquat Toxicol* **2007**, *82*, 296-307.

(24) Kuriyama, S. N.; Talsness, C. E.; Grote, K.; Chahoud, I., Developmental exposure to low dose PBDE 99: effects on male fertility and neurobehavior in rat offspring. *Environ Health Perspect* **2005**, *113*, 149-154.

(25) Viberg, H.; Fredriksson, A.; Eriksson, P., Neonatal exposure to polybrominated diphenyl ether (PBDE 153) disrupts spontaneous behaviour, impairs learning and memory, and decreases hippocampal cholinergic receptors in adult mice. *Toxicol Appl Pharmacol* **2003**, *192*, 95-106.

(26) Madia, F.; Giordano, G.; Fattori, V.; Vitalone, A.; Branchi, I.; Capone, F.; Costa, L. G., Differential in vitro neurotoxicity of the flame retardant PBDE-99 and of the PCB Aroclor 1254 in human astrocytoma cells. *Toxicol Lett* **2004**, *154*, 11-21.

(27) Muirhead, E. K.; Skillman, A. D.; Hook, S. E.; Schultz, I. R., Oral exposure of PBDE-47 in fish: toxicokinetics and reproductive effects in Japanese Medaka (Oryzias latipes) and fathead minnows (Pimephales promelas). *Environ Sci Technol* **2006**, *40*, 523-528.

(28) Føreid, S.; Knudsen, L.; Gabrielsen, G.; Barrett, R.; Polder, A.; Lie, E.; Skåre, J., Temporal trends of pollution patterns (chlorinated hydrocarbons and brominated flame retardants) in eggs of seabirds from Northern Norway. *Organohalogen Compounds* **2006**, *68* 1462-1465.

(29) Hale, R. C.; Alaee, M.; Manchester-Neesvig, J. B.; Stapleton, H. M.; Ikonomou, M. G., Polybrominated diphenyl ether flame retardants in the North American environment. *Environ Int* **2003**, *29*, 771-779.

(30) Eriksson, J.; Green, N.; Marsh, G.; Bergman, A., Photochemical Decomposition of 15 Polybrominated Diphenyl Ether Congeners in Methanol/Water. *Environ Sci Technol* **2004**, *38*, 3119-3125.

(31) Bezares-Cruz, J.; Jafvert, C. T.; Hua, I., Solar photodecomposition of decabromodiphenyl ether: products and quantum yield. *Environ Sci Technol* **2004**, *38*, 4149-4156.

(32) Barring, H.; Bucheli, T. D.; Broman, D.; Gustafsson, O., Soot-water distribution coefficients for polychlorinated dibenzo-p-dioxins, polychlorinated dibenzofurans and polybrominated diphenylethers determined with the soot cosolvency-column method. *Chemosphere* **2002**, *49*, 515-523.

(33) Braekevelt, E.; Tittlemier, S. A.; Tomy, G. T., Direct measurement of octanol-water partition coefficients of some environmentally relevant brominated diphenyl ether congeners. *Chemosphere* **2003**, *51*, 563-567.

(34) Watanabe, I.; Sakai, S., Environmental release and behavior of brominated flame retardants. *Environ Int* **2003**, *29*, 665-682.

(35) Safe, S., Polychlorinated biphenyls (PCBs), dibenzo-p-dioxins (PCDDs), dibenzofurans (PCDFs), and related compounds: environmental and mechanistic considerations which support the development of toxic equivalency factors (TEFs). *Critical Reviews in Toxicology* **1990**, *21*, 51-88.

(36) Lee, J. E.; Choi, W.; Mhin, B. J., DFT Calculation on the Thermodynamic Properties of Polychlorinated Dibenzo-p-dioxins: Intramolecular Cl-Cl Repulsion Effects and Their Thermochemical Implications. *Journal of Physical Chemistry A* **2003**, *107*, 2693-2699.

(37) Wong, A.; Lei, Y. D.; Alaee, M.; Wania, F., Vapor Pressures of the Polybrominated Diphenyl Ethers. *Journal of Chemical and Engineering Data* **2001**, *46*, 239-242.

(38) Wania, F.; Lei, Y. D.; Harner, T., Estimating octanol-air partition coefficients of nonpolar semivolatile organic compounds from gas chromatographic retention times. *Analytical Chemistry* **2002**, *74*, 3476-3483.

(39) Li, X.-W.; Shibata, E.; Nakamura, T., Theoretical Calculation of Thermodynamic Properties of Polybrominated Dibenzo-p-dioxins. *Journal of Chemical and Engineering Data* **2003**, *48*, 727-735.

(40) Zhu, L.; Bozzelli, J. W., Thermochemical Properties, DfH Deg(298.15 K), S Deg(298.15 K), and Cp Deg(T), of 1,4-Dioxin, 2,3-Benzodioxin, Furan, 2,3-Benzofuran, and Twelve Monochloro and Dichloro Dibenzo-p-dioxins and Dibenzofurans. *Journal of Physical and Chemical Reference Data* **2003**, *32*, 1713-1735.

(41) Zeng, X.; Freeman, P. K.; Vasil'ev, Y. V.; Voinov, V. G.; Simonich, S. L.; Barofsky, D. F., Theoretical Calculation of Thermodynamic Properties of Polybrominated Diphenyl Ethers. *Journal of Chemical and Engineering Data* **2005**, *50*, 1548-1556.

(42) Soderstrom, G.; Sellstrom, U.; de Wit, C. A.; Tysklind, M., Photolytic debromination of decabromodiphenyl ether (BDE 209). *Environ Sci Technol* **2004**, *38*, 127-132.

(43) Sanchez-Prado, L.; Lores, M.; Llompart, M.; Garcia-Jares, C.; Bayona, J. M.; Cela, R., Natural sunlight and sun simulator photolysis studies of tetra- to hexa-brominated diphenyl ethers in water using solid-phase microextraction. *J Chromatogr A* **2006**, *1124*, 157-166.

(44) Hua, I.; Kang, N.; Jafvert, C. T.; Fabrega-Duque, J. R., Heterogeneous photochemical reactions of decabromodiphenyl ether. *Environ Toxicol Chem* **2003**, *22*, 798-804.

(45) Schmidt, S.; Wittich, R. M.; Erdmann, D.; Wilkes, H.; Francke, W.; Fortnagel, P., Biodegradation of diphenyl ether and its monohalogenated derivatives by Sphingomonas sp. strain SS3. *Appl Environ Microbiol* **1992**, *58*, 2744-2750.

(46) Pfeifer, F.; Truper, H. G.; Klein, J.; Schacht, S., Degradation of diphenylether by Pseudomonas cepacia Et4: enzymatic release of phenol from 2,3-dihydroxydiphenylether. *Arch Microbiol* **1993**, *159*, 323-329.

(47) Hundt, K.; Jonas, U.; Hammer, E.; Schauer, F., Transformation of diphenyl ethers by Trametes versicolor and characterization of ring cleavage products. *Biodegradation* **1999**, *10*, 279-286.

(48) Rayne, S.; Ikonomou, M. G.; Whale, M. D., Anaerobic microbial and photochemical degradation of 4,4'-dibromodiphenyl ether. *Water Res* **2003**, *37*, 551-560.

(49) He, J.; Robrock, K. R.; Alvarez-Cohen, L., Microbial reductive debromination of polybrominated diphenyl ethers (PBDEs). *Environ Sci Technol* **2006**, *40*, 4429-4434.

(50) Gerecke, A. C.; Giger, W.; Hartmann, P. C.; Heeb, N. V.; Kohler, H. P.; Schmid, P.; Zennegg, M.; Kohler, M., Anaerobic degradation of brominated flame retardants in sewage sludge. *Chemosphere* **2006**, *64*, 311-317.

(51) Gerecke, A. C.; Hartmann, P. C.; Heeb, N. V.; Kohler, H. P.; Giger, W.; Schmid, P.; Zennegg, M.; Kohler, M., Anaerobic degradation of decabromodiphenyl ether. *Environ Sci Technol* **2005**, *39*, 1078-1083.

(52) Johnson, T. L.; Scherer, M. M.; Tratnyek, P. G., Kinetics of Halogenated Organic Compound Degradation by Iron Metal. *Environmental Science and Technology* **1996**, *30*, 2634-2640.

(53) Keum, Y. S.; Li, Q. X., Reductive debromination of polybrominated diphenyl ethers by zerovalent iron. *Environ Sci Technol* **2005**, *39*, 2280-2286.

(54) Scherer, M. M.; Balko, B. A.; Gallagher, D. A.; Tratnyek, P. G., Correlation Analysis of Rate Constants for Dechlorination by Zero-Valent Iron. *Environmental Science and Technology* **1998**, *32*, 3026-3033.

(55) Zhou, Z.; Parr, R. G., Activation hardness: new index for describing the orientation of electrophilic aromatic substitution. *Journal of the American Chemical Society* **1990**, *112*, 5720-5724.

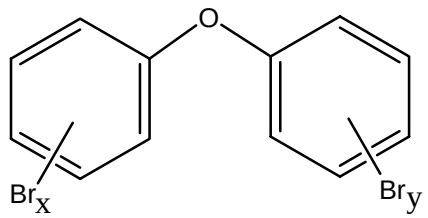

Figure 1.1. Structure of a PBDE congener, x + y = 1 to 10.

Table 1.1. Concentrations (%, w/w) of some major PBDEs in penta-, octa-, and deca-technical products. (Revised from La Guardia, M. J. et al., 2006) (*6*).

	Penta-BDE		**Octa-BDE**		**Deca-BDE**	
	DE-71	**Bromkal 70-5DE**	**DE-79**	**Bromkal 79-8DE**	**Saytex 102E**	**Bromkal 82-0DE**
BDE-47	38.2	42.8				
BDE-100	13.1	7.82				
BDE-99	48.6	44.8				
BDE-154	4.54	2.68				
BDE-153	5.44	5.32	8.66	0.15		
BDE-175/183			42	12.6		
BDE-197			22.2	10.5		
BDE-203			4.4	8.14		
BDE-196			10.5	3.12		
BDE-207			11.5	11.2		
BDE-206			1.38	7.66	2.1	5.13
BDE-209			1.31	49.6	96.8	91.6

CHAPTER 2. THEORETICAL CALCULATION OF THERMODYNAMIC PROPERTIES OF POLYBROMINATED DIPHENYL ETHERS

Xia Zeng, Peter K. Freeman, Yury V. Vasil'ev, Valery G. Voinov, Staci L. Simonich,

Douglas F. Barofsky

Journal of Chemical and Engineering Data

American Chemical Society

Member & Subscriber Services

PO Box 3337

Columbus, OH, 43210, USA

Journal of Chemical and Engineering Data **2005**, 50, 1548-1556.

Abstract

The thermodynamic properties of 39 Polybrominated Diphenyl Ethers (PBDEs) in the ideal gas phase have been calculated using Gaussian 03 on the B3LYP/6-31G(d)//B3LYP/6-31G(d) level. Their thermodynamic and other physicochemical properties show a strong dependence on the bromine substitution pattern. The PBDE congeners' enthalpies of formation increase with increasing number of bromines. The thermodynamic properties of congeners with the same number of bromines also show dependence on the bromine substitution pattern, especially for ortho-substituted congeners. PBDE congeners with one phenyl ring fully brominated, such as 2,3,4,5,6-PeBDE, 2,3,4,4',5,6-HxBDE, 2,2',3,4,4',5,6-HpBDE, and 2,3,3',4,4',5,6-HpBDE, were found to be the least stable among the analogues. The effects of bromine substitution pattern have been quantitatively studied by group additivity method (GAM) based on the output of the theoretical calculations. The results of the GAM were consistent with theoretical calculations, proving that theoretical calculations are reliable. Furthermore, the GAM model can be used to predict the thermodynamic properties for all of the 209 PBDE congeners.

Introduction

Polybrominated Diphenyl Ether (PBDE) flame retardants are widely used as additives in polymers for textiles, electronics, and home furnishings. They have been widely detected in biotic and abiotic matrices including sediments, air, water, fish, marine mammals, human plasma, and human milk.(*1*-*5*) As the use of PBDEs has increased in recent years,(*6*) their concentrations in the environment have also increased.(*7*) A meta-analysis of the published PBDE concentration data carried out in a recent review(*8*)

indicates that PBDEs have migrated in large quantities from industrial products to the environment and to people and, furthermore, that their concentrations have increased exponentially.

Similar to the other polyhalogenated aromatic compounds, such as polychlorinated biphenyls (PCBs), polychlorodibenzo-*p*-dioxins (PCDDs), polychlorodibenzofurans (PCDFs), and polybromodibenzo-*p*-dioxins (PBDDs), the physical, chemical, and biological properties of PBDE congeners strongly depend on the halogen substitution pattern.(*9,10*) Although extensive studies have been conducted to measure the presence of PBDEs in the environment, their vapor pressures,(*11*) and their octanol-air partition coefficients,(*12*) none have been conducted to measure their thermodynamic properties. This is due to the limited availability of pure compounds and to experimental difficulties, such as photodegradation of highly brominated PBDE congeners, associated with some of the congeners. Therefore, theoretical calculations are of interest for estimating the thermodynamic properties of PBDEs. Since there are no experimental values of thermodynamic properties available for PBDEs to compare with the calculated quantities, the uncertainty of the thermodynamic quantities can not be estimated.Density Functional Theory (DFT) calculations were carried out in this work to estimate the enthalpy of formation, ΔH_f, and the Gibbs free energy of formation, ΔG_f, of PBDEs in the gas phase at 298.15 K and 101.325 kPa. Similar calculations have been performed on PBDDs,(*13*) PCDDs(*10*) and PCDFs.(*14*) Unlike dibenzo-*p*-dioxin and dibenzofuran and their halogenated derivatives, diphenyl ether (DE), and thus the PBDEs, has an ether bond about which the two phenyl rings can rotate relatively freely. Finding the most energetically favorable geometries for PBDEs is a complicated, time consuming process;

therefore, it would be impractical to perform DFT calculations for all of the 209, theoretically possible, PBDE congeners. Consequently, commercial availability of standards and importance in environmental research(*7*),(*15*) were used to select the 39 congeners listed in Table 2.1 to illustrate this theoretical approach for PBDEs.

Computational Methods

Using Gaussian 03(*16*), geometry optimizations and energy calculations were performed at the B3LYP/6-31G(d) level. Frequency calculations were also performed for all of the possible geometries to ensure they were minimal on the potential energy surface. Thermal energy ($E_{thermal}$) was calculated as the sum of zero point energy and thermal energy corrections for molecular translation (E_{trans}), rotation (E_{rot}), and vibration (E_{vib}) at 298.15 K. Enthalpy (H), at 298.15 K and 1 atm, was obtained by adding RT to the electronic energy (E_e) and thermal energy. These data, as well as the Gibbs free energy (G), were obtained from the Gaussian output file in Hartrees and converted to kJ/mol (1 Hartree =2625.50 kJ/mol).

Like PCDDs and PBDDs, PBDEs have a variable number of halogens attached to two phenyl rings that are connected to each other by an ether bond. In this study, PBDE congeners with one to seven bromine atoms are represented by the notation MoBDE, DiBDE, TrBDE, TeBDE, PeBDE, HxBDE and HpBDE, respectively. The PBDE with ten bromine atoms on the phenyl ring is represented by DecaBDE.

In a previous study,(*13*) three methods were applied to estimate the thermodynamic properties of PBDDs: calculation from isolated atoms; calculation from isodesmic reactions; and, Benson's Method.(*17*) Among these methods, the second was found to yield the most accurate results. Lee *et al.*(*10*) also used the isodesmic reaction to calculate

the ΔH_f and ΔG_f of PCDDs and obtained results consistent to experimental results. Isodesmic reactions were also applied to calculate ΔH_f of dibenzo-*p*-dioxin, dibenzofuran, PCDDs, and PCDFs using DFT calculations.(*14*) Given the accuracy of these theoretical calculations for PBDDs and PCDDs, it seems reasonable to expect that estimates of the thermodynamic properties of PBDEs, from DFT calculations based on isodesmic reactions, will be similarly accurate.

In this study, Reaction 1, which is similar to the isodesmic reaction used to calculate thermodynamic data for the PCDDs(*10*) and PBDDs,(*13*) served as the basis for calculating ΔH_f and ΔG_f for the PBDEs. In an isodesmic reaction, the number of each type of chemical bond does not change. Therefore, systematic errors associated with, for instance, low basis sets and incomplete correction for electron correlation, can be cancelled out in these reactions.(*18*) Bromobenzene is structurally similar to a PBDE, and the experimental values of ΔH_f for bromobenzene and benzene are reliable.(*19,20*) Compared to the direct reaction of DE with Br_2 or CH_4Br, as described by Li *et al.*,(*13*) Reaction 1 should lead to more accurate results, given by,

$$DE + \mathrm{n}\,bromobenzene = PBDE + \mathrm{n}\,benzene\,. \qquad (1)$$

The enthalpy change of the reaction, ΔH_r, is equal to the sum of the absolute enthalpies of the products as obtained from DFT calculations minus the sum of the absolute enthalpies of reactants,

$$\Delta H_r = [H_{PBDE} + \mathrm{n}\,H_{benzene}] - [H_{DE} + \mathrm{n}\,H_{bromobenzene}]. \qquad (2)$$

The sum of the enthalpies of formation of the products minus that of the reactants also yields ΔH_r,

$$\Delta H_r = [\Delta H_{f\ PBDE} + \mathrm{n}\,\Delta H_{f\ benzene}] - [\Delta H_{f\ DE} + \mathrm{n}\,\Delta H_{f\ bromobenzene}]. \qquad (3)$$

The ΔH_f for any given PBDE was calculated by substituting the calculated enthalpies of the respective compounds listed in Table 2.2 for the PBDE, benzene, DE, and bromobenzene into Equation 2, and substituting the literature values of ΔH_f listed in Table 2.2 for benzene, DE and bromobenzene into Equation 3, eliminating ΔH_r between the two equations, and solving for ΔH_f of PBDEs.

The same method was used to calculate ΔG_f for the PBDEs from the calculated values of G and the literature values of ΔG_f listed in Table 2.2. An experimental value for ΔG_f of DE was not available; hence, eq 4 was used to calculate this quantity,

$$\Delta G_{f\ DE} = \Delta H_{f\ DE} - T(S_{DE} - [12 \times S_{graphite} + 5 \times S_{H_2} + \frac{1}{2} \times S_{O_2}]), \qquad (4)$$

where T is the specified temperature (298.15K) and S is the entropy.

According to Zhu *et al.*,(*14*) DFT calculations produce entropy data for dibenzodioxin (DD) and dibenzofuran (DF) that agree very well with experimental and statistical thermodynamic values. Since DE is structurally similar to DD and DF, it is reasonable to assume that the results obtained in the present study for DE are reliable

Results and Discussion

All of the energies and other thermodynamic quantities calculated for the 39 PBDEs investigated in this study are listed in Table 2.1.

Conformational isomers of PBDE congeners. Because of the low energy barrier for the phenyl rings' rotation about the ether bond, and the rotation of phenyl rings lead to multiple local minima on potential energy surface, each congener can have several stable conformations. After performing DFT calculations on all of the 39 PBDE congeners, it

was found that these stable conformations fell into three groups (Figure 2.1). Generally, for a given congener, the conformation with the largest dihedral angle (Figure 2.1C) had the lowest energy.

The conformational isomers for each congener differ in certain patterns. For the congeners with bromine in the ortho positions on both phenyl rings, i.e. with 2,2' bromines, the distance between the bromines determines the relative energy of the isomers. For most of the congeners studied with 2,2' bromines, the conformational isomer of any given congener with the greatest distance between the 2,2' bromines was the most stable.

Most of the congeners were found to have two or more conformational isomers; however, the following were found to have only one: 4-MoBDE; 2,6-DiBDE; 4,4'-DiBDE; 2,4,6-TrBDE; 2,4',6-TrBDE; 2,4,4',6-TeBDE; 2,2',3,4,4'-PeBDE; 2,3,4,5,6-PeBDE; 2,3,4,4',5,6-HxBDE; and, DecaBDE. Most of these latter congeners have symmetric structures: either C_S symmetry (2,6-DiBDE, 2,4,6-TrBDE, 2,4',6-TrBDE, 2,4,4',6-TeBDE, 2,3,4,5,6-PeBDE, and 2,3,4,4',5,6-HxBDE) or C_2 symmetry (4,4'-DiBDE and DecaBDE).

Energy difference between PBDE congeners. The energy differences between the different conformations of a PBDE congener were found, in general, to be much smaller than the energy differences between congeners within homologues (Figure 2.2). The ΔG_f of the PBDE congeners also exhibit similar differences.

It was determined in an earlier study(*13*) that the energy differences between PBDD congeners are strongly affected by the intramolecular halogenic repulsion, position, and

number. An analysis of these factors in the present study indicates that the inter-congener energy differences for PBDEs are similarly affected.

Mono-BDE. Mono-BDE with the ortho position bromine, 2-MoBDE, is distinguished by a higher energy than the other Mono-BDE congeners, 3-MoBDE and 4-MoBDE (Figure 2.2A). The difference between the latter two is very small, indicating that bromination in the meta and para positions does not yield an increase of energy as much as the ortho-isomer. Comparison of the stability of these three congeners leads to a quantitative estimation of the effect of bromine-position.

Di-BDE. 2,6-DiBDE is the least stable dibrominated PBDE studied (Figure 2.2B) because it has two ortho bromines in its structure. The congeners with no ortho bromines are more stable than those with only one ortho bromine. If the two bromines are on separate phenyl rings, the energy is considerably lower than when both bromines are on the same ring, for example 2,4-DiBDE vs. 2,4'-DiBDE and 3,4-DiBDE vs. 3,4'-DiBDE. This suggests that the effect of intramolecular Br-Br repulsion on one phenyl ring is much larger than the repulsion between the two rings.

Tri-BDE. The least stable of the tri-brominated PBDE studied is 2,4,6-TrBDE (Figure 2.2C) which has all of the bromines on the same phenyl ring and two of them in ortho-positions. The congeners with one ortho bromine are less stable than those with no ortho bromine: the energies of 2,3',4-TrBDE and 2,4,4'-TrBDE are very close, as are those of 3,3',4-TrBDE and 3,4,4'-TrBDE; this indicates that the positions of meta and para substitution contribute similarly to the energy. The calculated energies of 2,4,4'-TrBDE and 3,4,4'-TrBDE are nearly equal (Table 2.1) even though 2,4,4'-TrBDE has one ortho

bromine. This result suggests that the energy-contribution from the 3,4 Br-Br repulsion in 3,4,4'-TrBDE is similar to that of the ortho bromine in 2,4,4'-TrBDE.

Tetra-BDE. The least stable tetra brominated PBDE studied is 2,2',4',6-TetraBDE, which has three ortho bromines (Figure 2.2D); the next least stable compound is 2,3',4,6'-TetraBDE because it has two ortho bromines and two adjacent bromines on one ring. The electronic energy of one of the conformational isomers of 2,2',4,6'-TetraBDE was found to be 9.96 kJ/mol higher than that of the other isomer shown in Figure 2.2D. The former conformation is not stable and most likely converts to the more stable conformation.

Penta-BDE, Hexa-BDE, Hepta-BDE. The least stable of the Penta-BDE congeners studied is 2,3,4,5,6-PeBDE, which has five adjacent bromines on the same phenyl ring (Figure 2.2E). Similarly, the least stable of the Hexa- and Hepta-BDEs studied are 2,3,4,4',5,6-HexaBDE (Figure 2.2F) and 2,2',3,4,4',5,6-HpBDE (Figure 2.2G), respectively.

Calculated enthalpy and Gibbs free energy of formation of the PBDEs. Most of the conformations of a given congener differ in energy by no more than 1.0 kJ/mol (Figure 2.2). Because the different conformations could exist in nature with comparable abundances, the less stable conformations can not simply be disregarded in favor of the most stable conformations when characterizing a congener. The energies of the various conformations should be weighted in accordance with their relative abundances when computing the average energy of the congener. The weighted averages of thermodynamic data, for a congener, should be more realistic and, thus, more reliable, than simple averages or averages that disregard the less stable conformations. The equilibrium

constant, k, for conversion from one conformation to another can be calculated from the difference in ΔG_f between the conformations, as in the relation,

$$\Delta(\Delta G_f) = -RT\ln(k)\,. \qquad (5)$$

Effect of bromine substitution pattern on PBDE thermodynamic properties. It has been shown experimentally in a previous study(*21*) that PBDE congeners with one fully-brominated phenyl ring, such as 2,3,4,5,6-PeBDE, 2,3,4,4',5,6-HxBDE, 2,2',3,4,4',5,6-HpBDE, and 2,3,3',4,4',5,6-HpBDE, are the most susceptible to photochemical decomposition among the highly brominated PBDEs. The results calculated in our study, shown in Figures 2.2E through G, indicate that these congeners are the least stable among the respective homologues, which is consistent with experimental observation.(*21*)

The dependence of PBDE thermodynamic properties on the number of bromines was investigated. Based on the thermodynamic values calculated in this study, PBDE congeners become less stable as the number of bromines increases (Figure 2.3A). Deca-BDE, which has a fully brominated structure, has the highest ΔG_f. The fitted lines for ΔH_f and ΔG_f seem to converge at deca-BDE, but the thermodynamic data indicate that ΔG_f is smaller than ΔH_f for deca-BDE, and thus, this perbrominated structure is entropically unfavorable. Indeed, deca-BDE has been observed in previous studies(*22*,*23*) to be photolytically unstable. The other 38 PBDE congeners studied here have an entropy increase during formation. The order of stability calculated in this study (Figure 2.3A) is in agreement with the increasing rate of PBDE decomposition with increasing numbers of bromine reported in an early study.(*22*)

The PBDDs, which have structures and physicochemical properties that are similar to those of the PBDEs, have been extensively studied. For example, the value of ΔH_f and ΔG_f for the PBDDs, as calculated by Li *et al.*(*13*) (Figure 2.3B), increase with successive bromination in a manner analogous to that of PBDEs, and the congeners with one fully brominated phenyl ring are the least stable among the PBDDs' homologues. We can conclude from Li's study and, this study, that bromination of DD and DE is thermodynamically unfavorable and that chlorination of DD is thermodynamically favored, as stated in a previous study.(*10*)

In the latter study, Lee *et al.*,(*10*) based on Benson's group additivity method (GAM),(*17*) analyzed the effect of chlorination position and Cl-Cl intramolecular repulsion on the energy of formation for PCDDs. This method has been adapted in this study to quantitatively analyze the effect of Br substitution patterns on the energy of formation for PBDEs. All of the components of this method are listed in Table 2.3 and illustrated schematically in Figure 2.4 for a PBDE congener. The enthalpies discussed in the remainder of this report will be a weighted average of all of the conformations studied for the PBDE congener in question.

ΔH_1 is the difference in enthalpy between a specific Br position in study and the most stable position on the phenyl ring. 3-MoDE was found to be the most stable of the Mono-BDEs so therefore, ΔH_1 is 0 kJ/mol for the meta-position. ΔH_2 and ΔH_3 are the Br-Br repulsions in one phenyl ring and between two phenyl rings, respectively.

ΔH_2 for bromines at position 2 and 3 is calculated using the following equations:

$$2,3\text{-}DiBDE + DE = 2\text{-}MoBDE + 3\text{-}MoBDE, \qquad (6)$$

$$\Delta H_2(2,3) = H_{2,3-DiBDE} + H_{DE} - H_{2-MoBDE} - H_{3-MoBDE} \ . \quad (7)$$

The calculation of ΔH_3 for bromines at the position 2 and 2' is demonstrated by the following equations:

$$2,2'\text{-}\ DiBDE + DE = 2\text{-}\ MoBDE + 2\text{-}\ MoBDE, \quad (8)$$

$$\Delta H_3(2,2') = H_{2,2'-DiBDE} + H_{DE} - 2 \times H_{2-MoBDE} \ . \quad (9)$$

Additional DFT calculations were performed for the enthalpies of 2,3-DiBDE, 2,5-DiBDE, 3,5-DiBDE, 2,2'-DiBDE, 2,3'-DiBDE, and 3,3'-DiBDE (Table 2.4) because they were not among the 39 congeners initially studied.

The results of the group additivity approach for the 39 congeners are shown in Table 2.5. In this table, relative ΔH_f DFT is the difference in ΔH_f (from DFT calculation) between the congener in question and the first congener in its homolog group (Figure 2.5A through 5G). Relative ΔH_f GAM is the difference of the sum of ΔH_1, ΔH_2 and ΔH_3 for the same congener compared to the first congener of the homolog group. Plotting the values of relative ΔH_f DFT and relative ΔH_f GAM together on the same bar graph (Figure 2.5) shows that GAM predicts essentially the same effect of a given bromine substitution pattern on thermodynamic properties as does the corresponding DFT calculation. However, some congeners, especially for those with two ortho bromines on a same phenyl ring, the differences between relative ΔH_f DFT and relative ΔH_f GAM are fairly great, which may due to the fact that GAM model can not describe the thermodynamic properties as accurate as DFT method, especially for ortho bromines.

Intramolecular repulsion causes the ΔH_f to increase nonlinearly with increasing number of bromines. This is reflected in the positive non-linear curvature of a plot of DFT

calculated ΔH_f vs. bromine number (Figure 2.6). Furthermore, the congeners with the same number of bromines also differ due to various substitution positions and different repulsion effects. This is also demonstrated in Figure 2.6 by the scattered points for the DFT calculated values.

It is of interest to look at the trend of ΔH_f without considering the Br substitution position and intramolecular Br-Br repulsion. GAM corrected ΔH_f is the result of ΔH_f from DFT calculation subtracted by the sum of ΔH_1, ΔH_2 and ΔH_3. In contrast to the curve of ΔH_f from DFT calculation, the values of GAM corrected ΔH_f fall very well on a straight line when plotted against the number of bromines (Figure 2.6). The collapse of ΔH_f values on to a straight line indicates that the correction from GAM eliminates the difference between congeners with the same degree of bromination. The slope of the line resulting from linear regression implies that the ΔH_f increases 21.98 kJ/mol for each addition of a single bromine when the substitution position and intramolecular repulsion are not considered.

By using the reaction,

$$DE + bromobenzene = 3\text{-}MoBDE + benzene, \qquad (10)$$

the change in enthalpy due to bromination of DE at the 3-position can be calculated. The product of this reaction, 3-MoBDE, has the substitution position of lowest energy and can not exhibit any effect due to intramolecular Br-Br repulsion. The increase of ΔH_f in going from DE to 3-MoBDE is 23.85 kJ/mol, which is only 1.87 kJ/mol more than predicted by the slope obtained from ΔH_f GAM corrected versus Br number (Figure 2.6). The consistency between the results from GAM model and those obtained from DFT calculation give credence to the latter's use for calculating the thermodynamic properties

of PBDEs. The linear correlation between the GAM corrected ΔH_f and bromine number makes it possible to predict ΔH_f for any PBDE congeners.

Conclusions

After optimization by DFT calculation, the geometries of the 39 PBDE congeners studied all fall into the three groups (Figure 2.1). It is likely that other undiscovered conformations may exist for some of these PBDE congeners; however, the thermodynamic properties calculated in this study should not be affected by the missing conformations because the energy differences between different conformations of PBDE congeners are much smaller than the energy differences within homologues.

Use of the isodesmic reaction is a valid method for predicting the enthalpy and Gibbs free energy of formation of PBDEs from the results of DFT calculations and from known experimental values for other compounds. GAM yields results that are consistent with DFT calculation. The GAM model describes the effect of Br substitution pattern very well and can be potentially useful in predicting the thermodynamic properties of all of the 209 PBDE congeners.

Acknowledgment

This publication was made possible in part by grant number P30ES00210 from the National Institute of Environmental Health Sciences, NIH through a pilot project awarded by Oregon State University's Environmental Health Sciences Center. Its contents are solely the responsibility of the authors and do not necessarily represent the official view of the NIEHS, NIH. The authors would like to acknowledge OSU's EHSC's mass spectrometry core facility for assistance, and Max Deinzer and Luke Ackerman for helpful suggestions.

Reference

(1)Dodder, N. G.; Strandberg, B.; Hites, R. A., Concentrations and Spatial Variations of Polybrominated Diphenyl Ethers and Several Organochlorine Compounds in Fishes from the Northeastern United States. *Environ Sci Technol* **2002**, *36*, 146-151.

(2)Strandberg, B.; Dodder, N. G.; Basu, I.; Hites, R. A., Concentrations and Spatial Variations of Polybrominated Diphenyl Ethers and Other Organohalogen Compounds in Great Lakes Air. *Environmental Science and Technology* **2001**, *35*, 1078-1083.

(3)Darnerud, P. O.; Eriksen, G. S.; Johannesson, T.; Larsen, P. B.; Viluksela, M., Polybrominated diphenyl ethers: Occurrence, dietary exposure, and toxicology. *Environmental Health Perspectives Supplements* **2001**, *109*, 49-68.

(4)Rahman, F.; Langford, K. H.; Scrimshaw, M. D.; Lester, J. N., Polybrominated diphenyl ether (PBDE) flame retardants. *Science of the Total Environment* **2001**, *275*, 1-17.

(5)Palm, A.; Cousins, I. T.; Mackay, D.; Tysklind, M.; Metcalfe, C.; Alaee, M., Assessing the environmental fate of chemicals of emerging concern: a case study of the polybrominated diphenyl ethers. *Environmental Pollution (Oxford, United Kingdom)* **2002**, *117*, 195-213.

(6)Bromine Science and environmental Forum. Total Market Demand 2003. available at www.bsef.com.

(7)de Wit, C. A., An overview of brominated flame retardants in the environment. *Chemosphere* **2002**, *46*, 583-624.

(8)Hites, R. A., Polybrominated Diphenyl Ethers in the Environment and in People: A Meta-Analysis of Concentrations. *Environ Sci Technol* **2004**, *38*, 945-956.

(9)Safe, S., Polychlorinated biphenyls (PCBs), dibenzo-p-dioxins (PCDDs), dibenzofurans (PCDFs), and related compounds: environmental and mechanistic considerations which support the development of toxic equivalency factors (TEFs). *Critical Reviews in Toxicology* **1990**, *21*, 51-88.

(10)Lee, J. E.; Choi, W.; Mhin, B. J., DFT Calculation on the Thermodynamic Properties of Polychlorinated Dibenzo-p-dioxins: Intramolecular Cl-Cl Repulsion Effects and Their Thermochemical Implications. *Journal of Physical Chemistry A* **2003**, *107*, 2693-2699.

(11)Wong, A.; Lei, Y. D.; Alaee, M.; Wania, F., Vapor Pressures of the Polybrominated Diphenyl Ethers. *Journal of Chemical and Engineering Data* **2001**, *46*, 239-242.

(12)Wania, F.; Lei, Y. D.; Harner, T., Estimating octanol-air partition coefficients of nonpolar semivolatile organic compounds from gas chromatographic retention times. *Analytical Chemistry* **2002**, *74*, 3476-3483.

(13)Li, X.-W.; Shibata, E.; Nakamura, T., Theoretical Calculation of Thermodynamic Properties of Polybrominated Dibenzo-p-dioxins. *Journal of Chemical and Engineering Data* **2003**, *48*, 727-735.

(14)Zhu, L.; Bozzelli, J. W., Thermochemical Properties, DfH Deg(298.15 K), S Deg(298.15 K), and Cp Deg(T), of 1,4-Dioxin, 2,3-Benzodioxin, Furan, 2,3-Benzofuran, and Twelve Monochloro and Dichloro Dibenzo-p-dioxins and Dibenzofurans. *Journal of Physical and Chemical Reference Data* **2003**, *32*, 1713-1735.

(15)Ackerman, L. K.; Wilson, G. R.; Simonich, S. L., Quantitative analysis of 39 polybrominated diphenyl ethers by isotope dilution GC/low-resolution MS. *Analytical Chemistry* **2005**, *77*, 1979-1987.

(16) Frisch, M. J., Gaussian 03, revision B.05. *Gaussian Inc. Pittsburg, PA* **2003**.

(17)Benson, S. W. *Thermochemical Kinetics: Methods for the Estimation of Thermochemical Data and Rate Parameters. 2nd Ed*; Wiley: New York, 1976.

(18)Irikura, K. K.; Frurip, D. J.; Editors *Computational Thermochemistry: Prediction and Estimation of Molecular Thermodynamics. (Proceedings of a Symposium at the 212th National Meeting of the American Chemical Society, Orlando, Florida, 25-29 August 1996.) [In: ACS Symp. Ser., 1998; 677]*, 1998.

(19)Pedley, J. B.; Naylor, R. D.; Kirby, S. B. *Thermochemical Data of Organic Compounds. 2nd Ed*; Chapman and Hall: New York, 1986.

(20)Anon, CRC Handbook of Chemistry and Physics. 83rd Edition. Edited by David R. Lide (National Institute of Standards and Technology). CRC Press: Boca Raton. 2002. + 2664 pp. $139.95. ISBN 0-8493-0483-0. *Journal of the American Chemical Society* **2002**, *124*, 14280.

(21)Peterman, P. H.; Orazio, C. E.; Feltz, K. P., Sunlight photolysis of 39 mono-hepta PBDE congeners in lipid. *Organohalogen Compounds* **2003**, *63*, 357-360.

(22)Eriksson, J.; Green, N.; Marsh, G.; Bergman, A., Photochemical Decomposition of 15 Polybrominated Diphenyl Ether Congeners in Methanol/Water. *Environ Sci Technol* **2004**, *38*, 3119-3125.

(23)Herrmann, T.; Schilling, B.; Paepke, O., Photolysis of PBDEs in solvents by exposure to daylight in a routine laboratory. *Organohalogen Compounds* **2003**, *63*, 361-364.

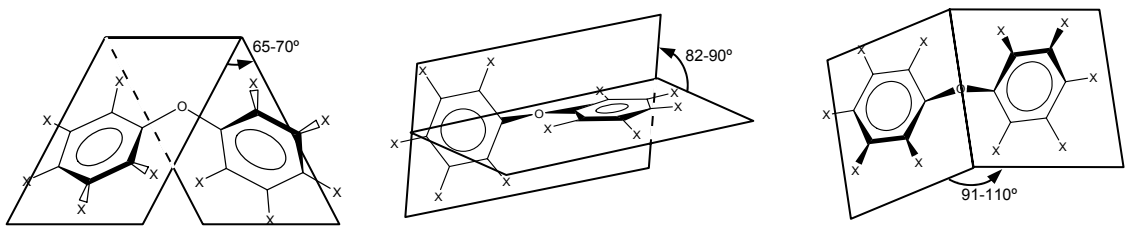

Figure 2.1. Stable conformations of PBDE congeners (X = H or Br): (A) the planes of the phenyl rings form an acute angle (65-70º); (B) the planes form a dihedral close to a right angle, with one phenyl ring in the same plane as the C-O-C bond and the other ring perpendicular to the ether plane (82-90º); (C) the planes form an obtuse dihedral angle (91-110º).

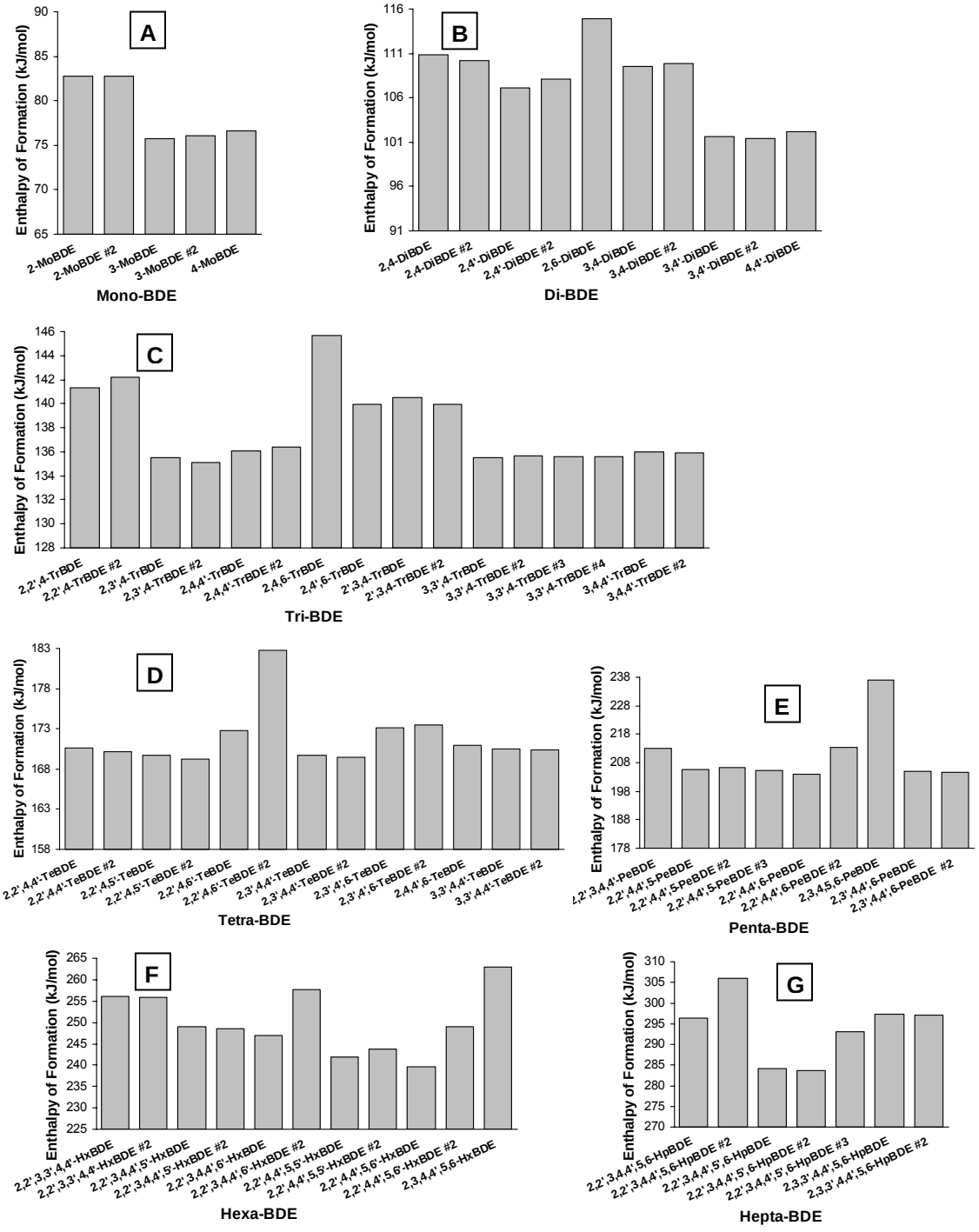

Figure 2.2. ΔH_f for the studied conformations of PBDEs from DFT calculation, with congeners in homologue groups displayed in A through G. For the congeners with more than one conformation isomer, "#2" was added to the congener name representing the second conformation, "#3" for the third conformation, and so on.

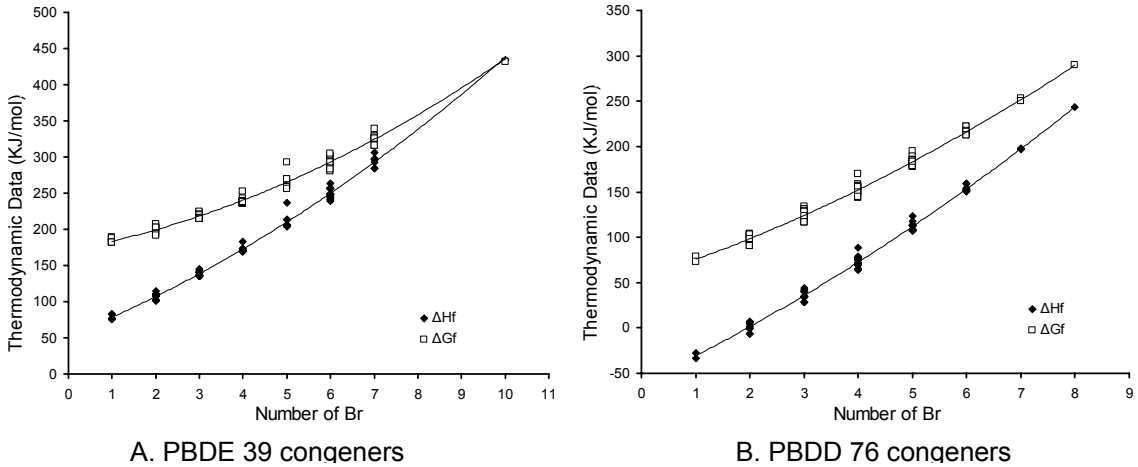

Figure 2.3. ΔH_f and ΔG_f for PBDE and PBDD(*13*) congeners from DFT calculations. The trend lines are results of polynomial fitting.

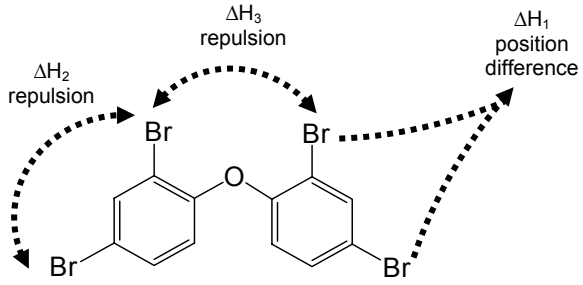

Figure 2.4. Group additivity components for 2,2',4,4'-TeBDE.

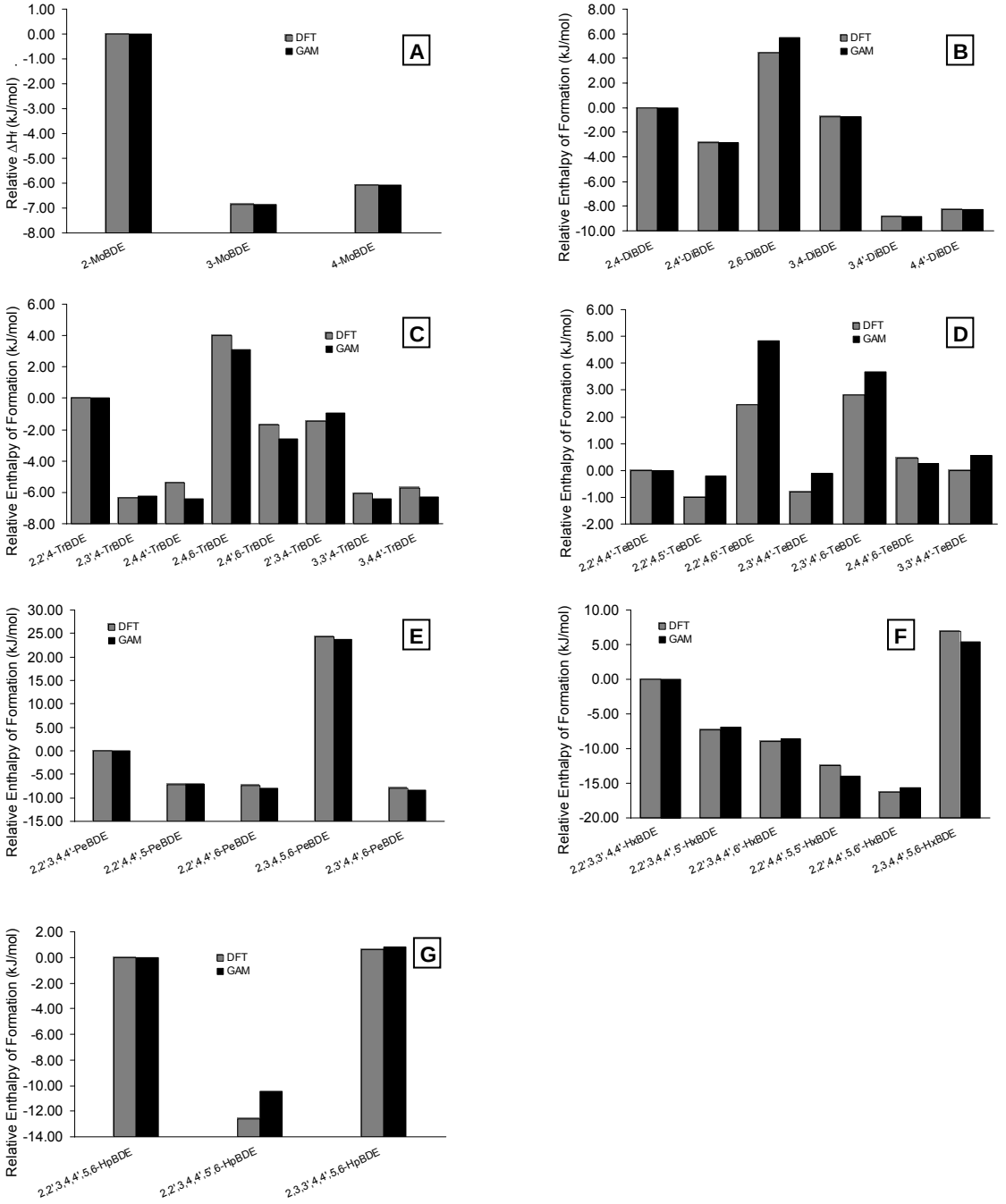

Figure 2.5. Comparison of relative ΔH_f from DFT calculation to GAM model, with congeners in homologue groups plotted in A through G. Relative ΔH_f DFT is the difference in ΔH_f (from DFT calculation) between the congener in question and the first congener in the homologue group. Relative ΔH_f GAM is the difference of the sum of ΔH_1, ΔH_2 and ΔH_3 for the same congener compared to the first congener of the group.

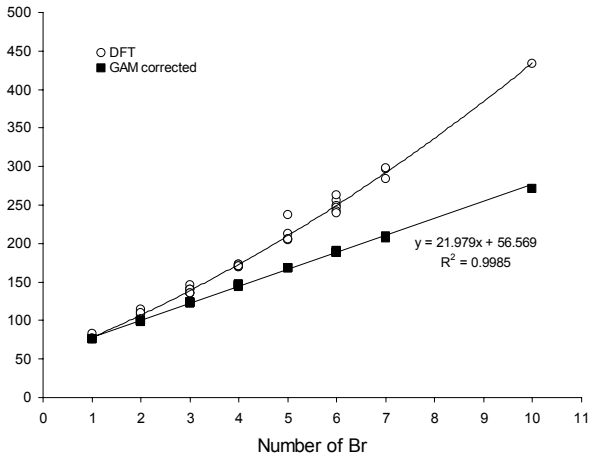

Figure 2.6. Comparison of enthalpy of formation between DFT calculation and GAM corrected results. The nonlinear trend line is the result of polynomial fitting, and linear trend line is from linear regression.

Table 2.1. Thermodynamic Data of PBDEs from DFT Calculations

Congener number	Congener name [a]	E_e/Hartree	H/Hartree	G/Hartree	ΔH_f/kJ/mol	ΔG_f/kJ/mol	S/J/mol·K	Relative abundanc	H Average /Hartree
BDE-1	2-MoBDE	-3109.61470	-3109.42678	-3109.47944	82.72	189.05	463.28	0.7201	-3109.42678
	2-MoBDE #2	-3109.61480	-3109.42678	-3109.47975	82.71	188.24	465.98	1	
BDE-2	3-MoBDE	-3109.61737	-3109.42944	-3109.48235	75.73	181.40	465.51	1	-3109.42939
	3-MoBDE #2	-3109.61724	-3109.42933	-3109.48206	76.02	182.15	463.95	0.7371	
BDE-3	4-MoBDE	-3109.61707	-3109.42909	-3109.48222	76.64	181.76	467.37	1	-3109.42909
BDE-7	2,4-DiBDE	-5680.71757	-5680.53828	-5680.59532	110.89	204.50	501.78	0.4331	-5680.53845
	2,4-DiBDE #2	-5680.71792	-5680.53853	-5680.59611	110.22	202.43	506.50	1	
BDE-8	2,4'-DiBDE	-5680.71905	-5680.53971	-5680.59705	107.13	199.94	504.47	1	-5680.53954
	2,4'-DiBDE #2	-5680.71878	-5680.53936	-5680.59698	108.06	200.13	506.94	0.9246	
BDE-10	2,6-DiBDE	-5680.71609	-5680.53675	-5680.59415	114.90	207.55	505.02	1	-5680.53675
BDE-12	3,4-DiBDE	-5680.71811	-5680.53880	-5680.59610	109.52	202.44	504.07	0.9072	-5680.53873
	3,4-DiBDE #2	-5680.71795	-5680.53867	-5680.59619	109.85	202.20	506.01	1	
BDE-13	3,4'-DiBDE	-5680.72109	-5680.54179	-5680.59936	101.65	193.87	506.45	1	-5680.54183
	3,4'-DiBDE #2	-5680.72117	-5680.54187	-5680.59932	101.46	193.99	505.40	0.9545	
BDE-15	4,4'-DiBDE	-5680.72094	-5680.54160	-5680.60034	102.16	191.30	516.77	1	-5680.54160
BDE-17	2,2',4-TrBDE	-8251.81967	-8251.64892	-8251.71022	141.31	222.50	539.31	1	-8251.64879
	2,2',4-TrBDE #2	-8251.81931	-8251.64859	-8251.70984	142.17	223.50	538.82	0.6665	
BDE-25	2,3',4-TrBDE	-8251.82173	-8251.65113	-8251.71329	135.51	214.44	546.87	0.9197	-8251.65120
	2,3',4-TrBDE #2	-8251.82187	-8251.65127	-8251.71337	135.14	214.23	546.31	1	
BDE-28	2,4,4'-TrBDE	-8251.82164	-8251.65093	-8251.71267	136.03	216.07	543.13	0.5370	-8251.65084
	2,4,4'-TrBDE #2	-8251.82154	-8251.65080	-8251.71326	136.39	214.53	549.49	1	
BDE-30	2,4,6-TrBDE	-8251.81790	-8251.64725	-8251.70946	145.69	224.51	547.23	1	-8251.64725
BDE-32	2,4',6-TrBDE	-8251.82020	-8251.64944	-8251.71165	139.96	218.75	547.31	1	-8251.64944
BDE-33	2',3,4-TrBDE	-8251.81988	-8251.64924	-8251.71090	140.49	220.73	542.46	0.7232	-8251.64935
	2',3,4-TrBDE #2	-8251.82012	-8251.64943	-8251.71120	139.97	219.92	543.42	1	
BDE-35	3,3',4-TrBDE	-8251.82174	-8251.65114	-8251.71319	135.47	214.71	545.83	1	-8251.65110
	3,3',4-TrBDE #2	-8251.82162	-8251.65106	-8251.71314	135.70	214.84	546.17	0.9504	
	3,3',4-TrBDE #3	-8251.82170	-8251.65111	-8251.71301	135.55	215.17	544.57	0.8317	
	3,3',4-TrBDE #4	-8251.82171	-8251.65109	-8251.71305	135.61	215.07	545.06	0.8631	
BDE-37	3,4,4'-TrBDE	-8251.82159	-8251.65095	-8251.71292	135.98	215.41	545.20	0.9091	-8251.65097
	3,4,4'-TrBDE #2	-8251.82163	-8251.65098	-8251.71301	135.90	215.17	545.73	1	
BDE-47	2,2',4,4'-TeBDE	-10822.92214	-10822.76001	-10822.82656	170.57	236.73	585.54	1	-10822.76005
	2,2',4,4'-TeBDE #2	-10822.92241	-10822.76015	-10822.82570	170.20	239.01	576.64	0.3988	
BDE-49	2,2',4,5'-TeBDE	-10822.92236	-10822.76032	-10822.82622	169.75	237.62	579.78	0.8290	-10822.76043
	2,2',4,5'-TeBDE #2	-10822.92258	-10822.76052	-10822.82640	169.23	237.16	579.58	1	
BDE-51	2,2',4,6'-TeBDE	-10822.92134	-10822.75917	-10822.82428	172.76	242.74	572.73	1	-10822.75917
	2,2',4,6'-TeBDE #2	-10822.91732	-10822.75538	-10822.82043	182.72	252.83	572.30	0.0171	
BDE-66	2,3',4,4'-TeBDE	-10822.92233	-10822.76035	-10822.82672	169.67	236.33	583.83	0.8604	-10822.76040
	2,3',4,4'-TeBDE #2	-10822.92243	-10822.76045	-10822.82686	169.42	235.96	584.25	1	
BDE-71	2,3',4',6-TeBDE	-10822.92113	-10822.75905	-10822.82573	173.08	238.93	586.58	1	-10822.75897
	2,3',4',6-TeBDE #2	-10822.92093	-10822.75889	-10822.82566	173.51	239.11	587.40	0.9285	
BDE-75	2,4,4',6-TeBDE	-10822.92191	-10822.75987	-10822.82692	170.92	235.80	589.81	1	-10822.75987
BDE-77	3,3',4,4'-TeBDE	-10822.92197	-10822.76005	-10822.82656	170.46	236.73	585.14	1	-10822.76005
	3,3',4,4'-TeBDE #2	-10822.92201	-10822.76006	-10822.82618	170.44	237.74	581.69	0.6658	
BDE-85	2,2',3,4,4'-PeBDE	-13394.01961	-13393.86611	-13393.93563	212.90	270.05	611.60	1	-13393.86611
BDE-99	2,2',4,4',5-PeBDE	-13394.02239	-13393.86883	-13393.93878	205.78	261.80	615.37	0.5186	-13393.86888
	2,2',4,4',5-PeBDE #2	-13394.02199	-13393.86864	-13393.93879	206.27	261.76	617.17	0.5274	
	2,2',4,4',5-PeBDE #3	-13394.02247	-13393.86904	-13393.93940	205.23	260.17	618.99	1	
BDE-100	2,2',4,4',6-PeBDE	-13394.02209	-13393.86954	-13393.93709	203.91	266.22	594.29	1	-13393.86891
	2,2',4,4',6-PeBDE #2	-13394.01915	-13393.86590	-13393.93561	213.45	270.11	613.22	0.2077	
BDE-116	2,3,4,5,6-PeBDE	-13394.00976	-13393.85689	-13393.92705	237.13	292.60	617.20	1	-13393.85689
BDE-119	2,3',4,4',6-PeBDE	-13394.02246	-13393.86911	-13393.94020	205.03	258.07	625.36	0.5567	-13393.86919
	2,3',4,4',6-PeBDE #2	-13394.02259	-13393.86923	-13393.94075	204.72	256.62	629.19	1	
BDE-128	2,2',3,3',4,4'-HxBDE	-15965.11633	-15964.97190	-15965.04592	256.09	300.18	651.20	1	-15964.97194
	2,2',3,3',4,4'-HxBDE	-15965.11668	-15964.97201	-15965.04556	255.78	301.13	647.00	0.6823	
BDE-138	2,2',3,4,4',5'-HxBDE	-15965.11940	-15964.97459	-15965.04831	249.02	293.91	648.52	0.4841	-15964.97470
	2,2',3,4,4',5'-HxBDE	-15965.11938	-15964.97476	-15965.04899	248.57	292.11	653.05	1	
BDE-140	2,2',3,4,4',6'-HxBDE	-15965.11999	-15964.97539	-15965.04926	246.91	291.40	649.89	1	-15964.97535
	2,2',3,4,4',6'-HxBDE	-15965.11568	-15964.97126	-15965.04497	257.76	302.67	648.47	0.0106	
BDE-153	2,2',4,4',5,5'-HxBDE	-15965.12222	-15964.97731	-15965.05152	241.89	285.47	652.93	0.1495	-15964.97670
	2,2',4,4',5,5'-HxBDE	-15965.12136	-15964.97661	-15965.05332	243.72	280.76	674.83	1	
BDE-154	2,2',4,4',5,6'-HxBDE	-15965.12294	-15964.97819	-15965.05235	239.56	283.29	652.45	1	-15964.97812
	2,2',4,4',5,6'-HxBDE	-15965.11912	-15964.97455	-15965.04863	249.11	293.06	651.70	0.0194	
BDE-166	2,3,4,4',5,6-HxBDE	-15965.11356	-15964.96928	-15965.04402	262.95	305.16	657.51	1	-15964.96928
BDE-181	2,2',3,4,4',5,6-HpBDE	-18536.21440	-18536.07879	-18536.15675	296.36	328.88	685.88	1	-18536.07872
	2,2',3,4,4',5,6-HpBDE	-18536.21061	-18536.07514	-18536.15293	305.95	338.91	684.37	0.0174	
BDE-183	2,2',3,4,4',5',6-HpBDE	-18536.21938	-18536.08345	-18536.16163	284.11	316.06	687.76	0.8613	-18536.08353
	2,2',3,4,4',5',6-HpBDE	-18536.21961	-18536.08367	-18536.16177	283.55	315.69	687.12	1	
	2,2',3,4,4',5',6-HpBDE	-18536.21576	-18536.08002	-18536.15819	293.12	325.10	687.69	0.0225	
BDE-190	2,3,3',4,4',5,6-HpBDE	-18536.21395	-18536.07840	-18536.15751	297.39	326.90	695.96	0.5131	-18536.07848
	2,3,3',4,4',5,6-HpBDE	-18536.21407	-18536.07853	-18536.15814	297.05	325.24	700.36	1	
BDE-209	DecaBDE	-26249.50214	-26249.39314	-26249.48288	433.79	431.67	789.54	1	-26249.39314

[a] For the congeners with more than one conformation isomer, "#2" was added to the congener name representing the second conformation, "#3" for the third conformation, and so on. The relative abundance is 1 for the most stable conformation of a congener.

Table 2.2. Thermodynamic Data used to Calculate ΔH_f and ΔG_f of PBDEs

	DE	bromobenzene	benzene	graphite	H_2	O_2
H/Hartree	-538.31625[a]	-2803.25621[a]	-232.14255[a]			
ΔH_f/kJ/mol	52.0[c]	105.4[c]	82.9[d]			
G/Hartree	-538.36453[a]	-2803.29372[a]	-232.17535[a]			
ΔG_f/kJ/mol	171.04384[b]	138.6[e]	129.7[d]			
S/J/mol·K	425.22501[a]			5.7[d]	130.7[d]	205.2[d]

[a] data from DFT calculation. [b] calculated from Equation 4. [c] data from reference 19. [d] data from reference 20. [e] data from reference 13.

Table 2.3. Group Additivity Components for PBDEs

Name	Definition	Calculated by	Example
ΔH_1	the difference in enthalpy compared to meta position on phenyl ring	comparing the enthalpy of 2-MoBDE, 3-MoBDE and 4-MoBDE	0 kJ/mol for meta 6.86 kJ/mol for ortho 0.79 kJ/mol for para
ΔH_2	intramolecular Br-Br repulsion in one phenyl ring	isodesmic reactions of 2,3-DiBDE, 2,4-DiBDE, 2,5-DiBDE, 2,6-DiBDE, 3,4-DiBDE, 3,5-DiBDE	Equation (6)(7)
ΔH_3	intramolecular Br-Br repulsion between two phenyl rings	isodesmic reactions of 2,2'-DiBDE, 2,3'-DiBDE, 2,4'-DiBDE, 3,3'-DiBDE, 3,4'-DiBDE, 4,4'-DiBDE	Equation (8)(9)

Table 2.4. Enthalpies of Additional PBDE Congeners

Congeners	*H*/Hartree
2,3-DiBDE	-5680.53625
2,5-DiBDE	-5680.53891
3,5-DiBDE	-5680.54124
2,2'-DiBDE	-5680.53684
2,3'-DiBDE	-5680.53954
3,3'-DiBDE	-5680.54194

Table 2.5. Enthalpy Data of Position and Repulsion Effects for PBDE Congeners

Congener Name	ΔH_f	Relative ΔH_f DFT	ΔH_1	ΔH_2	ΔH_3	Relative ΔH_f GAM
			kJ/mol			
2-MoBDE	82.72	0.00	6.86	0.00	0.00	0.00
3-MoBDE	75.85	-6.86	0.00	0.00	0.00	-6.86
4-MoBDE	76.64	-6.07	0.79	0.00	0.00	-6.07
2,4-DiBDE	110.42	0.00	7.65	3.06	0.00	0.00
2,4'-DiBDE	107.57	-2.85	7.65	0.00	0.22	-2.85
2,6-DiBDE	114.90	4.48	13.73	1.47	1.23	5.71
3,4-DiBDE	109.69	-0.73	0.79	9.20	0.00	-0.73
3,4'-DiBDE	101.56	-8.86	0.79	0.00	1.06	-8.86
4,4'-DiBDE	102.16	-8.26	1.58	0.00	0.88	-8.26
2,2',4-TrBDE	141.66	0.00	14.52	3.06	1.44	0.00
2,3',4-TrBDE	135.32	-6.34	7.65	3.06	2.07	-6.24
2,4,4'-TrBDE	136.26	-5.39	8.44	3.06	1.09	-6.42
2,4,6-TrBDE	145.69	4.03	14.52	7.60	0.00	3.09
2,4',6-TrBDE	139.96	-1.70	14.52	1.47	0.44	-2.60
2',3,4-TrBDE	140.19	-1.47	7.65	9.20	1.22	-0.95
3,3',4-TrBDE	135.58	-6.07	0.79	9.20	2.63	-6.41
3,4,4'-TrBDE	135.94	-5.72	1.58	9.20	1.94	-6.31
2,2',4,4'-TeBDE	170.47	0.00	15.31	6.13	2.54	0.00
2,2',4,5'-TeBDE	169.46	-1.00	14.52	5.73	3.51	-0.21
2,2',4,6'-TeBDE	172.93	2.46	21.38	4.54	2.89	4.83
2,3',4,4'-TeBDE	169.67	-0.80	8.44	12.26	3.16	-0.11
2,3',4',6-TeBDE	173.29	2.82	14.52	10.67	2.45	3.66
2,4,4',6-TeBDE	170.92	0.46	15.31	7.60	1.31	0.25
3,3',4,4'-TeBDE	170.45	-0.01	1.58	18.39	4.57	0.57
2,2',3,4,4'-PeBDE	212.90	0.00	15.31	24.96	4.61	0.00
2,2',4,4',5-PeBDE	205.64	-7.26	15.31	17.99	4.61	-6.97
2,2',4,4',6-PeBDE	205.55	-7.35	22.17	10.66	3.98	-8.06
2,3,4,5,6-PeBDE	237.13	24.22	14.52	54.02	0.00	23.66
2,3',4,4',6-PeBDE	204.84	-8.07	15.31	16.80	4.39	-8.38
2,2',3,3',4,4'-HxBDE	255.96	0.00	15.31	43.79	8.24	0.00
2,2',3,4,4',5'-HxBDE	248.72	-7.25	15.31	36.82	8.24	-6.97
2,2',3,4,4',6'-HxBDE	247.03	-8.94	22.17	29.50	7.06	-8.61
2,2',4,4',5,5'-HxBDE	243.48	-12.49	15.31	29.86	8.24	-13.94
2,2',4,4',5,6'-HxBDE	239.75	-16.22	22.17	22.53	7.06	-15.58
2,3,4,4',5,6-HxBDE	262.95	6.98	15.31	54.02	3.44	5.42
2,2',3,4,4',5,6-HpBDE	296.53	0.00	22.17	57.08	8.12	0.00
2,2',3,4,4',5',6-HpBDE	283.92	-12.61	22.17	44.03	10.69	-10.48
2,3,3',4,4',5,6-HpBDE	297.17	0.64	15.31	63.21	9.64	0.79
DecaBDE	433.79	0.00	29.03	108.03	25.20	0.00

CHAPTER 3. DEVELOPMENT AND VALIDATION OF A CONGENER SPECIFIC PHOTODEGRADATION MODEL FOR POLYBROMINATED DIPHENYL ETHERS

Xia Zeng[†], *Staci L. Simonich*[†‡*], *Kristin R. Robrock*[§], *Peter Korytár*[€], *Lisa Alvarez-Cohen*[§], *Douglas F. Barofsky*[†]

[†]Department of Chemistry, Oregon State University, Corvallis, OR 97331, USA; [‡]Department of Environmental and Molecular Toxicology, Oregon State University, Corvallis, OR 97331, USA; [§]Department of Civil and Environmental Engineering, University of California, Berkeley, California 94720, USA; [€] Wageningen Institute for Marine Resources and Ecosystem Studies, Haringkade 1, 1976 CP IJmuiden, The Netherlands

*Corresponding author. Telephone: (541) 737-9194. Fax: (541) 737-2062. Email: staci.simonich@orst.edu

Abstract

With the phase-out of the manufacture of some polybrominated diphenyl ether (PBDE) formulations, namely penta-BDE and octa-BDE, and the continued use of the deca-BDE formulation, it is important to be able to predict the photodegradation of the highly brominated congeners. A model was developed and validated to predict the products, and their relative concentrations, from the photodegradation of PBDEs. The enthalpies of formation of the 209 PBDE congeners were calculated and the relative reaction rate constants were obtained. The predicted reaction rate constants for PBDEs show linear correlation with previous experimental results. Because of their large volume use, high concentrations in the environment, and/or importance in the photodegradation of the deca-BDE formulation, BDE-209, BDE-184, BDE-100 and BDE-99 were chosen for further UV photodegradation experiments in isooctane. The photodegradation model successfully predicted the products of the photochemical reactions of PBDEs in experimental studies. A GC retention time model for PBDEs was developed using a multiple linear regression analysis and, together with the photodegradation model and additional PBDE standards, provided a way to identify unknown products from PBDE photodegradation. Based on the results of the photodegradation experiments, as well as the model predictions, it appears that the photodegradation of PBDEs is a first order reaction and, further, that the rate determining step is the stepwise loss of bromine. Our results suggest that, over time, BDE-99 will remain as the most abundant penta-BDE, while BDE-49 and BDE-66 will increase greatly and will be comparable in abundance to BDE-47.

Introduction

Polybrominated diphenyl ether (PBDE) flame retardants are widely used in consumer products to reduce flammability (*1*). Increasing consumer use has led to increasing PBDE concentrations in the environment and the human body (*2-5*). Because of their potential toxicity (*6,7*), the use of penta-BDE and octa-BDE formulations has been banned in Europe and voluntarily phased out in the U.S. (*8*). However, with the continued use of the deca-BDE formulation, large quantities of PBDEs are still being released into the environment. BDE-209, the major ingredient of deca-BDE technical mixture, has been reported to photodegrade under UV and natural sunlight to give lower PBDEs, including the banned penta and octa-BDEs (*9,10*). This finding has led to a need for a model to explain and predict the products of the photodegradation of PBDEs and their relative abundances. In our previous study, the enthalpies of formation of 39 PBDE congeners were calculated using Gaussian 03 and a Group Additivity Method (GAM) was developed (*11*). This made it possible in the current study to predict the stability of all 209 PBDE congeners using the GAM model and develop a photodegradation model to predict the relative abundances of their photodegradation products.

Previous studies on the photodegradation rate of PBDEs have been conducted (*9,10,12,13*). However, the identification and interpretation of products and reaction pathways has been limited. In one of the studies, BDE-209 and 14 other PBDE congeners were shown to undergo first order photodegradation reactions and stepwise

loss of bromine (*9*). Bezares-Cruz et al. proposed a limited reaction pathway for BDE-209 photodegradation to BDE-47 (*10*).

To better understand PBDE photodegradation and validate the photodegradation model, experiments were conducted on the photodegradation of BDE-209, BDE-184, BDE-100 and BDE-99 under UV light. BDE-209 is the major ingredient of deca-BDE technical mixture which is still being used in large quantity; BDE-184 is one of the previously unreported products of BDE-209 photodegradation; BDE-100 and BDE-99 are the major penta-BDEs detected in the environment (*3-5*). The stepwise debromination to form lower BDE congeners was monitored and products identified using gas chromatography/mass spectrometry (GC-MS), a new PBDE GC retention time model, and PBDE standards (*14*) (*15*). In this study, the relative abundances of PBDE photodegradation products from experiments were compared to those predicted by the photodegradation model. Specifically, these calculations and the model indicate that bromine dissociation energy is correlated with the photodegradation energy barrier, a relationship that can be used to predict the photodegradation products and their relative abundances.

Experimental section

Chemicals

A standard mixture of 39 PBDEs was obtained from Cambridge Isotope (*14*). Individual standards of BDE-99, 100, 121, 140, 146, 148, 168, 184, 196, 197, 203, 206, 207, 208 were purchased from AccuStandard. BDE-209 was purchased from Aldrich.

Some of the PBDE photodegradation products, which were not identified using the above standards, were confirmed with an additional 126 individual PBDE congeners (*15*).

Methods

UV Photodegradation studies were conducted using a Rayonet RPR-100 photochemical reactor with RMR-2537A (250nm) UV lamps purchased from Southern New England Ultra Violet Company. PBDE congeners were dissolved in isooctane and these solutions were irradiated in sealed quartz vials. Isooctane was chosen as the solvent because the PBDE standards were purchased in isooctane and previous studies in hexane (*10*) and toluene (*12*) have shown that organic solvent type does not affect the PBDE debromination pattern (*12*). Isooctane has been previously used to study the photodegradation of chlorinated dioxins (*16*). Starting concentrations of BDE-99, BDE-100, and BDE-184 were 1 to 10 μmol/L and the BDE-209 solution was saturated at 196 μmol/L. The irradiated samples were analyzed using a JEOL GC mate II GC-HRMS in electron capture negative ionization (ECNI) mode. The GC column was a 30m J&W DB-5 column (0.25mm I.D. and 0.25μm film thickness), and the GC temperature program was: 100ºC (hold for 1 min); 10ºC/min to 320ºC (hold for 27 min). The temperatures of the splitless injector, GC interface, and ion source were 280ºC, 250ºC and 250ºC, respectively. The PBDE congeners were quantified using external calibration. PBDE congeners without available standards were quantified using the average ECNI response of the homologous PBDE group.

Multiple linear regression analysis was used to predict the GC retention time of the photodegradation products. ΔH_f, the number of ortho-, meta-, and para-bromines,

polarizability, highest occupied molecular orbital (HOMO) energy, lowest unoccupied molecular orbital (LUMO) energy, dipole moment, and natural logarithm of molecular weight (ln(MW)) were included in the GC retention time model as molecular descriptors. All of the molecular descriptors, except for ln(MW) were obtained using Gaussian 03 (*17*) on the B3LYP/6-31G(d)//B3LYP/6-31G(d) level, which is much more precise than the results obtained by semi-empirical methods (*18-20*). Molecular descriptors, such as ΔH_f, polarizability, HOMO, LUMO, and especially dipole moments, are different for different conformational isomers of a given PBDE congener. These molecular descriptors were averaged for PBDE congeners that had more than one stable conformation.

Photodegradation Model

The enthalpies of formation of all 209 PBDE congeners were obtained using a previously developed GAM model (*11*). Briefly, for a specific PBDE congener:

$$\Delta H_f\,(kJ/mol) = 21.979 \times BrNumber + 56.569 + \Delta H_1 + \Delta H_2 + \Delta H_3. \qquad (1)$$

ΔH_1 is the difference in enthalpy between the specific Br position in question and the most stable position on the phenyl ring; ΔH_2 and ΔH_3 are the energies due to repulsion, respectively, between two bromines on one phenyl ring and between two bromines on opposite phenyl rings (*11*).

As a unimolecular reaction, the photodegradation of a PBDE is a pseudo-first-order reaction according to Lindemann theory (*21*). In the model developed in this study, the photodegradation of a PBDE congener is presumed to proceed by detachment of a bromine, followed by addition of H from a H-donor. The loss of bromine is the rate

determining step. In the photodegradation of PBDEs, the reaction rate of a specific PBDE congener *i* is:

$$-\frac{d[i]}{dt} = \sum k_i[i] - \alpha_{hi} k_h^i[h] \quad (2)$$

$$\sum k_i = \sum \alpha_{ij} k_i^j \quad (3)$$

In Eqn 2, $[i]$ is the concentration of the PBDE congener *i*, and $\sum k_i$ is the total degradation rate constant for PBDE congener *i.* Since *i* can also be a product of higher PBDE congener (*h*) degradation, the reaction rate of *i* also included $-\alpha_{hi} k_h^i[h]$ in Eqn 2, in which $[h]$ is the concentration of the parent PBDE congener, k_h^i is the rate constant for *h* degradation to *i*, and α_{hi} is the number of equivalent pathways for the degradation of *h* to *i*. $\sum k_i$ is calculated in Eqn 3 where k_i^j is the reaction rate constants for *i* degradation to the lower PBDE *j* and α_{ij} is the number of equivalent pathways for the degradation of *i* to *j*. For example, in the photodegradation of BDE-209, the reaction rate of BDE-209 is expressed:

$$-\frac{d[209]}{dt} = \sum k_{209} \times [209], \quad (4)$$

$$\sum k_{209} = 2 \times k_{209}^{208} + 4 \times k_{209}^{207} + 4 \times k_{209}^{206}. \quad (5)$$

Similarly, BDE-208, which is one of the products of BDE-209 photodegradation, photodegrades to produce BDE-198, BDE-199, BDE-200, BDE-201, and BDE-202 at the rate

$$-\frac{d[208]}{dt} = \sum k_{208} \times [208] - 2 \times k_{209}^{208} \times [209] \quad (6)$$

where

$$\sum k_{208} = 2 \times k_{208}^{198} + 2 \times k_{208}^{199} + 2 \times k_{208}^{200} + 2 \times k_{208}^{201} + k_{208}^{202} \ . \quad (7)$$

The photodegradation rate constant can be calculated from the following expression:

$$k = A \times \exp\left(\frac{-Ea}{RT}\right) \quad (8)$$

where A is a pre-exponential factor and Ea is the bromine dissociation energy. To simplify the model, we assume the A and T are the same for all 209 PBDE congeners; therefore, the rate constant is only correlated to Ea. Also, the positional isomerization that is possible during debromination is not likely to occur because of the excessive energy required. For example, for the two photodegradation pathways BDE-209 to BDE-207 and BDE-209 to BDE-208, the ratio of reaction rates would be:

$$\frac{k_{209}^{207}}{k_{209}^{208}} = \exp\left(\frac{-D(C-Br)_{meta} + D(C-Br)_{para}}{RT}\right), \quad (9)$$

in which $D(C\text{-}Br)_{para}$ and $D(C\text{-}Br)_{meta}$ are the bond dissociation energies of para and meta C-Br bonds in BDE-209. The difference in ΔH_f, as given by Eqn 1, between BDE-208 and BDE-207 is equivalent to the difference in bond dissociation energies between the para and meta C-Br bonds of BDE-209:

$$-D(C-Br)_{meta} + D(C-Br)_{para} = -\Delta H_{f207} + \Delta H_{f208} \, . \quad (10)$$

Eqn 9 and 10 together give:

$$\frac{k_{209}^{207}}{k_{209}^{208}} = \exp\left(\frac{\Delta H_{f207} - \Delta H_{f208}}{-RT}\right). \quad (11)$$

For all the PBDEs, a general expression of Eqn 11 is:

$$\frac{k_h^i}{k_h^j} = \exp\left(\frac{\Delta H_{fi} - \Delta H_{fj}}{-RT}\right). \quad (12)$$

Because the model in this study provides the ratio of the rate constants between different reaction pathways, the photodegradation rate constants are all relative rate constants. To predict the photodegradation of PBDEs in experiments, at least one experimental value of the rate constant must be known. In all cases of our study, that is the degradation rate constant of the reactant PBDE.

A Visual BASIC program was developed to calculate the relative abundances of reactant and photodegradation products by calculating the change in the concentration over a small time interval:

$$-d[i] = \left(\sum k_i \times [i] - \alpha_{hi} k_h^i [h]\right) dt . \quad (13)$$

The initial concentration and experimental rate constant of the reactant PBDE were used in this model to estimate the final concentration at a specific reaction time.

Results and Discussion

Calculated Enthalpy of formation of PBDE congeners

We have previously shown that the GAM model yields values for ΔH_f that are consistent with those calculated using a density functional theory (DFT) method in Gaussian 03 at the B3LYP/6-31G(d)//B3LYP/6-31G(d) level for 39 PBDEs (*11*). Therefore, ΔH_f values for each of the 209 PBDE congeners were calculated using the GAM model (*11*) and are shown in Figure 3.1. Among homologue groups, the higher energy PBDE congeners tend to have more adjacent bromines and more ortho bromines than other PBDE congeners, for example, BDE-1 (2-monoBDE), BDE-5 (2,3-diBDE),

BDE-21 (2,3,4-triBDE), BDE-24 (2,3,6-triBDE), BDE-61 (2,3,4,5-tetraBDE), BDE-62 (2,3,4,6-tetraBDE), BDE-116 (2,3,4,5,6-pentaBDE), BDE-142 (2,2,'3,4,5,6-hexaBDE), BDE-173 (2,2',3,3',4,5,6-heptaBDE), and BDE-195 (2,2',3,3',4,4',5,6-octaBDE). However, some PBDE congeners with the highest number of ortho bromines, for example BDE-54 (2,2',6,6'-tetraBDE), BDE-96 (2,2',3,6,6'-pentaBDE), and BDE-155(2,2',4,4',6,6'-hexaBDE), do not have the highest energies. Clearly, repulsion energies, caused by adjacent bromine atoms, make the greatest contribution to ΔH_f within a homologous PBDE group.

In general, the PBDE congeners with the lowest energies among homologues are the congeners with lowest number of adjacent bromines and lowest number of ortho bromines, examples include BDE-11 (3,3'-diBDE), BDE-13 (3,4'-diBDE), BDE-36 (3,3',5-triBDE), BDE-39 (3,4',5-triBDE), BDE-80 (3,3',5,5'-tetraBDE), BDE-120 (2,3',4,5,5'-pentaBDE), BDE-121 (2,3',4,5,6'-pentaBDE), BDE-155 (2,2',4,4',6,6'-hexaBDE), BDE-184 (2,2',3,4,4',6,6'-heptaBDE), and BDE-197 (2,2',3,3',4,4',6,6'-octaBDE). However, among these examples, BDE-155, BDE-184 and BDE-197 are fully ortho-brominated. Therefore, it appears that ortho bromine substitution does not contribute to the energy as much as adjacent bromine substitution does.

It should be noted that the most abundant PBDE photodegradation products are not always the most stable congeners. For example, of the penta-BDEs, the ΔH_f for BDE-99 is slightly higher than the ΔH_f for BDE-121 and BDE-120. Never the less, experiments show that BDE-99 is the most abundant penta-BDE product resulting from BDE-209 photodegradation (*10*), which indicates that photodegradation of BDE-209 follows

certain reaction pathways and that the stability is not the only factor to decide the relative abundance of the photodegradation products. The possible photodegradation products of PBDE congeners, and their relative abundances, can be predicted from the calculated values of ΔH_f for all 209 PBDEs assuming that the positional isomerization, which requires substantial energy, does not occur.

GC retention time prediction of photodegradation products

To obtain reliable predictions of the photodegradation product GC retention times, it was necessary to use eight molecular descriptors of physicochemical properties. Specifically, the following linear expression was used to predict PBDE photodegradation product GC retention times:

$$\textit{Retention time(min)} = \beta_0 + \beta_1 \times \Delta H_f + \beta_2 \times \textit{polarizability} + \beta_3 \times \textit{HOMO} + \beta_4 \times \textit{LUMO} + \beta_5 \times \textit{ln(MW)} + \beta_6 \times \textit{ortho bromine} + \beta_7 \times \textit{para bromine} + \beta_8 \times \textit{meta bromine} + \beta_9 \times \textit{dipole moment} \quad (14)$$

where ΔH_f is the enthalpy of formation in kJ/mol; polarizability is the average molecular polarizability in a.u.; HOMO and LUMO are molecular orbital energies in eV; ln(MW) is the natural logarithm of molecular weight; ortho bromine, para bromine, and meta bromine are the number of bromines at ortho, para and meta bromines respectively; dipole moment is the average dipole moment in Debye; and β_0 to β_9 are empirically determined by multiple linear regression, and are, therefore, specific for the DB-5 column and GC temperature program used in this study. Previous GC retention time models have been used to identify the number of bromines on an unknown PBDE congener (*18-20*). However, these models can not be used to identify PBDEs within a homologous group. In

contrast, values computed from Eqn 14 for 47 of the PBDEs (Table 3.1) show good linearity and, in particular, within homologous groups (R^2=0.9939, P<0.0001) (Figure 3.2A). The values of β_0 to β_9 in Figure 3.2A are -27.3227, 0.0586, 0.0027, -15.6492, 19.6598, 5.5465, -1.1053, -0.4677, 0.0141, and 0.2243, respectively. A residual plot (Figure 3.2B) shows that, with only two exceptions, the predicted GC retention times are within 0.6 min of their corresponding measured retention times and there is no systematic trend. The outliers, BDE-168 (2,3',4,4',5',6-hexaBDE) and BDE-196 (2,2',3,3',4,4',5,6'-octaBDE), have one of the greatest dipole moments (2.33 Debye and 1.74 Debye, respectively) within their homologue groups.

PBDE photodegradation model validation

In a recent study (*22*), quantitative structure-property relationship (QSPR) models were used to predict the photodegradation rates of 15 PBDEs based on experimental reaction rate (*9*); however, the photodegradation rates for the remaining 194 PBDEs were not predicted. In this study, the photodegradation rate constants of the 208 PBDE congeners that are potential photodegradation products of BDE-209 were calculated using Eqns 3 and 12 relative to an arbitrarily assigned rate constant of 1 min^{-1} for BDE-209 (Table 3.2). From among these values, 15 congeners were plotted (Figure 3.3) against the corresponding photodegradation rate constants measured in methanol/water (80/20) under UV light (*9*). The linear correlation between the experimental rate constants (*9*) and those predicted from Eqn 2 and 13 is good (R^2=0.8958, P<0.0001) (Figure 3.3).

Using Eqn 13, the abundances of hepta-BDEs relative to total PBDE concentration were computed at different reaction times (Figure 3.4). The predicted relative abundance

of PBDE congeners was inversely correlated with their ΔH_f at short reaction time (Figure 3.4A compared to the hepta-BDE in Figure 3.1). However, at longer reaction times, the congeners with the slowest total degradation rates had the highest relative abundance (BDE-187 and 188) (Figure 3.4B).

A recent study (*13*) reported the time profile for the photodegradation products of several PBDE congeners, namely BDE 47, BDE 100, BDE 99, BDE 154 and BDE 153, coated on a Solid Phase Micro Extraction (SPME) fiber and irradiated with simulated sunlight. Using the rate constants from their study ($\sum k_{100}$ = 0.096min^{-1} and $\sum k_{153}$ = 0.401min^{-1}) (*13*), we calculated the photodegradation time profile of BDE-100 and BDE-153 (Figure 3.5A and 3.5B). Using our photodegradation model, we also predicted the photodegradation of BDE-209 from previous studies (*10,12*). Using the reported rate constants, the prediction of the solar photodegradation of BDE-209 in hexane (*10*) is shown in Figure 3.5C and the prediction of the photodegradation of BDE-209 on silica gel under UV-light (*12*) is shown in Figure 3.5D. When compared to the corresponding literature results (*10,12,13*), our photodegradation model predicts PBDE photodegradation time profiles under different conditions very well.

Photodegradation experiments and model predictions

Using our theoretical model of PBDE photodegradation and GC retention time prediction, we conducted laboratory photodegradation experiments on BDE-209, BDE-184, BDE-100 and BDE-99 to better understand PBDE photodegradation time profiles. BDE-184 has not been previously reported to be a photodegradation product of BDE-209. However, BDE-184 is one of the predicted important BDE-209 photodegradation

products (Figure 3.4), and the prediction was confirmed experimentally (data not shown). In addition, it was both predicted by the model and experimentally observed that the major products of BDE-184 photodegradation are BDE-154, BDE-155 and BDE-100 (Figure 3.6). With only three exceptions, the predicted photodegradation products of BDE-184 after 120 min (Figure 3.6C) correlate with the corresponding product peaks in the GC/MS chromatogram from the BDE-184 photodegradation experiment after 120 min UV irradiation (R^2=0.4882, P=0.0168 overall and R^2=0.9786, P<0.0001 without the three exceptions) (Figure 3.7) (Figure 3.6D). Two of the exceptions, BDE-139 and BDE-140, were predicted at concentrations much lower than observed, whereas the other exception, BDE-155, was predicted at a much higher concentration than observed experimentally. BDE-155 (2,2',4,4',6,6'-hexaBDE) is fully brominated in the ortho positions. The stability of the ortho bromine may be over predicted by the model, which results in higher predicted concentrations relative to the experiment. All of the major chromatographic peaks in Figure 3.6D were identified using PBDE standards except for the two peaks at 19.95 min and 23.05 min. The chromatographic peak at 19.95 min was predicted to be BDE-103 based on the GC retention time model (Table 3.1) and photodegradation model (Figure 3.6C); the peak at 23.05 min was assigned as BDE-139, which has a predicted retention time of 22.88 min. The identities of BDE-103 and BDE-139 were confirmed using the 126 PBDE standards (*15*).

The photodegradation of BDE-100 and BDE-99, which are the most abundant penta-BDEs detected in the environment (*3-5*), has been previously studied (*9,13*). However, all of the products were not identified and the reaction mechanism was not explained.

Therefore, we chose to also study the photodegradation of these important penta-BDEs. The experimentally determined time profile for the photodegradation of BDE-100 (Figure 3.8A) was predicted from the photodegradation model in all but one case (BDE-28) (Figure 3.8B). Compared to the all the other photodegradation products, which have two or more ortho bromines, BDE-28 (2,4,4'-triBDE) has only one bromine in the ortho positions. The stability of the ortho bromine may be over predicted by the model, which results in higher predicted concentrations relative to the experiment, except for BDE-28. As was observed in the photodegradation of BDE-184, the total concentration of PBDEs decreased with time.

The most abundant photodegradation products of BDE-100 at 10 min were predicted from the photodegradation model to be BDE-75, BDE-47 and BDE-28 (Figure 3.8C); these predictions corresponded to the most abundant photodegradation products observed in the GC-MS chromatogram of a BDE-100 sample after 10 min of irradiation (Figure 3.8D). All of the major chromatographic peaks were identified using PBDE standards except for the peaks at 18.16 min and 18.55 min (which co-elute with BDE-75). A recent study (*15*) showed that BDE-75 and BDE-51 co-elute and, further, that BDE-50 has a shorter retention time than BDE-51 on a DB-5 column under a GC temperature program similar to the one used in the present study. Based on this information and photodegradation model, the peaks at 18.16 min and 18.55 min are most likely BDE-50 and BDE-51, respectively. The identities of BDE-50 and BDE-51 were confirmed by the 126 PBDE standards (*15*). Linear correlation between the experimental concentrations

and those predicted by the model for the photodegradation of BDE-100 after 5 min irradiation is good (R^2=0.7892, P=0.0180) (Figure 3.9).

For BDE-99, the photodegradation model predicted that the four primary products, BDE-66, BDE-74, BDE-47, and BDE-49, reached their maximum concentrations after about 2 min of irradiation (Figure 3.10B); this result closely matched the experiment (Figure 3.10A). Again, the total concentration of PBDEs in the BDE-99 photodegradation experiment decreased significantly with time after 5 min irradiation.

As was true for BDE-100 photodegradation, all of the predicted major photodegradation products of BDE-99 at 5 min (Figure 3.10C) appeared in the GC-MS chromatogram of a BDE-99 sample irradiated for 5 min (Figure 3.10D). The chromatographic peaks at 16.21 min, 16.67 min and 19.20 min were predicted to be BDE-18, BDE-31 and BDE-74, respectively, based on the GC retention time model prediction of 15.65 min, 16.31 min, and 18.96 min, respectively. The identities of BDE-18, BDE-31 and BDE-74 were confirmed by the 126 PBDE standards (*15*). The correlation between the experimental results and predicted concentrations of BDE-99's photodegradation products after 5 min irradiation was not very linear but was statistically significant (R^2=0.4441, P=0.0133) (Figure 3.11).

Figure 3.12A shows the experimental result of the time profile of BDE-209 photodegradation by homologous group. The predicted time profile of BDE-209 photodegradation was calculated and is shown in Figure 3.12B. After 8 days of irradiation, only 0.16% of mono-BDEs and 0.02% of di-BDEs were detected in the solution. At the level of homologous group, the theoretical model reproduced the results

of the experiment well and both show stepwise debromination of PBDEs over time. The experimental results (Figure 3.12C) and model prediction (Figure 3.12D) at congener level for penta-BDE and tetra-BDE products indicates that at the congener level, the model did not predict as well as it did for BDE-184, BDE-100 and BDE-99. Furthermore, the concentrations of the tetra-BDEs were underestimated by the model (Figure 3.12E and 3.12F), and the correlation between model and experiment also confirmed this (Figure 3.13). Because the photodegradation of BDE-209 has up to ten steps of debromination and could result in 208 possible products, the estimation error may accumulate for each step of debromination and lead to relatively large error.

Photodegradation pathways

The major photodegradation pathways mapped out in this study for BDE-209, BDE-184, BDE-100, and BDE-99 are summarized in Figure 3.14. The thicker lines pass through those photodegradation products with higher concentrations; these pathways are more probable than the rest. The relative abundances of photodegradation products were concluded from the experimental results when the model prediction did not agree well with the experimental results. For the photodegradation of BDE-209, BDE-99 is the most abundant penta-BDE product even though it is not the most stable penta-BDE, because it is on the pathway of the highest probability for each step. Similarly, BDE-28 is on the pathway of the highest probability in the photodegradation of BDE-100, therefore it is the most abundant tri-BDE product.

In all of the photodegradation experiments conducted, the total amounts of PBDEs were observed to decrease with time. This is contradictory to the photodegradation model

that assumes constant mass balance. It is possible that the ether bond breaks under wavelength UV light (*23*). In addition, there was greater loss of PBDEs when the photo reaction shifted to lower PBDEs. Also, ECNI is not as sensitive for mono and di-BDEs as other highly brominated PBDEs (*14*). Therefore, mono- and di-BDEs were rarely detected in the photodegradation products, and may not be fully accounted for in the mass balance of the experiments.

The PBDE photodegradation model is based on the GAM model which is an approximation to calculate the ΔH_f of PBDEs. ΔH_f may not be the only factor determining the PBDE photodegradation rate constant. Other factors may include molecular weight, molecular orbital energy, and charge distribution (*22*). Furthermore, the model assumes that the solvent effect and light conditions have the same effect on all PBDE congeners. These limitations may cause the observed deviations from the experiment results.

Previous studies have shown that the current PBDE congeners in the environment are similar to the congener composition of the technical mixtures used (*3,4*). Assuming that most of the BDE-209 in the environment is eventually photodegraded by natural sunlight, the future pattern of the PBDE congeners caused by BDE-209 degradation in the environment may be comparable to our results. For example, BDE-99 will remain as the most abundant penta-BDE, while BDE-49 and BDE-66 will increase greatly and will be comparable in abundance to BDE-47. It is also possible that PBDE congeners that have not been used commercially, such as octa BDE-201 and hepta BDE-187, will be present in the environment at significant concentrations among their congener group.

Acknowledgement

This publication was made possible in part by grant number P30ES00210 from the National Institute of Environmental Health Sciences, NIH through a pilot project awarded by Oregon State University's Environmental Health Sciences Center. Its contents are solely the responsibility of the authors and do not necessarily represent the official view of the NIEHS, NIH. The authors would like to acknowledge OSU's EHSC's mass spectrometry core facility for assistance, and Max Deinzer and Luke Ackerman for helpful suggestions and Harris Fellowship for summer support.

References

(1) Hale, R. C.; La Guardia, M. J.; Harvey, E.; Mainor, T. M., Potential role of fire retardant-treated polyurethane foam as a source of brominated diphenyl ethers to the US environment. *Chemosphere* **2002**, *46*, 729-735.

(2) de Wit, C. A., An overview of brominated flame retardants in the environment. *Chemosphere* **2002**, *46*, 583-624.

(3) Hites, R. A., Polybrominated Diphenyl Ethers in the Environment and in People: A Meta-Analysis of Concentrations. *Environ Sci Technol* **2004**, *38*, 945-956.

(4) Elliott, J. E.; Wilson, L. K.; Wakeford, B., Polybrominated diphenyl ether trends in eggs of marine and freshwater birds from British Columbia, Canada, 1979-2002. *Environ Sci Technol* **2005**, *39*, 5584-5591.

(5) Dodder, N. G.; Strandberg, B.; Hites, R. A., Concentrations and Spatial Variations of Polybrominated Diphenyl Ethers and Several Organochlorine Compounds in Fishes from the Northeastern United States. *Environ Sci Technol* **2002**, *36*, 146-151.

(6) Madia, F.; Giordano, G.; Fattori, V.; Vitalone, A.; Branchi, I.; Capone, F.; Costa, L. G., Differential in vitro neurotoxicity of the flame retardant PBDE-99 and of the PCB Aroclor 1254 in human astrocytoma cells. *Toxicol Lett* **2004**, *154*, 11-21.

(7) Muirhead, E. K.; Skillman, A. D.; Hook, S. E.; Schultz, I. R., Oral exposure of PBDE-47 in fish: toxicokinetics and reproductive effects in Japanese Medaka (Oryzias latipes) and fathead minnows (Pimephales promelas). *Environ Sci Technol* **2006**, *40*, 523-528.

(8) Hale, R. C.; Alaee, M.; Manchester-Neesvig, J. B.; Stapleton, H. M.; Ikonomou, M. G., Polybrominated diphenyl ether flame retardants in the North American environment. *Environ Int* **2003**, *29*, 771-779.

(9) Eriksson, J.; Green, N.; Marsh, G.; Bergman, A., Photochemical Decomposition of 15 Polybrominated Diphenyl Ether Congeners in Methanol/Water. *Environ Sci Technol* **2004**, *38*, 3119-3125.

(10) Bezares-Cruz, J.; Jafvert, C. T.; Hua, I., Solar photodecomposition of decabromodiphenyl ether: products and quantum yield. *Environ Sci Technol* **2004**, *38*, 4149-4156.

(11) Zeng, X.; Freeman, P. K.; Vasil'ev, Y. V.; Voinov, V. G.; Simonich, S. L.; Barofsky, D. F., Theoretical Calculation of Thermodynamic Properties of Polybrominated Diphenyl Ethers. *Journal of Chemical and Engineering Data* **2005**, *50*, 1548-1556.

(12) Soderstrom, G.; Sellstrom, U.; de Wit, C. A.; Tysklind, M., Photolytic debromination of decabromodiphenyl ether (BDE 209). *Environ Sci Technol* **2004**, *38*, 127-132.

(13) Sanchez-Prado, L.; Lores, M.; Llompart, M.; Garcia-Jares, C.; Bayona, J. M.; Cela, R., Natural sunlight and sun simulator photolysis studies of tetra- to hexa-brominated diphenyl ethers in water using solid-phase microextraction. *J Chromatogr A* **2006**, *1124*, 157-166.

(14) Ackerman, L. K.; Wilson, G. R.; Simonich, S. L., Quantitative analysis of 39 polybrominated diphenyl ethers by isotope dilution GC/low-resolution MS. *Analytical Chemistry* **2005**, *77*, 1979-1987.

(15) Korytar, P.; Covaci, A.; de Boer, J.; Gelbin, A.; Brinkman, U. A., Retention-time database of 126 polybrominated diphenyl ether congeners and two bromkal technical mixtures on seven capillary gas chromatographic columns. *J Chromatogr A* **2005**, *1065*, 239-249.

(16) Kieatiwong, S.; Nguyen, L. V.; Hebert, V. R.; Hackett, M.; Miller, G. C.; Miille, M. J.; Mitzel, R., Photolysis of chlorinated dioxins in organic solvents and on soils. *Environmental Science and Technology* **1990**, *24*, 1575-1580.

(17) Frisch, M. J., Gaussian 03, revision B.05. *Gaussian Inc. Pittsburg, PA* **2003**.

(18) Rayne, S.; Ikonomou, M. G., Predicting gas chromatographic retention times for the 209 polybrominated diphenyl ether congeners. *J Chromatogr A* **2003**, *1016*, 235-248.

(19) Harju, M.; Andersson, P. L.; Haglund, P.; Tysklind, M., Multivariate physicochemical characterisation and quantitative structure-property relationship modelling of polybrominated diphenyl ethers. *Chemosphere* **2002**, *47*, 375-384.

(20) Wang, Y.; Li, A.; Liu, H.; Zhang, Q.; Ma, W.; Song, W.; Jiang, G., Development of quantitative structure gas chromatographic relative retention time models on seven stationary phases for 209 polybrominated diphenyl ether congeners. *Journal of Chromatography, A* **2006**, *1103*, 314-328.

(21) Robinson, P. J.; Holbrook, K. A. *Unimolecular Reactions*, 1972.

(22) Niu, J.; Shen, Z.; Yang, Z.; Long, X.; Yu, G., Quantitative structure-property relationships on photodegradation of polybrominated diphenyl ethers. *Chemosphere* **2006**, *64*, 658-665.

(23) Hageman, H. J.; Louwerse, H. L.; Mijs, W. J., Photoreactions of some diaryl ethers. *Tetrahedron* **1970**, *26*, 2045-2052.

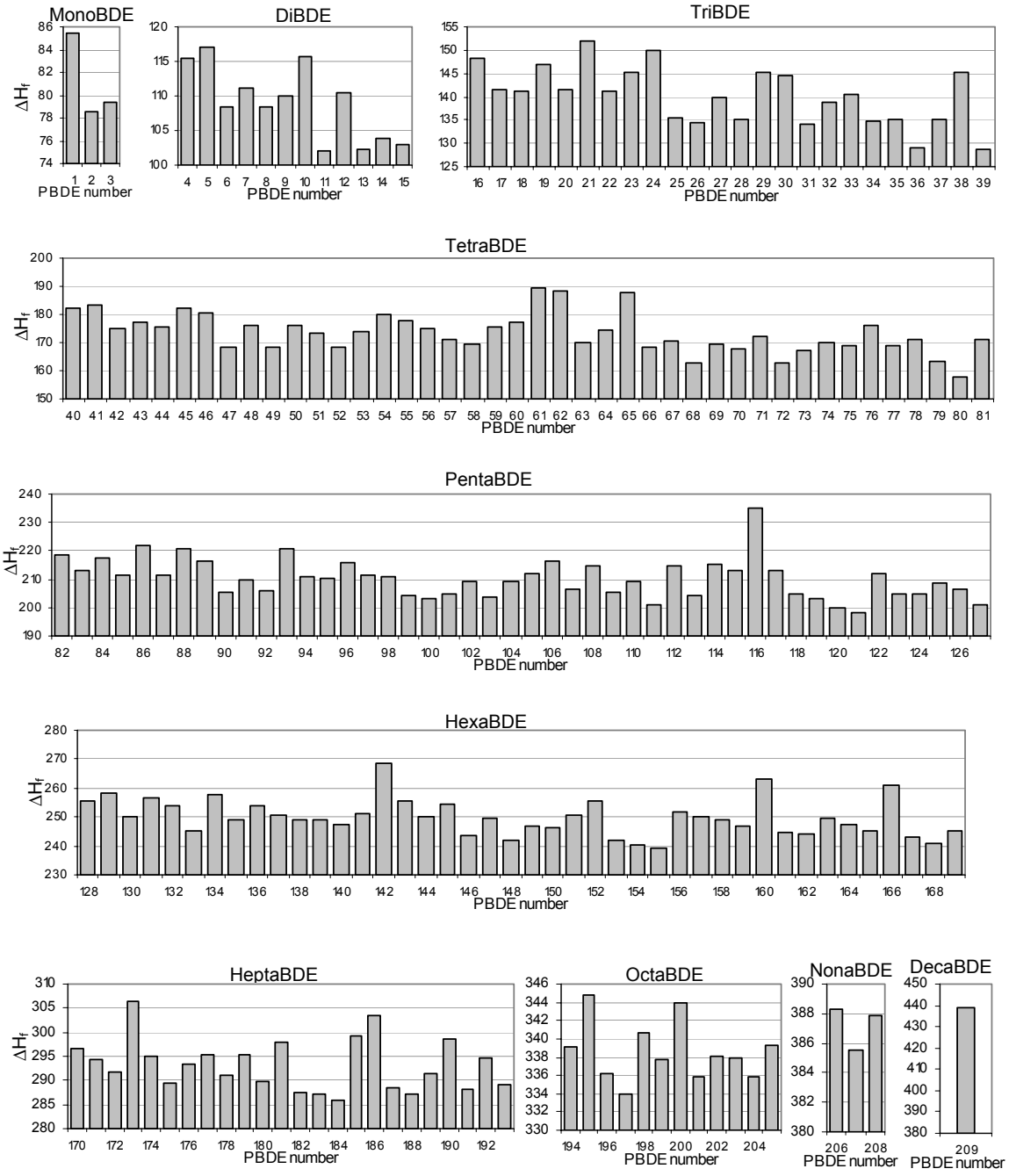

Figure 3.1. Enthalpy of formation of 209 PBDEs calculated using the GAM model (*11*).

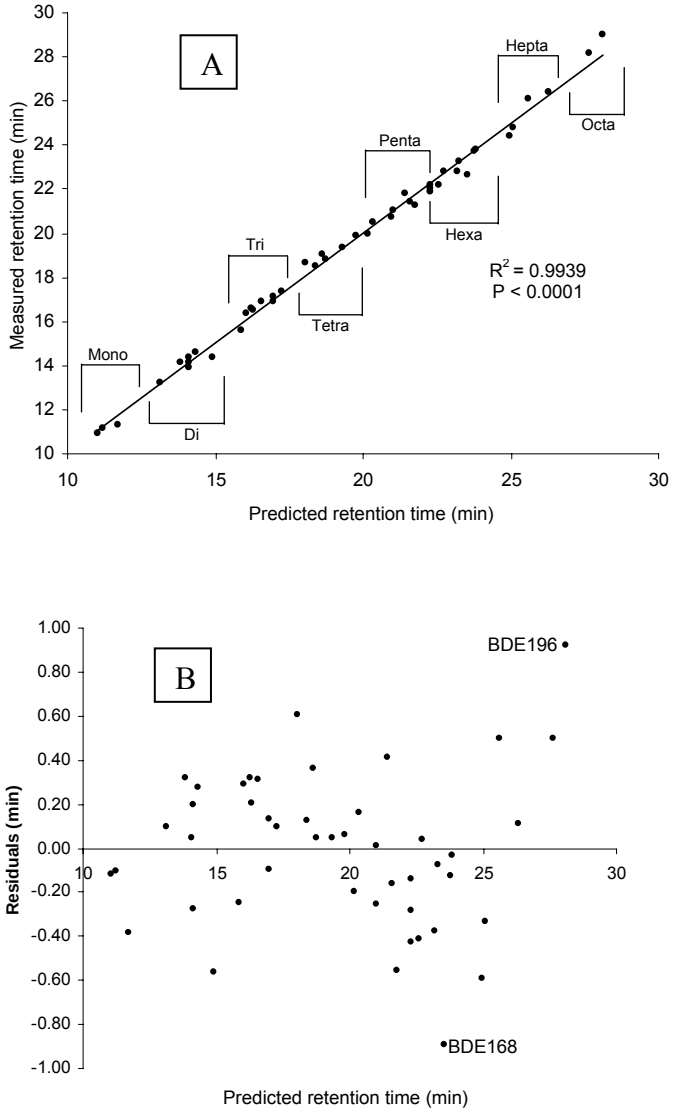

Figure 3.2. Correlation between measured and predicted GC retention time (A) and plot of residuals (B).

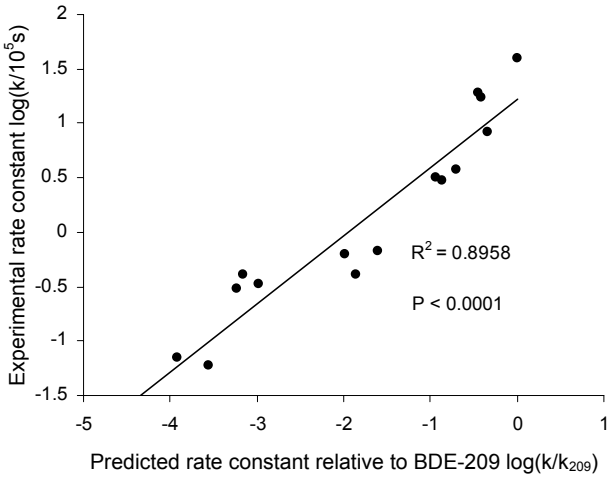

Figure 3.3. Correlation between predicted photodegradation rates (relative to BDE-209) and experimental rates(*9*).

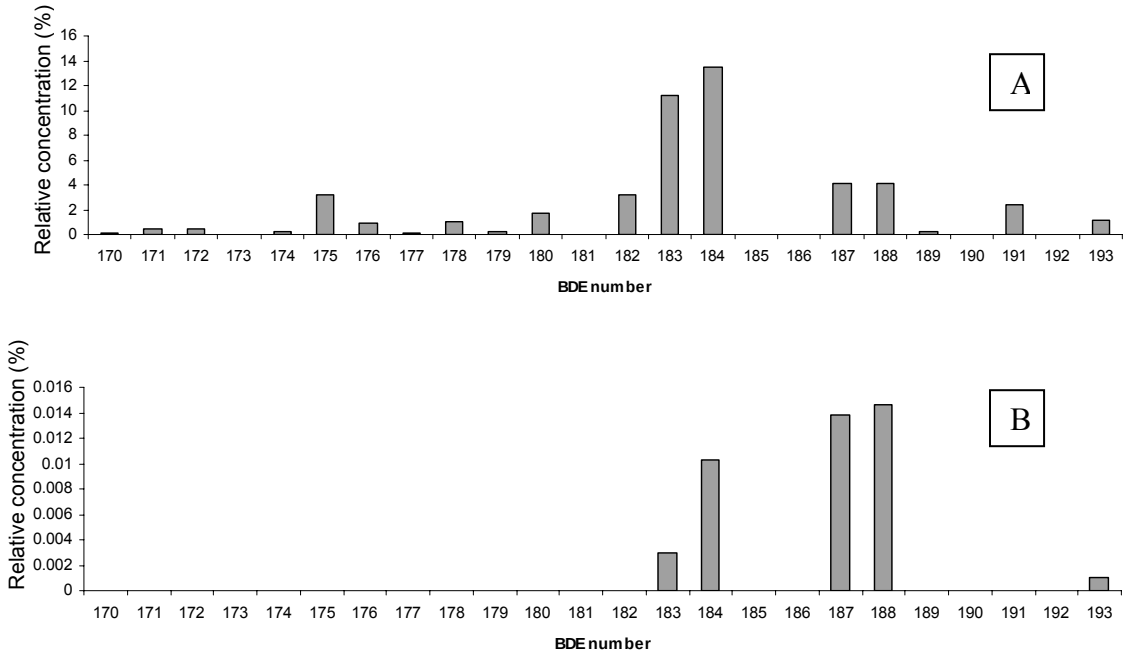

Figure 3.4. Predicted hepta-BDE products from BDE-209 photodegradation in methanol/water (80/20) and UV light. A is the product profile at 1.67×10^3min reaction time and B is the product profile at 2.3×10^4min. The concentrations are relative to the total BDE concentration.

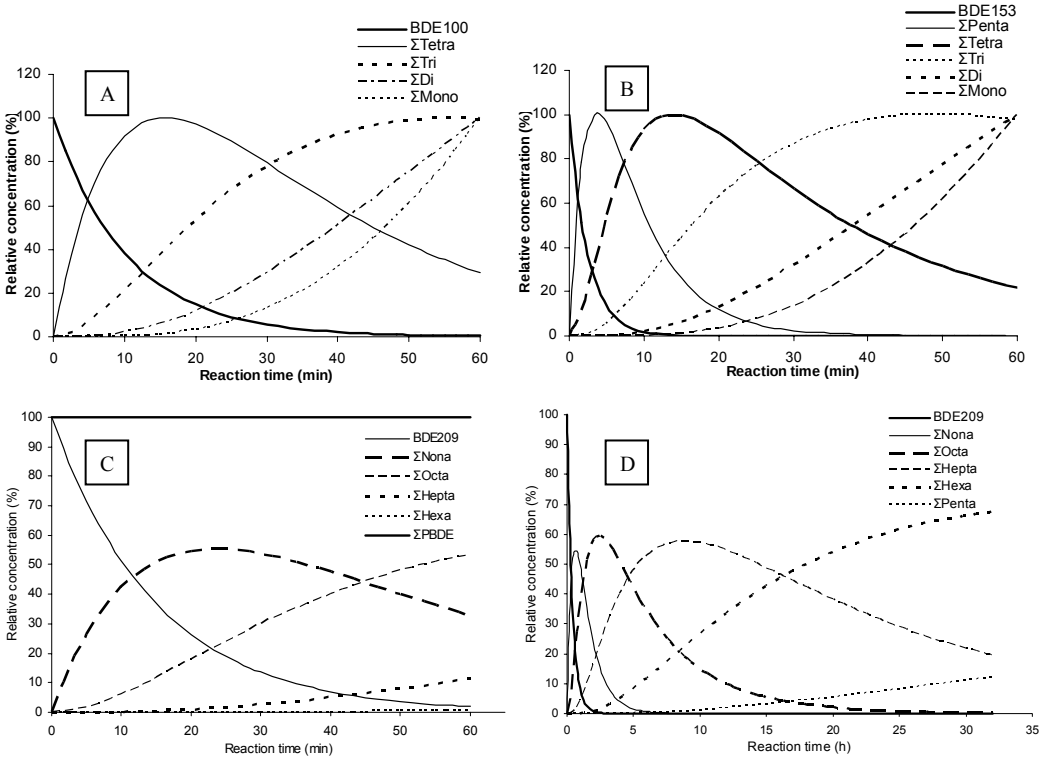

Figure 3.5. Predicted PBDE photodegradation time profiles. A and B are the predicted photodegradation of BDE-100 and BDE-153, respectively, after SPME fiber exposure to sunlight simulated irradiation normalized to the maximum concentration of each homologous group (*13*). C is the predicted solar photodecomposition of BDE-209 in hexane relative to total PBDE concentration (*10*). D is the predicted photodegradation of BDE-209 on silica gel under UV-light relative to total PBDE concentration (*12*).

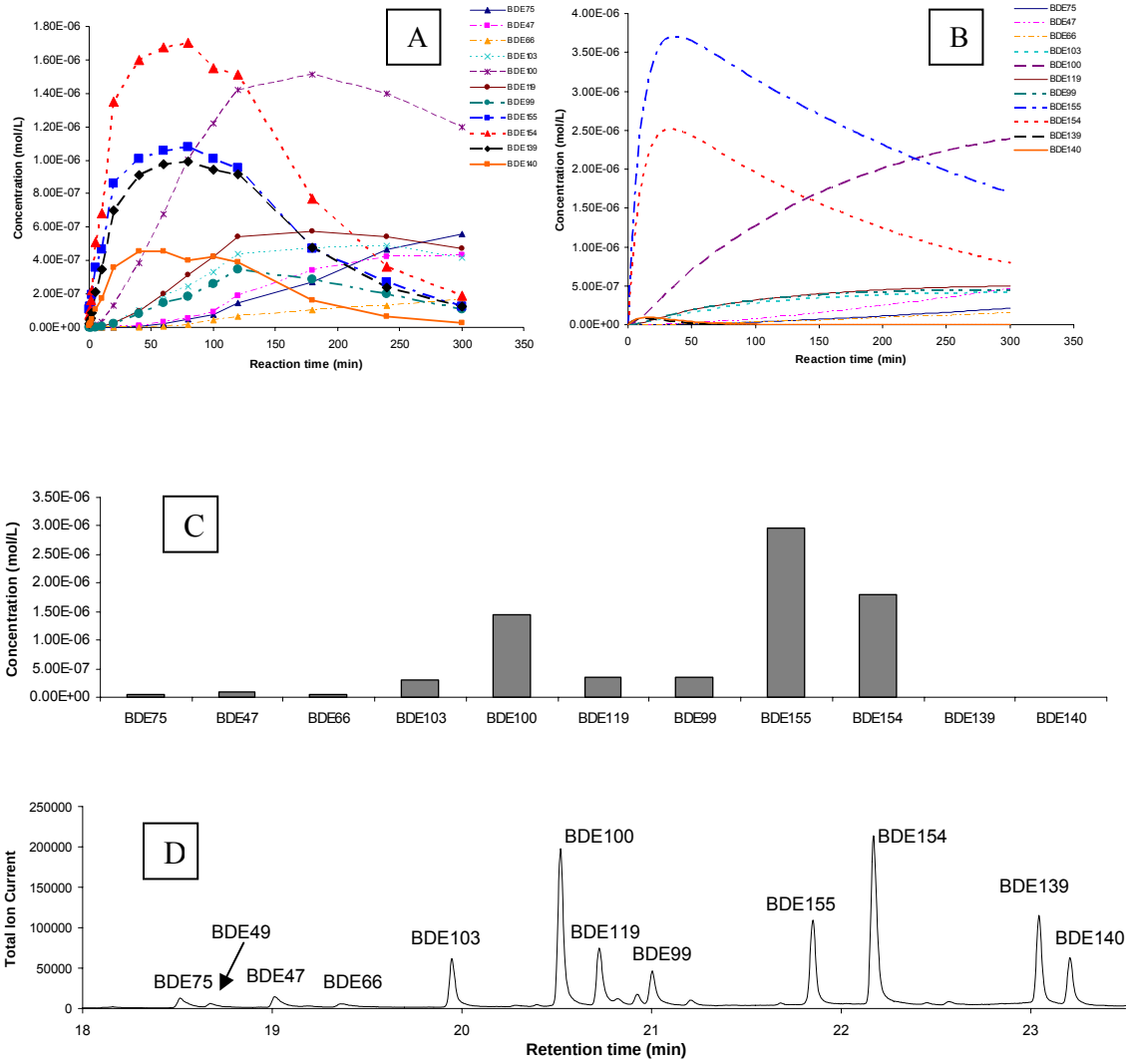

Figure 3.6. Photodegradation of BDE-184 in isooctane under UV. A is the experimental results and B is the model prediction. C is the model prediction and D is experimental results of BDE-184 photodegradation at 120 min.

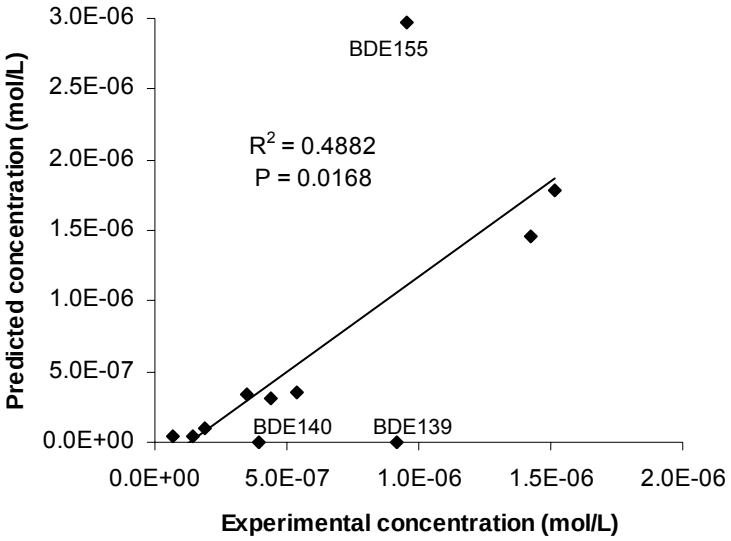

Figure 3.7. Correlation between experimental concentration and model predicted concentration for BDE-184 photodegradation products at 120 min.

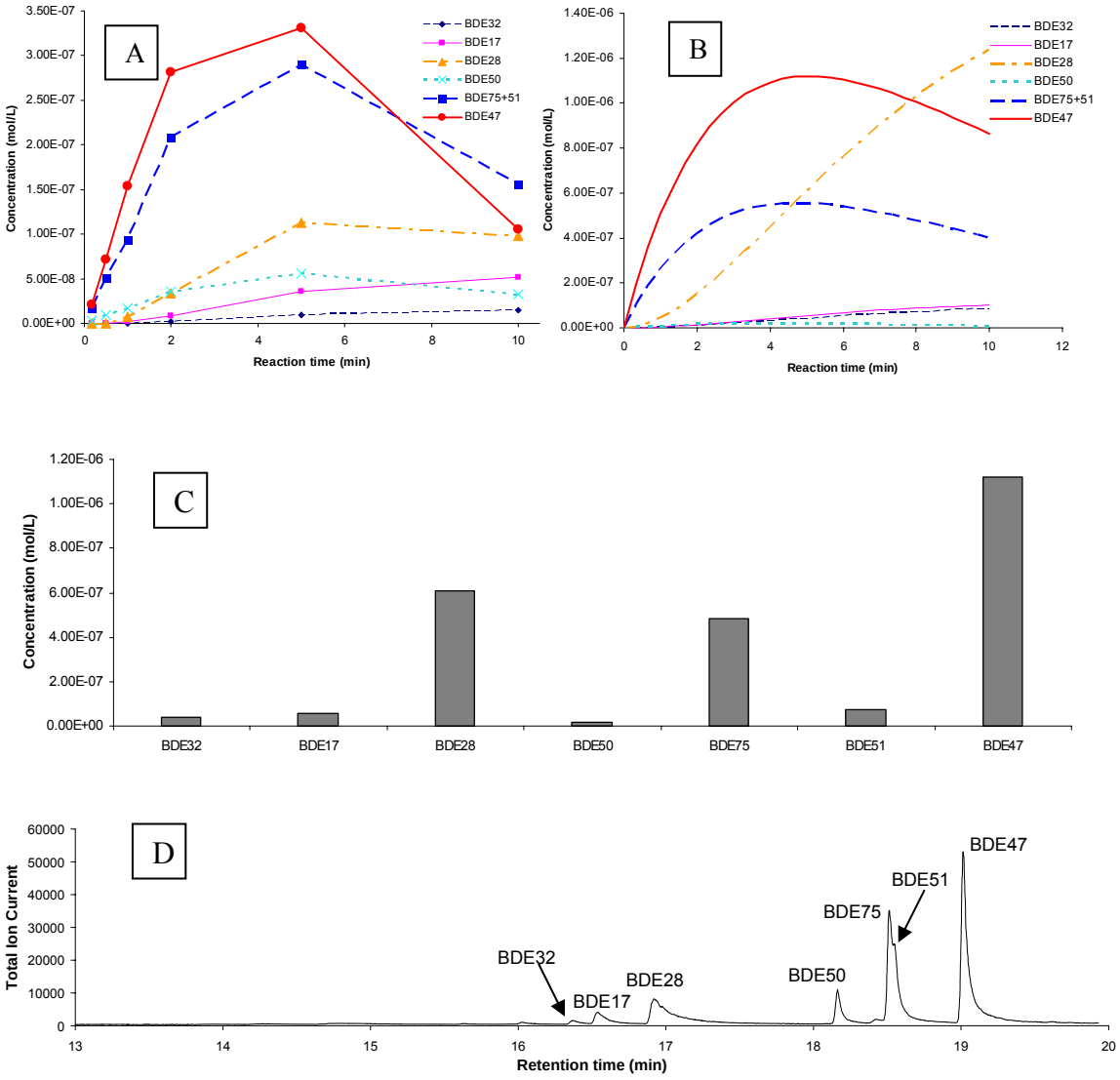

Figure 3.8. Photodegradation of BDE-100 in isooctane under UV. A is the experimental results and B is the model prediction for BDE-100. C is the model prediction and D is experimental results of BDE-100 photodegradation at 5 min.

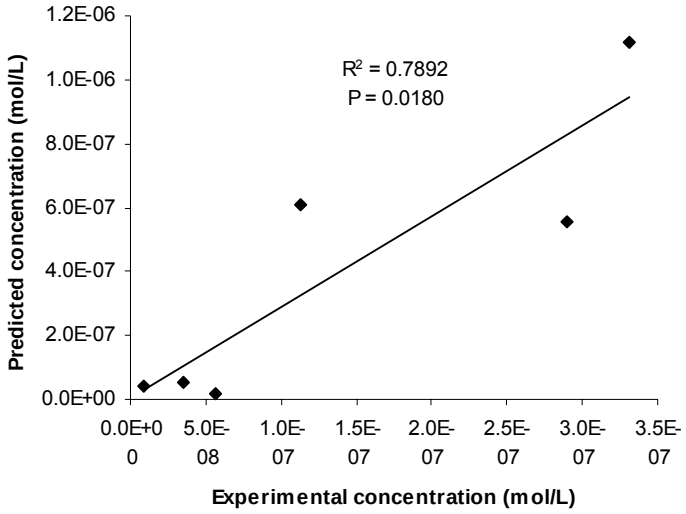

Figure 3.9. Correlation between experimental result and model simulation for BDE-100 photodegradation products at 5 min.

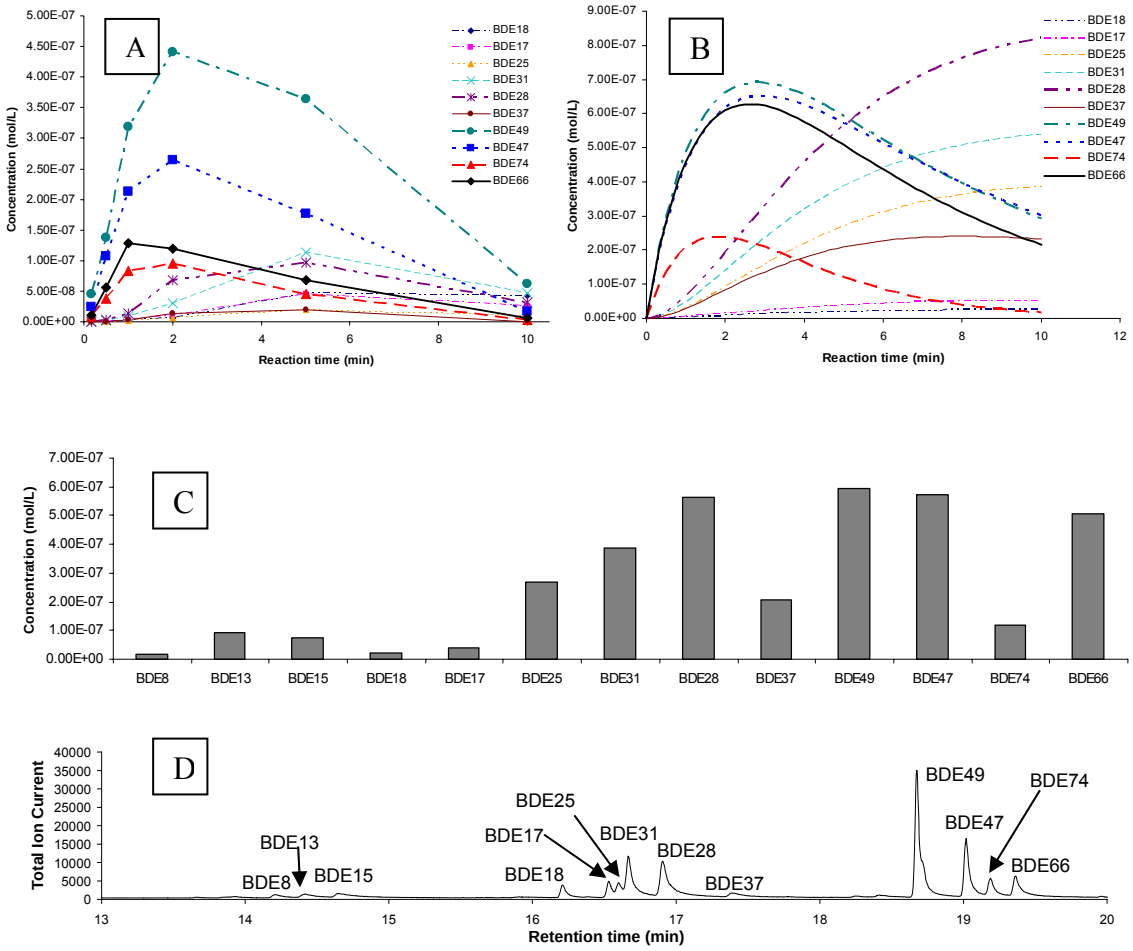

Figure 3.10. Photodegradation of BDE-99 in isooctane under UV. A is the experimental results and B is the model prediction for BDE-99. C is the model prediction and D is experimental results of BDE-99 photodegradation at 5 min.

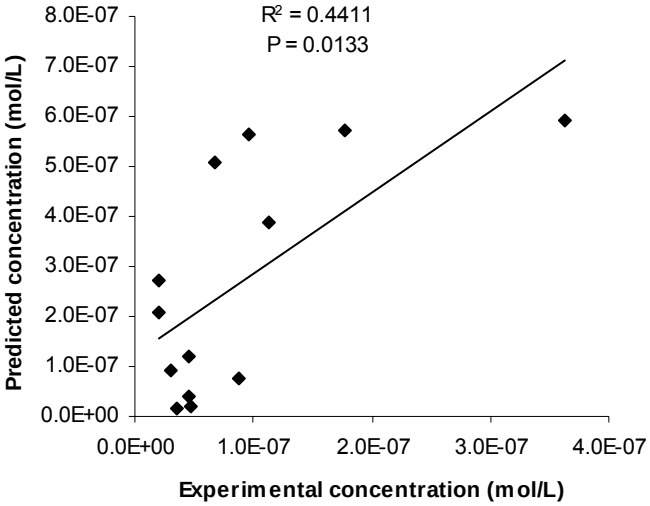

Figure 3.11. Correlation between experimental result and model simulation for BDE-99 photodegradation products at 5 min.

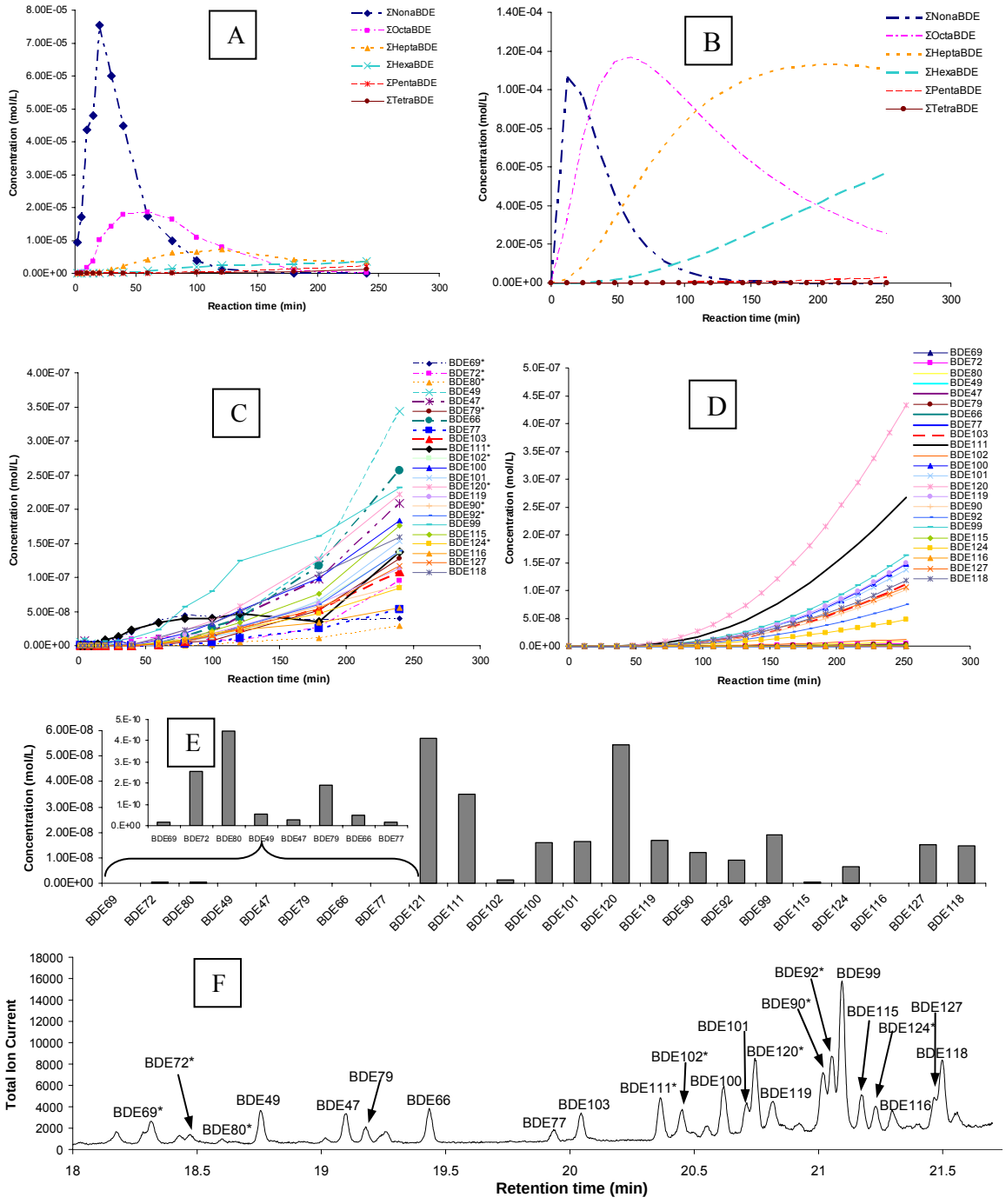

Figure 3.12. Photodegradation of BDE-209 in isooctane under UV. A is the experimental results and B is the model prediction by homologous groups. C is the experimental results and B is the model prediction by congener for penta-BDE and tetra-BDE products. E is the model prediction and F is experimental results of BDE-209 photodegradation at 120 min. "*" represents PBDE congeners not identified by standards.

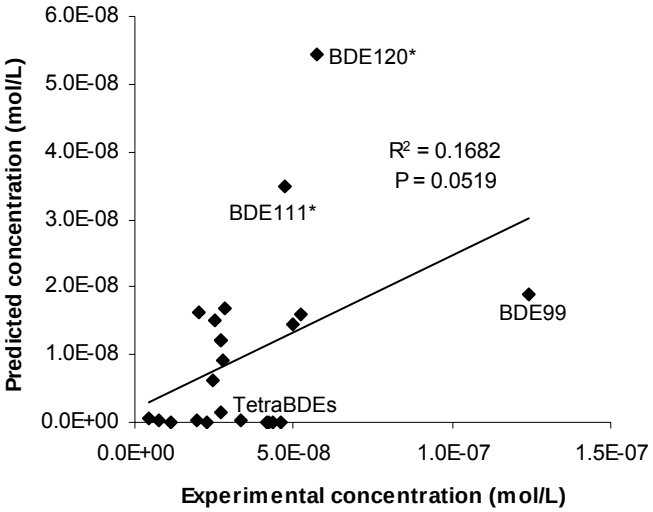

Figure 3.13. Correlation between experimental result and model simulation for tetra-BDEs and penta-BDEs in BDE-209 photodegradation products at 120 min.

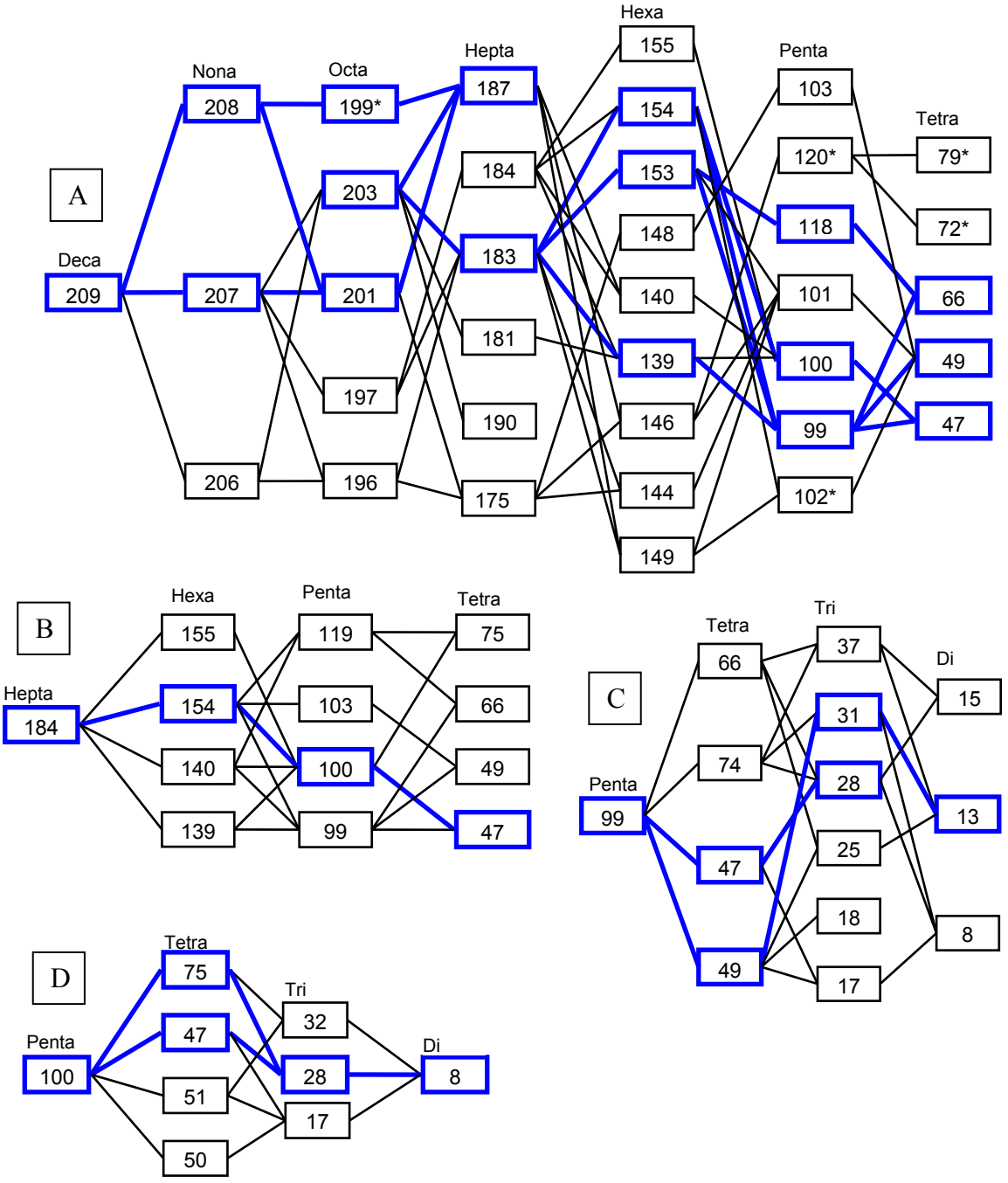

Figure 3.14. Reaction pathways of BDE-209, BDE-184, BDE-99 and BDE-100 photodegradation. The thicker lines pass through those photodegradation products with higher concentrations. Only major BDE-209 pathways are shown. "*" represents PBDE congeners not confirmed by standards.

Table 3.1. Experimental and multiple linear fit GC retention times for PBDE congeners

PBDE number	Retention time exp (min)	Retention time fit (min)	Residual	PBDE number	Retention time exp (min)	Retention time fit (min)	Residual
BDE-1	10.92	11.04	-0.12	BDE-153	22.83	23.20	-0.37
BDE-2	11.12	11.22	-0.10	BDE-154	22.18	22.59	-0.41
BDE-3	11.32	11.70	-0.38	BDE-155	21.87	22.29	-0.42
BDE-7	13.87	14.14	-0.27	BDE-166	23.82	23.85	-0.03
BDE-8	14.15	14.10	0.05	BDE-168	22.67	23.56	-0.89
BDE-10	13.25	13.15	0.10	BDE-181	26.13	25.63	0.50
BDE-11	14.15	13.83	0.32	BDE-183	24.77	25.10	-0.33
BDE-12	14.33	14.89	-0.56	BDE-184	24.38	24.97	-0.59
BDE-13	14.33	14.14	0.19	BDE-190	26.43	26.32	0.11
BDE-15	14.62	14.35	0.27	BDE-196	29.03	28.11	0.92
BDE-17	16.52	16.32	0.20	BDE-197	28.15	27.65	0.50
BDE-25	16.58	16.26	0.32				
BDE-28	16.88	16.57	0.31				
BDE-30	15.62	15.87	-0.25				
BDE-32	16.35	16.06	0.29				
BDE-33	16.88	16.98	-0.10				
BDE-35	17.12	16.99	0.13				
BDE-37	17.37	17.27	0.10				
BDE-47	19.02	18.66	0.36				
BDE-49	18.67	18.06	0.61				
BDE-66	19.37	19.32	0.05				
BDE-71	18.78	18.73	0.05				
BDE-75	18.52	18.39	0.13				
BDE-77	19.87	19.81	0.06				
BDE-85	21.83	21.42	0.41				
BDE-99	21.02	21.01	0.01				
BDE-100	20.53	20.37	0.16				
BDE-116	21.23	21.78	-0.55				
BDE-118	21.42	21.58	-0.16				
BDE-119	20.73	20.98	-0.25				
BDE-121	20.00	20.20	-0.20				
BDE-126	22.02	22.30	-0.28				
BDE-138	23.68	23.81	-0.13				
BDE-140	23.22	23.30	-0.08				
BDE-146	22.78	22.74	0.04				
BDE-148	22.17	22.31	-0.14				

Table 3.2. Calculated reaction rate constants relative to BDE-209 for all the 209 PBDEs

PBDE Number	relative $\sum k$	PBDE Number	relative $\sum k$	PBDE Number	relative $\sum k$	PBDE Number	relative $\sum k$	PBDE Number	relative $\sum k$
BDE1	9.25E-06	BDE44	1.26E-03	BDE87	7.34E-03	BDE130	1.62E-02	BDE173	1.46E-01
BDE2	5.80E-07	BDE45	1.58E-03	BDE88	1.04E-02	BDE131	1.97E-02	BDE174	5.15E-02
BDE3	7.98E-07	BDE46	1.36E-03	BDE89	7.00E-03	BDE132	1.40E-02	BDE175	3.65E-02
BDE4	3.03E-05	BDE47	1.23E-04	BDE90	2.77E-03	BDE133	1.10E-02	BDE176	3.14E-02
BDE5	4.79E-04	BDE48	4.05E-04	BDE91	1.87E-03	BDE134	1.66E-02	BDE177	3.46E-02
BDE6	1.47E-05	BDE49	1.35E-04	BDE92	3.70E-03	BDE135	9.47E-03	BDE178	3.01E-02
BDE7	3.46E-05	BDE50	2.27E-04	BDE93	8.90E-03	BDE136	7.69E-03	BDE179	2.80E-02
BDE8	1.10E-05	BDE51	1.49E-04	BDE94	3.95E-03	BDE137	2.66E-02	BDE180	4.56E-02
BDE9	2.88E-05	BDE52	1.43E-04	BDE95	2.48E-03	BDE138	1.03E-02	BDE181	1.16E-01
BDE10	3.35E-05	BDE53	1.59E-04	BDE96	2.65E-03	BDE139	1.39E-02	BDE182	3.84E-02
BDE11	2.18E-06	BDE54	1.80E-04	BDE97	1.95E-03	BDE140	9.07E-03	BDE183	2.48E-02
BDE12	5.63E-05	BDE55	4.67E-03	BDE98	1.72E-03	BDE141	3.27E-02	BDE184	2.17E-02
BDE13	2.12E-06	BDE56	9.42E-04	BDE99	5.94E-04	BDE142	8.47E-02	BDE185	1.43E-01
BDE14	4.60E-06	BDE57	2.21E-03	BDE100	3.19E-04	BDE143	2.88E-02	BDE186	1.24E-01
BDE15	2.27E-06	BDE58	1.13E-03	BDE101	6.94E-04	BDE144	1.77E-02	BDE187	1.72E-02
BDE16	8.05E-04	BDE59	1.46E-03	BDE102	6.31E-04	BDE145	1.63E-02	BDE188	1.71E-02
BDE17	7.17E-05	BDE60	3.63E-03	BDE103	3.85E-04	BDE146	5.07E-03	BDE189	5.93E-02
BDE18	6.98E-05	BDE61	1.40E-02	BDE104	4.20E-04	BDE147	1.03E-02	BDE190	1.40E-01
BDE19	7.98E-05	BDE62	6.76E-03	BDE105	6.30E-03	BDE148	4.74E-03	BDE191	3.17E-02
BDE20	7.31E-04	BDE63	1.63E-03	BDE106	2.30E-02	BDE149	3.56E-03	BDE192	1.69E-01
BDE21	2.82E-03	BDE64	1.07E-03	BDE107	7.85E-03	BDE150	3.31E-03	BDE193	2.06E-02
BDE22	5.37E-04	BDE65	5.45E-03	BDE108	1.14E-02	BDE151	1.38E-02	BDE194	1.49E-01
BDE23	1.44E-03	BDE66	1.63E-04	BDE109	2.72E-03	BDE152	1.46E-02	BDE195	2.23E-01
BDE24	9.49E-04	BDE67	4.45E-04	BDE110	1.82E-03	BDE153	1.64E-03	BDE196	1.05E-01
BDE25	5.33E-05	BDE68	8.87E-05	BDE111	3.42E-03	BDE154	1.04E-03	BDE197	7.23E-02
BDE26	4.55E-05	BDE69	1.90E-04	BDE112	8.43E-03	BDE155	7.09E-04	BDE198	2.54E-01
BDE27	5.16E-05	BDE70	1.71E-04	BDE113	2.26E-03	BDE156	3.18E-02	BDE199	1.04E-01
BDE28	3.99E-05	BDE71	1.47E-04	BDE114	1.90E-02	BDE157	1.44E-02	BDE200	2.16E-01
BDE29	2.75E-04	BDE72	8.00E-05	BDE115	9.01E-03	BDE158	1.57E-02	BDE201	7.14E-02
BDE30	1.25E-04	BDE73	8.58E-05	BDE116	5.92E-02	BDE159	3.82E-02	BDE202	6.84E-02
BDE31	3.36E-05	BDE74	3.70E-04	BDE117	6.24E-03	BDE160	9.95E-02	BDE203	2.00E-01
BDE32	3.75E-05	BDE75	1.41E-04	BDE118	7.79E-04	BDE161	1.96E-02	BDE204	1.69E-01
BDE33	8.63E-05	BDE76	1.76E-03	BDE119	3.47E-04	BDE162	8.32E-03	BDE205	2.47E-01
BDE34	2.77E-05	BDE77	2.79E-04	BDE120	7.40E-04	BDE163	1.00E-02	BDE206	4.51E-01
BDE35	9.63E-05	BDE78	2.40E-03	BDE121	2.98E-04	BDE164	5.81E-03	BDE207	3.51E-01
BDE36	1.07E-05	BDE79	1.74E-04	BDE122	4.02E-03	BDE165	1.31E-02	BDE208	3.97E-01
BDE37	8.46E-05	BDE80	3.25E-05	BDE123	2.59E-03	BDE166	8.18E-02	BDE209	1.00E+00
BDE38	1.52E-03	BDE81	2.19E-03	BDE124	2.84E-03	BDE167	4.98E-03		
BDE39	8.95E-06	BDE82	8.60E-03	BDE125	2.09E-03	BDE168	3.23E-03		
BDE40	2.38E-03	BDE83	5.40E-03	BDE126	3.69E-03	BDE169	1.10E-02		
BDE41	4.43E-03	BDE84	4.30E-03	BDE127	3.83E-03	BDE170	6.03E-02		
BDE42	9.55E-04	BDE85	5.71E-03	BDE128	1.89E-02	BDE171	3.82E-02		
BDE43	2.38E-03	BDE86	1.98E-02	BDE129	3.46E-02	BDE172	6.06E-02		

CHAPTER 4. APPLICATION OF A CONGENER SPECIFIC DEGRADATION MODEL TO STUDY PHOTODEGRADATION, ANAEROBIC BIODEGRADATION, AND Fe^0 REDUCTION OF PBDES

Xia Zeng[†], *Staci L. Simonich*[†‡*], *Douglas F. Barofsky*[†]

[†]Department of Chemistry, Oregon State University, Corvallis, OR 97331, USA;

[‡]Department of Environmental and Molecular Toxicology, Oregon State University, Corvallis, OR 97331, USA

*Corresponding author. Telephone: (541) 737-9194. Fax: (541) 737-2062. Email: staci.simonich@orst.edu

Abstract

A previously developed photodegradation model was used to predict the photodegradation of octa-polybrominated diphenyl ether (PBDE) technical mixture, and results were compared to the photodegradation experiments. The predicted reaction time profiles of the photodegradation products correlate very well with the experimental results. In addition, the slope of the linear regression between the measured product concentrations of first step debromination products and their enthalpies of formation was found to be close to the theoretical value. In the present work, the octa-BDE technical mixture photodegradation results were compared with anaerobic biodegradation results. The major products measured in the biodegradation experiments were also measured as major products in the photodegradation experiments. The photodegradation pathways of technical octa-BDE mixture are summarized. BDE-154, 99, 47 and 31 were found to be the most abundant hexa, penta, tetra and tri-BDE photodegradation products, respectively. These photodegradation products may become the most abundant products in their homologous groups when octa-BDE mixture degrades in the environment. The photodegradation and model prediction results were also compared with zero-valent iron treated reduction of BDE-209, 100 and 47 from a previous study and the same products were found in photo and Fe^0 degradation. Good correlation between 15 previous reported photodegradation rate constants of PBDE congeners and their calculated LUMO energies was found, indicating that, similar to the Fe^0 treated reduction, debromination by UV light is caused by electron transfer. Furthermore, the rate constants for the three different degradation processes are controlled by C-Br bond dissociation energy.

Introduction

As the major flame retardants used by volume, the environmental fate of polybrominated diphenyl ethers (PBDEs) has been studied extensively since the use of pentaBDE and octaBDE was banned in Europe and voluntarily phased out in the U.S. in 2004. However, because of the large quantity of the PBDEs previously used and released into the environment, their concentrations in the environment and human body continues to increase (*1*,*2*).

Several biotic and abiotic transformation reactions of PBDEs, and other brominated flame retardants, have been studied. Among them, photodegradation is one of the major abiotic transformations in the environment (*3*). Investigations into the photodegradation of PBDEs by both artificial and natural sunlight have been reported (*4*-*7*).

Halogenated aromatics have shown to biodegrade under aerobic conditions through the processes of hydroxylation, methoxylation, and aromatic ring cleavage (*8*-*10*), which may result in the formation of toxic halogenated aliphatic metabolites. In contrast, anaerobic biodegradation may only remove the halogen substituents, forming less hydrophobic compounds, and, eventually, complete mineralization (*11*). Octa-BDE technical mixture, which was widely used and classified as a teratogen (*12*), was reported to undergo stepwise debromination in *Dehalococcoides*-containing cultures and produce more toxic BDE-154, BDE-99, BDE-49 and BDE-47 (*13*). BDE-209, which is still used in large volume throughout the world, was also reported to biodegrade anaerobically to lower brominated diphenyl ethers in sewage sludge (*14*,*15*) and *Sulfurospirillum multivorans* culture (*13*).

A recent study reported that both photodegradation and anaerobic biodegradation of BDE-15 (4,4'-diBDE) followed the same degradation pathway and produced BDE-3 (4-monoBDE) and diphenyl ether in a stepwise manner (*11*). Neither rearrangement of Br nor C-O bond cleavage were found in the above reactions. This suggests that PBDE anaerobic biodegradation and photodegradation share the same reaction mechanism.

Zero-valent iron metal (Fe^0) has been studied for remediation of polyhalogenated organic compounds such as tetrachloromethane, 1,1,1-tricholoethane and tetrachloroethene, and the first order reaction rates were found (*16*). To explain the kinetics of dehalogenation and predict the rate constants, correlation analysis was used to predict the reactivity of a series of structurally related compounds. A linear correlation between the rate constants for Fe^0 dehalogenation and the LUMO energies has been reported for PBDEs (*17*) and other halogenated compounds (*18*).

The three different PBDEs degradation processes, namely anaerobic biodegradation, photodegradation, and Fe^0 reduction, have been recently studied, and first order, stepwise debromination reactions as well as the same degradation products were reported (*4,15,17*). This may indicate that the reaction mechanisms are similar. If this is true, a general model can be established to explain and predict these reactions. We have previously developed a theoretical model to predict the photodegradation of PBDEs based on the difference in bromine dissociation energies between PBDE congeners. The model was proved to be predictive for the photodegradation of PBDEs (see Chapter Three). Theoretically, it should be predictive for anaerobic biodegradation and Fe^0 reduction of PBDEs.

In order to test this possibility, we conducted detailed studies to compare different types of PBDE degradation processes. The PBDE congeners studied were the major ingredients of the octa-BDE technical mixture, i.e. BDE-196, 203, 197 and 153. The photodegradation of BDE-183 was not studied because of the lack of the BDE-183 pure standard. In addition, BDE-99 and 47, two of the most frequently detected congeners in the environment, were included in this study. The model predicted products, their concentrations, and the reactant degradation rate constants were also compared to the experimental results. In addition, the photodegradation of the octa-BDE technical mixture was studied and compared with results of anaerobic biodegradation experiments and model predictions. Using the photodegradation model, the relationship between the degradation rates and the LUMO energies of the PBDEs was explored.

Experimental

Materials

A standard mixture of 39 PBDEs was obtained from Cambridge Isotope (*19*). Individual standards of BDE-47, 99, 100, 121, 140, 146, 148, 153, 168, 184, 196, 197, 203, 206, 207, and 208 were purchased from AccuStandard. BDE-209, and octa-BDE technical mixture was purchased from Sigma Aldrich. The additional 126 PBDE standard used to identify the PBDE degradation products was provided by Peter Korytár (*20*).

Methods

UV Photodegradation studies were conducted using a Rayonet RPR-100 photochemical reactor with RMR-2537A (250nm) UV lamps purchased from Southern New England Ultra Violet Company. PBDE congeners were dissolved in isooctane, and these solutions

were irradiated in sealed quartz vials. The irradiated samples were collected at different time intervals and analyzed using a JEOL GC mate II GC-HRMS in electron capture negative ionization (ECNI) mode. The GC column was a 30m J&W DB-5 column (0.25mm I.D. and 0.25μm film thickness), and the GC temperature program was: 100ºC (hold for 1 min); 10ºC/min to 320ºC (hold for 27 min). The temperatures of the splitless injector, GC interface, and ion source were 280ºC, 250ºC, and 250ºC, respectively. The PBDE congeners were quantified using external calibration. PBDE congeners without available standards were quantified using the average ECNI response of the homologous PBDE group.

Using multiple linear regression analysis, a GC retention time model was built (see Chapter Three) to predict the GC retention time of the photodegradation products. All of the molecular descriptors, including the highest occupied molecular orbital (HOMO) energy and the lowest unoccupied molecular orbital (LUMO) energy, except for ln(MW), were obtained using Gaussian 03 on the B3LYP/6-31G(d)//B3LYP/6-31G(d) level.

Anaerobic biodegradation experiments of BDE-196, 203, 197, 183, 153, 99 and 47 were conducted at UC-Berkley. The microbial cultures used included: a trichloroethylene-dechlorinating enrichment culture containing multiple *Dehalococcoides* strains designated ANAS that was mixed in a 1:10 ratio with *D. ethenogenes* 195 (*Bomb195*), a tetrachloroethene to dichloroethene dechlorinating bacterium *Dehalobacter restrictus* PER-K23 (*Restrictus*), and a pentachlorophenol (PCP) degrading bacterium *Desulfitobacterium hafniense* PCP-1 (*Frappieri*). All cultures were grown in 160-mL serum bottles filled with 100-mL medium and sealed with blue butyl rubber septa, In

addition, the headspace of the bottles was filled with H_2/CO_2 (80:20 v/v) to ensure robust anaerobic environment. All samples and controls were incubated at 30°C in the dark without shaking. Experiments were conducted with triplicate biological samples and were repeated to confirm the results. PBDE congeners were detected using two-dimensional chromatography at the Wageningen IMARES laboratories in IJmuiden, Netherlands. An Agilent 6890 Gas Chromatograph equipped with an Electron Capture Detector (GC-ECD) and a loop-type carbon dioxide jet was employed for analysis.

The PBDE degradation model has been previously described (see Chapter Three). The same model was used to compare with photodegradation and biodegradation. The model predicted reaction rate constant (relative to BDE-209) was also used to compare with the Fe^0 treated degradation rate constant of PBDEs. For the degradation of the octa-BDE technical mixture, individual degradation models were developed for each BDE congener in the technical mixture, and the individual models were summed.

Results

Photodegradation of the individual octa-BDE technical mixture components

The time profile of both experimental and model prediction results for photodegradation of BDE-47, 153, 196, 197, and 203 is shown in Figure 4.1. The correlations between the experimental results and model predictions are shown in Figure 4.2.

The photodegradation of BDE-47 produced two tri-BDEs, BDE-28 and BDE-17 (Figure 4.1A), which confirmed the model prediction (Figure 4.1B). Both the model and the experimental result showed that BDE-28, an ortho debromination product of BDE-47,

has higher concentration than BDE-17, a para debromination product of BDE-47, indicating that the ortho bromine of BDE-47 is less stable and more liable to loss under UV light than para bromine of BDE-47. This is consistent with our previous study where we determined that on the same aromatic ring of a diphenyl ether system, bromine on the ortho position was 6.86 kJ/mol lower in energy than the para position (*21*). The experimental result indicated that BDE-28 reached its maximum concentration at 2.5 min reaction time (Figure 4.1A), while the model predicted at 3.7 min (Figure 4.1B). This inconsistency is also shown in Figure 4.2A, where the plot between experimental results and model predictions for BDE-47 resulted in a folded line instead of a straight line (Figure 4.2A). The slope of the linear regression between the predicted and experimental results for BDE-17 was much lower than for BDE-28 (Figure 4.2A), indicating that BDE-17 concentration was underestimated relative to BDE-28. No mono-BDEs were detected in this experiment. This is likely due to the lack of ECNI sensitivity and the loss of total PBDE mass (see Chapter Three).

BDE-153, the only penta-BDE in the octa-BDE technical mixture, was also shown to degrade under UV light. Our experimental results indicated that the three penta-BDE products from BDE-153 photodegradation were BDE-101, 99 and 118 and the most abundant tetra-BDE product was BDE-49 (Figure 4.1C), followed by two other tetra-BDE congeners, which were identified as BDE-70 and BDE-52 using the GC retention time model. The experimental results are consistent with the photodegradation model (Figure 4.1D), and the concentration of penta-BDE products reached their maximum at about 2 min in both cases. The slopes for the least-squares regression of the predicted

product concentrations and experimental results were similar for the different products of BDE-153 photodegradation (Figure 4.2C). The correlations were statistically significant for all of the photodegradation products except BDE-49. This is because the model predicted the concentration of BDE-49 to peak at 10 min (Figure 4.1D), while the experiment results showed a peak in concentration at 5 min (Figure 4.1C).

BDE-182 and 183 were found to be the most abundant hepta-BDE products from the photodegradation of BDE-196, both from the experimental results (Figure 4.1E) and the model prediction (Figure 4.1F). Both the model prediction and the experimental showed that BDE-154 and 153 were the most abundant hexa-BDE products of BDE-196 photodegradation. The predicted time profile from model matched the experimental results very well, and, the correlations between them were all statistically significant for all the major photodegradation products (Figure 4.2D).

The experimentally determined product time profile for the photodegradation of BDE-197 (Figure 4.1G) was also predicted by the photodegradation model (Figure 4.1H). BDE-184 and 183 were predicted to be the most abundant hepta-BDE products and this was confirmed by the experimental results. However, BDE-176, which was predicted by the model to be much lower in concentration than BDE-184 (Figure 4.1H), was detected with comparable concentration to BDE-184 (Figure 4.1G). This is also shown in the correlation between the experimental and the predicted product concentrations (Figure 4.2E), where the linear regression slope of BDE-176 is much lower than the other BDE-197 photodegradation products.

In the photodegradation of BDE-203, the identities of BDE-187, 185 and 180 were assigned by the GC retention model and confirmed using the 126 PBDE standard (*20*) at UC-Berkley. Quantification of BDE-187, 185 and 180 was done using the average ECNI response of hepta-BDEs. BDE-180, 187 and 183 were predicted to be the most abundant products of BDE-203 photodegradation, and BDE-183 was predicted to have the highest concentration (Figure 4.1J). However, the experimental results showed that BDE-187 had the highest concentration, followed by BDE-183 (Figure 4.1I). This is also obvious in that the slope of BDE-187 correlation in Figure 4.2F is lower than that of BDE-183. The predicted times of maximum concentrations for BDE-187 and 183 were later than determined by experiment. Therefore, the curves for BDE-183 and BDE187 in Figure 4.2F were folded lines instead of straight ones.

Since the photodegradation of PBDEs is a first order reaction (*4*):

$$-\frac{d[h]}{dt} = k_h[h], \qquad (1)$$

and $$k_h = \sum_i \left(\alpha_{hi} k_h^i\right), \qquad (2)$$

in which $[h]$ is the concentration of the parent PBDE congener h, and k_h is the degradation rate constant for PBDE congener h, k_h^i is the rate constant for h degradation to i, and α_{hi} is the number of pathways for the degradation of h to i (see Chapter Three). The reduced amount of the reactant PBDE h is equal to the increased amount of the first step debromination products:

$$-d[h] = \sum_i d[i]. \qquad (3)$$

For each individual product, the increased amount can be obtained by:

$$\frac{d[i]}{dt} = \alpha_{hi} k_h^i [h]. \quad (4)$$

In the initial stage of the reaction, assuming [*h*] is constant, Eqn 4 becomes:

$$\Delta[i] = \alpha_{hi} k_h^i [h] \Delta t. \quad (5)$$

Since the starting concentrations of the PBDE products are 0 mol/L and starting time is 0 sec, Eqn 5 becomes:

$$[i] = \alpha_{hi} k_h^i [h] t, \quad (6)$$

and the natural logarithm format of Eqn 6 is:

$$\ln \frac{[i]}{\alpha_{hi}} = \ln k_h^i + \ln([h]t). \quad (7)$$

The difference in ΔH_f, between product *i* and *j* in exponential format is correlated to the ratio of their individual rate constant (see Chapter Three):

$$\frac{k_h^i}{k_h^j} = \exp\left(\frac{\Delta H_{fi} - \Delta H_{fj}}{-RT}\right). \quad (8)$$

natural logarithm format of both side is:

$$\ln k_h^i - \ln k_h^j = \frac{\Delta H_{fi} - \Delta H_{fj}}{-RT}, \quad (9)$$

therefore, for these first step debromination products, the slope of correlation between ln*k* and ΔH_f should be $-\frac{1}{RT}$. According to Eqn 7, $\ln \frac{[i]}{\alpha_{hi}}$ should also have a similar correlation with ΔH_f, i.e. the slope should also be $-\frac{1}{RT}$, which equals -0.4036 when the

gas constant R is 8.314 J/molK , reaction temperature T is 298K, and the unit for ΔH_f is kJ/mol.

In Figure 4.3, the correlation between $\ln\frac{[i]}{\alpha_{hi}}$ and ΔH_f was plotted for the first step debromination products of BDE-47, 99, 153, 196, 197 and 203 photodegradation. [i] are the concentrations measured in the photodegradation experiments. All of the slopes of the plots in Figure 4.3 were negative and ranged from -0.07 to -1.37, which, for kinetic data, are reasonably close to the theoretical value of -0.4036. This confirmed that the photodegradation of PBDEs is controlled by the enthalpy of formation and the model can describe the experiment well.

The major photodegradation pathways for BDE-47, 153, 196, 197 and 203 are summarized in Figure 4.4, and the pathway for BDE-99 was summarized in Chapter 3. The thicker lines pass through those photodegradation products with higher concentrations; these pathways are more probable than the rest. The relative abundances of photodegradation products were determined from the experimental results when the model prediction did not agree well with the experimental results. From the photodegradation of BDE-203, BDE-187 and 183 are the most abundant hepta-BDE products, BDE-153 is the most abundant hexa-BDE product, and BDE-101 is the most abundant penta-BDE product. From the photodegradation of BDE-197, BDE-184 and 183 are the most abundant hepta-BDE product, BDE-139 and 154 are the most abundant hexa-BDE products, and BDE-100 is the most penta-BDE product. BDE-183, BDE-154 and BDE-99 are the most abundant hepta-BDE, hexa-BDE and penta-BDE products, respectively, generated from BDE-196 photodegradation. BDE-101, BDE-49 and BDE-

31 are the most abundant hexa-BDE, penta-BDE and tetra-BDE products, respectively, generated from BDE-153 photodegradation. Photodegradation of BDE-47 has two tri-BDE products in which BDE-28 is the most abundant.

These parent PBDE congeners are major component of the octa-BDE technical mixture. By adding all of these photodegradation reactions together, the fate of the octa-BDE technical mixture under UV light can be estimated. However, a more accurate result can be obtained by studying the photodegradation of octa-BDE technical mixture itself.

Photodegradation of octa-BDE technical mixture and comparison to anaerobic biodegradation

The commercial octa-BDE mixture was dissolved in isooctane and irradiated under UV light. The reaction time profiles for the reactants and products are shown in Figure 4.5A for the experimental results and in Figure 4.5B for the model prediction. The model was based on the first order degradation rate constant of BDE-207 obtained from the experiment. BDE-154, BDE-99 and BDE-49 were found to be the most abundant hepta, hexa and tetra-BDE products, respectively, from both experiment and model prediction. The reaction time profiles for PBDE congeners by homologous group were shown in Figure 4.5C for experiment and in Figure 4.5D for model prediction. The cumulative experimental concentrations for BDE-154, 99, 49 and 47 were plotted in Figure 4.6A and compared with the model prediction in Figure 4.6C. Cumulative experimental concentrations by homologous group are also plotted in Figure 4.6B and the model predictions in Figure 4.6D. Due to the loss of mass, the experimental results showed that

the total concentration of PBDEs were much lower than the model prediction after 10 min reaction.

In a previous study, the anaerobic biodegradation of the octa-BDE technical mixture produced several lower brominated diphenyl ethers in which BDE-154 was the most abundant among the positively identified products (*13*). These results are shown in Figure 4.7 and are very similar to the photodegradation results in the early stage up to 5 min (Figure 4.6). Due to the nature of anaerobic biodegradation, the reactions were slow compared to photodegradation. In the photodegradation experiments, the concentrations of the hepta and hexa-BDEs started to decrease after 10 min of UV irradiation, while their concentrations were still increasing after 322 days in the anaerobic biodegradation experiment (*13*). The relative photodegradation product abundances at 5 min were very similar to that of the anaerobic biodegradation at 322 days, where the order of concentrations are BDE-154 > BDE-99 > BDE-49 > BDE-47 and hexa-BDE > hepta-BDE > penta-BDE > tetra-BDE for both degradation processes. This similarity between the photodegradation and anaerobic biodegradation products suggested that these degradation processes may share similar reaction mechanisms.

From the photodegradation of the octa-BDE technical mixture, the reaction pathways are summarized in Figure 4.8. BDE-154, which is the product of BDE-207, BDE-203, BDE-196, and BDE-183, is the most abundant hexa-BDE product. BDE-99, which is the product of BDE-154 and BDE-153, is the most abundant penta-BDE product. BDE-49 and BDE-31 are the most abundant tetra and tri-BDEs, respectively. All of these abundant PBDE congeners, except for BDE-31, were measured as products in the

anaerobic biodegradation experiments (*13*). These products are likely to become the most abundant products in their homologous groups when the octa-BDE technical mixture degrades in the environment.

Anaerobic Biodegradation of BDE-47, 99, 153, 183, 196, 197 and 203

The anaerobic biodegradation study was performed at UC-Berkley and, except for BDE-183, the biodegradation products are shown in the degradation pathways in Figure 4.4, together with the photodegradation products. Since the anaerobic biodegradation was much slower than the photodegradation, only the first step biodegradation products were measured in most cases. The products measured in the anaerobic biodegradation were also the major products measured in photodegradation.

The correlation between ΔH_f of the first step anaerobic biodegradation products and their ln(concentration/number of pathways) are shown in Figure 4.9. The product concentrations were recorded after 30 days and were relative to total PBDE concentration. Only one product (BDE-17) was measured in the anaerobic biodegradation of BDE-47 in cultures *Frappieri* and *Restrictus*. BDE-17, a para debromination product of BDE-47, and small amount of BDE-28, a ortho debromination product of BDE-47 were found in *Bomb195* from the biodegradation of BDE-47. These results were much different from the results of photodegradation of BDE-47 (Figure 4.3A), where BDE-28 was measure at higher abundance than BDE-17. The ortho position C-Br bond in BDE-47, which is easier to break than para C-Br bond in photodegradation, seems to be hard to break in anaerobic biodegradation, most likely due to the stereo effect in the ortho position. The slopes for the plots in Figure 4.9 for BDE-99, 153, 183, 196, 197 and 203, except for a

few cases, were all found to be negative and range from -0.0788 to -6.535, which is similar but greater than the range for photodegradation. This indicates that the anaerobic biodegradation rate may be controlled by the enthalpy of formation, but also affected by other factors, such as the type of bacteria and stereo effect.

Zero-valent iron reduction of PBDEs

The degradation of PBDEs with Fe^0 was previously studied with BDE-209, 100, 66, 47 28 and 7 (*17*). The results indicated stepwise accumulation of the lower brominated diphenyl ether congeners, which is similar to the photodegradation and anaerobic biodegradation. The products measured in Fe^0 degradation of BDE-209 were all detected in the photodegradation experiments described in Chapter Three, and most had the highest concentrations in the homologous PBDE groups (Figure 4.5A in Chapter Three). The reaction time profiles of the Fe^0 degradation products of BDE-209 were shown in Figure 4.10A. For comparison, the corresponding data for BDE-209 photodegradation were also plotted in Figure 4.10B. BDE-183 was not included in Figure 4.10B because it coeluted with BDE-175 in the photodegradation experiment. The reported Fe^0 degradation products of BDE-47, namely BDE-17 and 28, and the Fe0 degradation products of BDE-100, namely 47, 50, 51 and 75, were all measured in the photodegradation experiments.

The relative abundances of the products from Fe^0 degradation of BDE-100, 66, 47, 28 were also previously reported (*17*). The correlation between the natural logarithm of the Fe^0 degradation product relative abundance per reaction pathway and the ΔH_f of the corresponding degradation products are shown in Figure 4.11. Except for BDE-66, the

slopes for BDE-100, 47 and 28 degradation products were negative, and ranged from -0.087 to -0.2459, which are higher than the theoretical value -0.4036.

In our previous study, the relative photodegradation rate constants for all 209 PBDEs were calculated using the theoretical model (see Chapter 3 Table 2). These rate constants were found to have good correlation with the measured Fe^0 degradation rates for BDE-100, 66, 47, 28 and 7 (Figure 4.12), which may indicate that the rate constants of the two different degradation processes are controlled by the same energy barrier, namely C-Br bond dissociation energy.

LUMO energies and degradation rate constants

A linear correlation between the rate constants of Fe^0 reduction of PBDEs and the LUMO energies was found in a previous study (*20*). The photodegradation rate constants for 15 PBDEs in methanol/water have also been previously reported (*4*). Our predicted LUMO energies, using DFT method (Chapter 2) for these 15 PBDE congeners, had a good linear correlation with these reported rate constants (*4*) in log scale (R^2=0.8541 and P<0.0001) (Figure 4.13). These linear relationships indicate that debromination of PBDEs by Fe^0 treatment and UV light may both be caused by electron transfer. The lower of the LUMO energy, the easier it is for the PBDE molecule to go to the excited state or accept an electron and, eventually, to cleave the C-Br bond.

In this study, photodegradation experiments and the photodegradation model were used to study the photodegradation of the octa-BDE technical mixture and its individual components. In addition, the photodegradation results were also compared with anaerobic biodegradation. The PBDE products measured in the anaerobic biodegradation were

found to be the major products in the photodegradation experiments. The photodegradation experiments and the model predictions were also compared with zero-valent iron reduction of BDE-209, 100 and 47 from a previous study and the same products were found in both photo and Fe^0 degradation. Good correlation between 15 previously reported photodegradation rate constants of PBDE congeners and their calculated LUMO energies was found. This indicates that, similar to the Fe^0 reduction, debromination by UV light is caused by electron transfer.

Acknowledgement

This publication was made possible in part by grant number P30ES00210 from the National Institute of Environmental Health Sciences, NIH through a pilot project awarded by Oregon State University's Environmental Health Sciences Center. Its contents are solely the responsibility of the authors and do not necessarily represent the official view of the NIEHS, NIH. The authors would like to acknowledge OSU's EHSC's mass spectrometry core facility for assistance, Kristin Robrock for performing the anaerobic biodegradation experiments, and Peter Korytár for providing additional standards.

References

(1) Hites, R. A., Polybrominated Diphenyl Ethers in the Environment and in People: A Meta-Analysis of Concentrations. *Environ Sci Technol* **2004**, *38*, 945-956.

(2) de Wit, C. A., An overview of brominated flame retardants in the environment. *Chemosphere* **2002**, *46*, 583-624.

(3) Niu, J.; Shen, Z.; Yang, Z.; Long, X.; Yu, G., Quantitative structure-property relationships on photodegradation of polybrominated diphenyl ethers. *Chemosphere* **2006**, *64*, 658-665.

(4) Eriksson, J.; Green, N.; Marsh, G.; Bergman, A., Photochemical Decomposition of 15 Polybrominated Diphenyl Ether Congeners in Methanol/Water. *Environ Sci Technol* **2004**, *38*, 3119-3125.

(5) Bezares-Cruz, J.; Jafvert, C. T.; Hua, I., Solar photodecomposition of decabromodiphenyl ether: products and quantum yield. *Environ Sci Technol* **2004**, *38*, 4149-4156.

(6) Soderstrom, G.; Sellstrom, U.; de Wit, C. A.; Tysklind, M., Photolytic debromination of decabromodiphenyl ether (BDE 209). *Environ Sci Technol* **2004**, *38*, 127-132.

(7) Sanchez-Prado, L.; Lores, M.; Llompart, M.; Garcia-Jares, C.; Bayona, J. M.; Cela, R., Natural sunlight and sun simulator photolysis studies of tetra- to hexa-brominated diphenyl ethers in water using solid-phase microextraction. *J Chromatogr A* **2006**, *1124*, 157-166.

(8) Schmidt, S.; Wittich, R. M.; Erdmann, D.; Wilkes, H.; Francke, W.; Fortnagel, P., Biodegradation of diphenyl ether and its monohalogenated derivatives by Sphingomonas sp. strain SS3. *Appl Environ Microbiol* **1992**, *58*, 2744-2750.

(9) Pfeifer, F.; Truper, H. G.; Klein, J.; Schacht, S., Degradation of diphenylether by Pseudomonas cepacia Et4: enzymatic release of phenol from 2,3-dihydroxydiphenylether. *Arch Microbiol* **1993**, *159*, 323-329.

(10) Hundt, K.; Jonas, U.; Hammer, E.; Schauer, F., Transformation of diphenyl ethers by Trametes versicolor and characterization of ring cleavage products. *Biodegradation* **1999**, *10*, 279-286.

(11) Rayne, S.; Ikonomou, M. G.; Whale, M. D., Anaerobic microbial and photochemical degradation of 4,4'-dibromodiphenyl ether. *Water Res* **2003**, *37*, 551-560.

(12) Darnerud, P. O.; Eriksen, G. S.; Johannesson, T.; Larsen, P. B.; Viluksela, M., Polybrominated diphenyl ethers: Occurrence, dietary exposure, and toxicology. *Environmental Health Perspectives Supplements* **2001**, *109*, 49-68.

(13) He, J.; Robrock, K. R.; Alvarez-Cohen, L., Microbial reductive debromination of polybrominated diphenyl ethers (PBDEs). *Environ Sci Technol* **2006**, *40*, 4429-4434.

(14) Gerecke, A. C.; Giger, W.; Hartmann, P. C.; Heeb, N. V.; Kohler, H. P.; Schmid, P.; Zennegg, M.; Kohler, M., Anaerobic degradation of brominated flame retardants in sewage sludge. *Chemosphere* **2006**, *64*, 311-317.

(15) Gerecke, A. C.; Hartmann, P. C.; Heeb, N. V.; Kohler, H. P.; Giger, W.; Schmid, P.; Zennegg, M.; Kohler, M., Anaerobic degradation of decabromodiphenyl ether. *Environ Sci Technol* **2005**, *39*, 1078-1083.

(16) Johnson, T. L.; Scherer, M. M.; Tratnyek, P. G., Kinetics of Halogenated Organic Compound Degradation by Iron Metal. *Environmental Science and Technology* **1996**, *30*, 2634-2640.

(17) Keum, Y. S.; Li, Q. X., Reductive debromination of polybrominated diphenyl ethers by zerovalent iron. *Environ Sci Technol* **2005**, *39*, 2280-2286.

(18) Scherer, M. M.; Balko, B. A.; Gallagher, D. A.; Tratnyek, P. G., Correlation Analysis of Rate Constants for Dechlorination by Zero-Valent Iron. *Environmental Science and Technology* **1998**, *32*, 3026-3033.

(19) Ackerman, L. K.; Wilson, G. R.; Simonich, S. L., Quantitative analysis of 39 polybrominated diphenyl ethers by isotope dilution GC/low-resolution MS. *Analytical Chemistry* **2005**, *77*, 1979-1987.

(20) Korytar, P.; Covaci, A.; de Boer, J.; Gelbin, A.; Brinkman, U. A., Retention-time database of 126 polybrominated diphenyl ether congeners and two bromkal technical mixtures on seven capillary gas chromatographic columns. *J Chromatogr A* **2005**, *1065*, 239-249.

(21) Zeng, X.; Freeman, P. K.; Vasil'ev, Y. V.; Voinov, V. G.; Simonich, S. L.; Barofsky, D. F., Theoretical Calculation of Thermodynamic Properties of Polybrominated Diphenyl Ethers. *Journal of Chemical and Engineering Data* **2005**, *50*, 1548-1556.

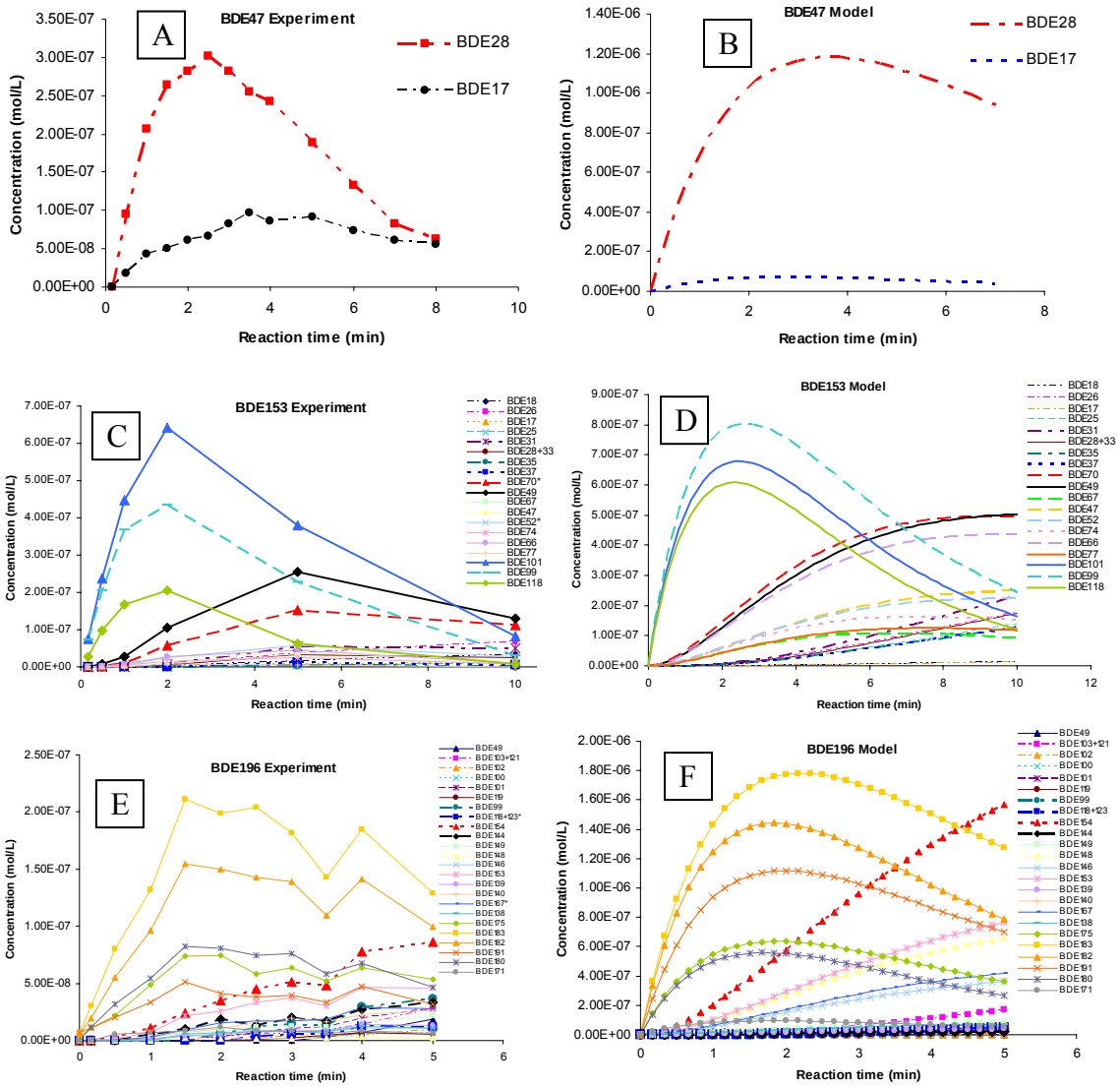

Figure 4.1. Reaction time profile for photodegradation products of BDE-47,153,196,197 and 203.

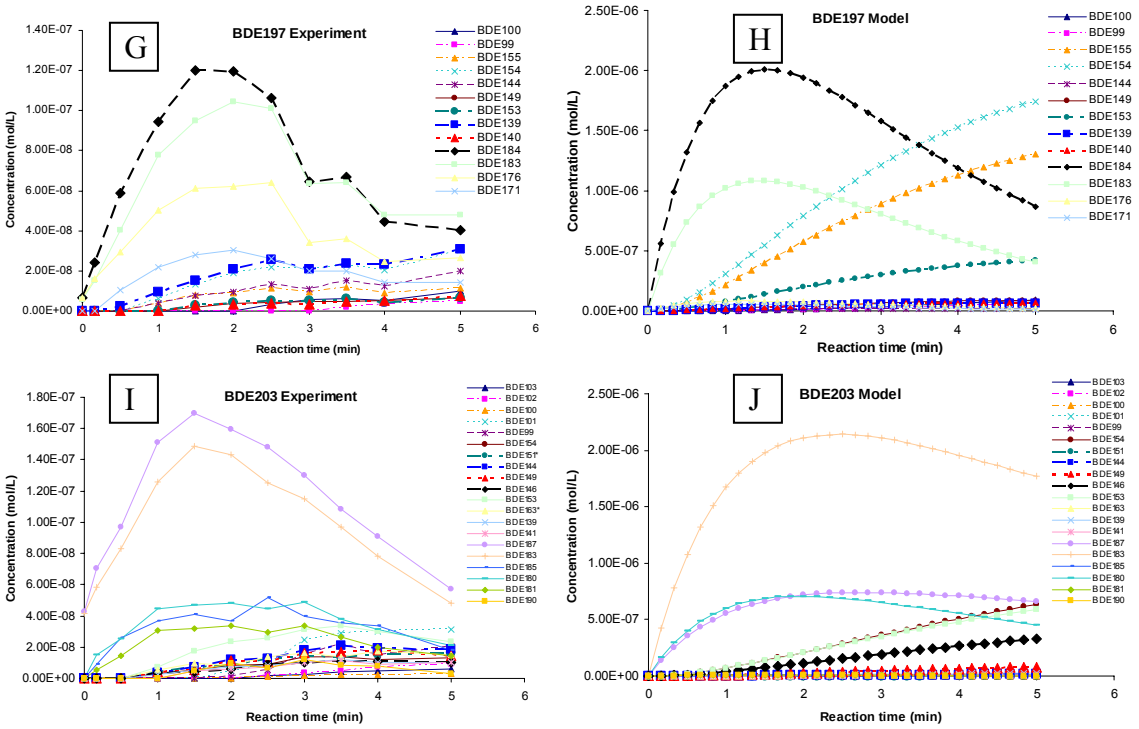

Figure 4.1. (Continued) Reaction time profile for photodegradation products of BDE-47,153,196,197 and 203.

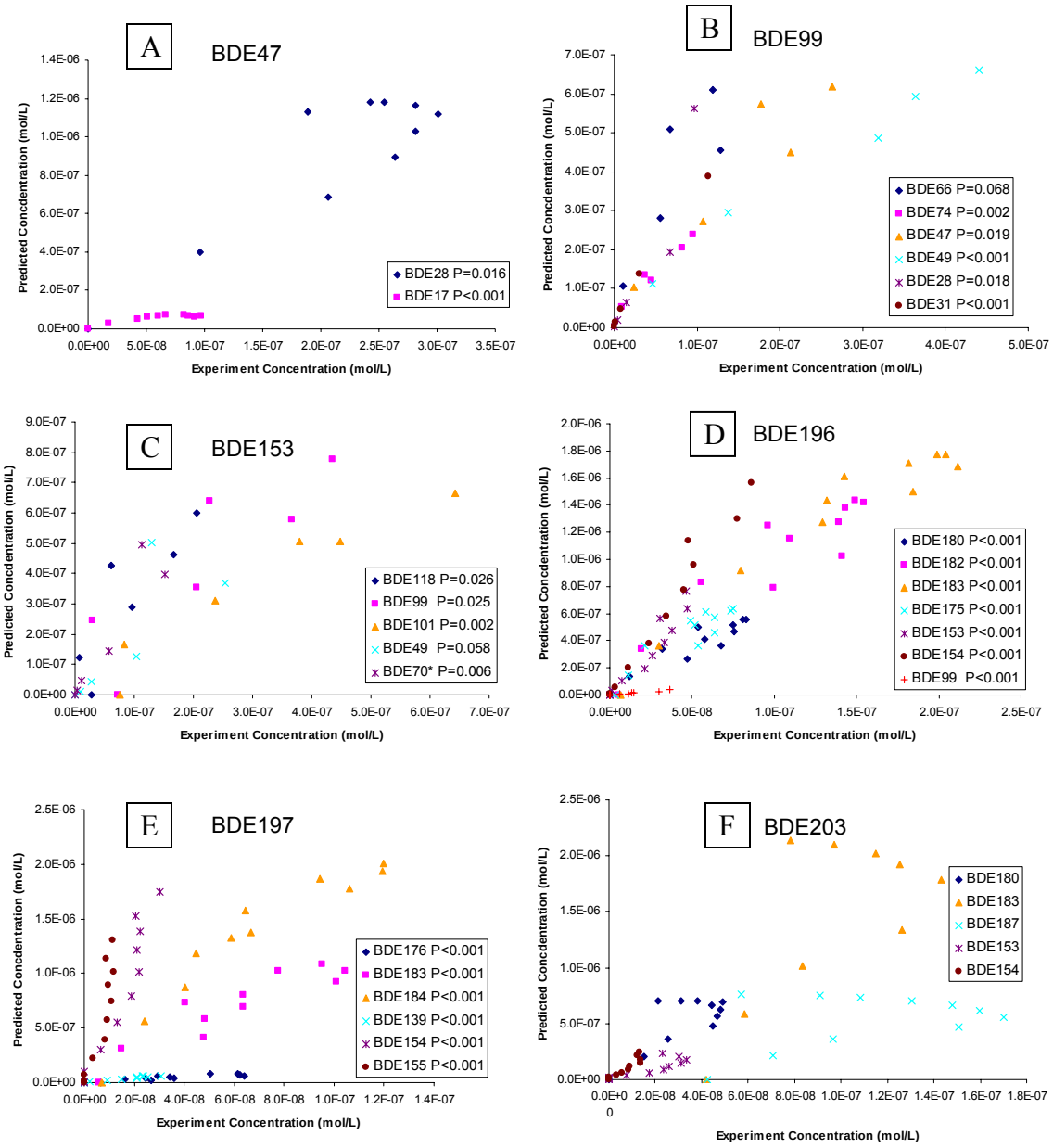

Figure 4.2. Correlation between experimental results and model predicted results for the major photodegradation products of BDE-47, 99,153,196,197 and 203.

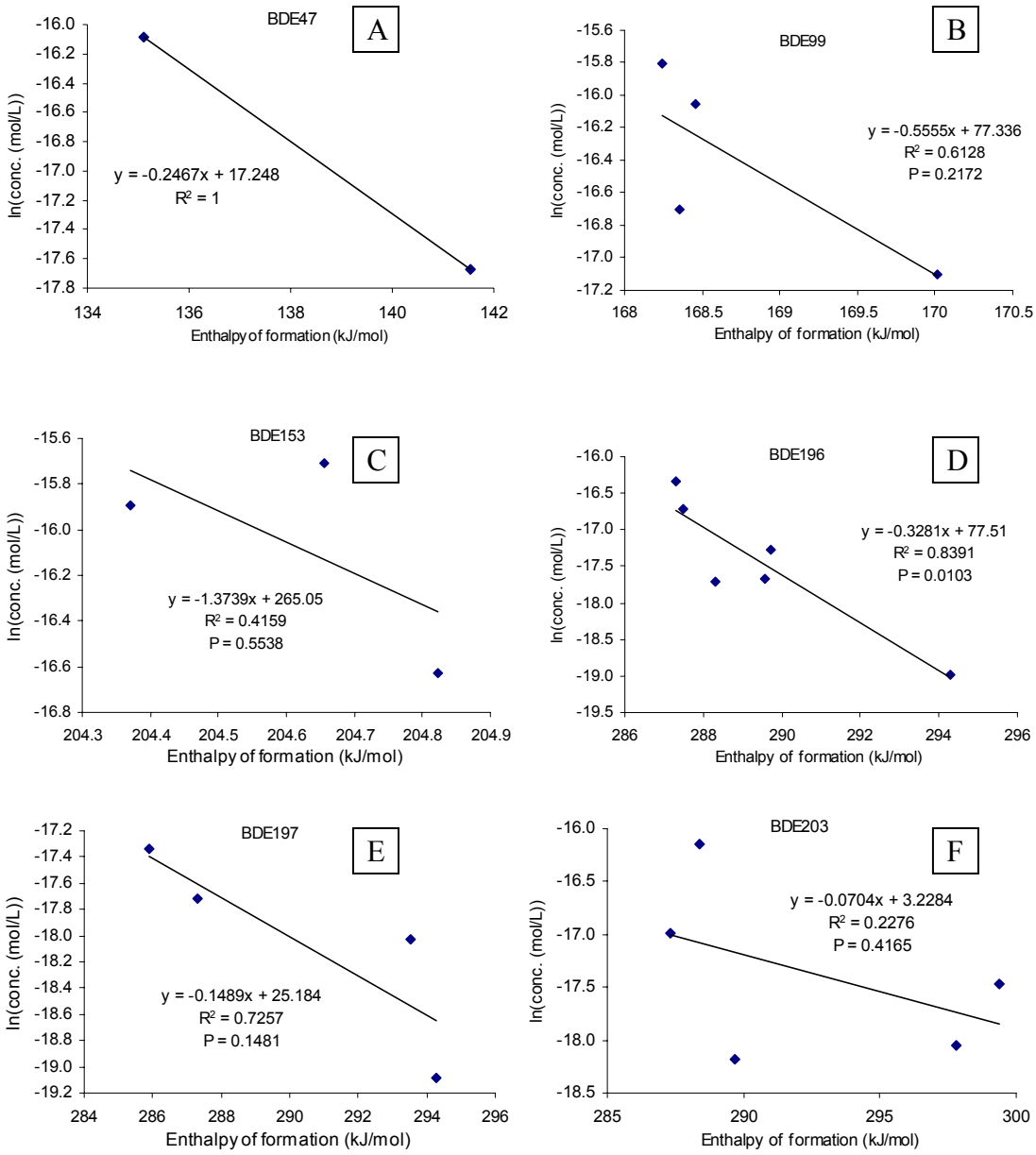

Figure 4.3. Correlation between natural logarithm of the first step photodegradation products concentration/(number of reaction pathways) at 0.5 min and the corresponding enthalpy of formation.

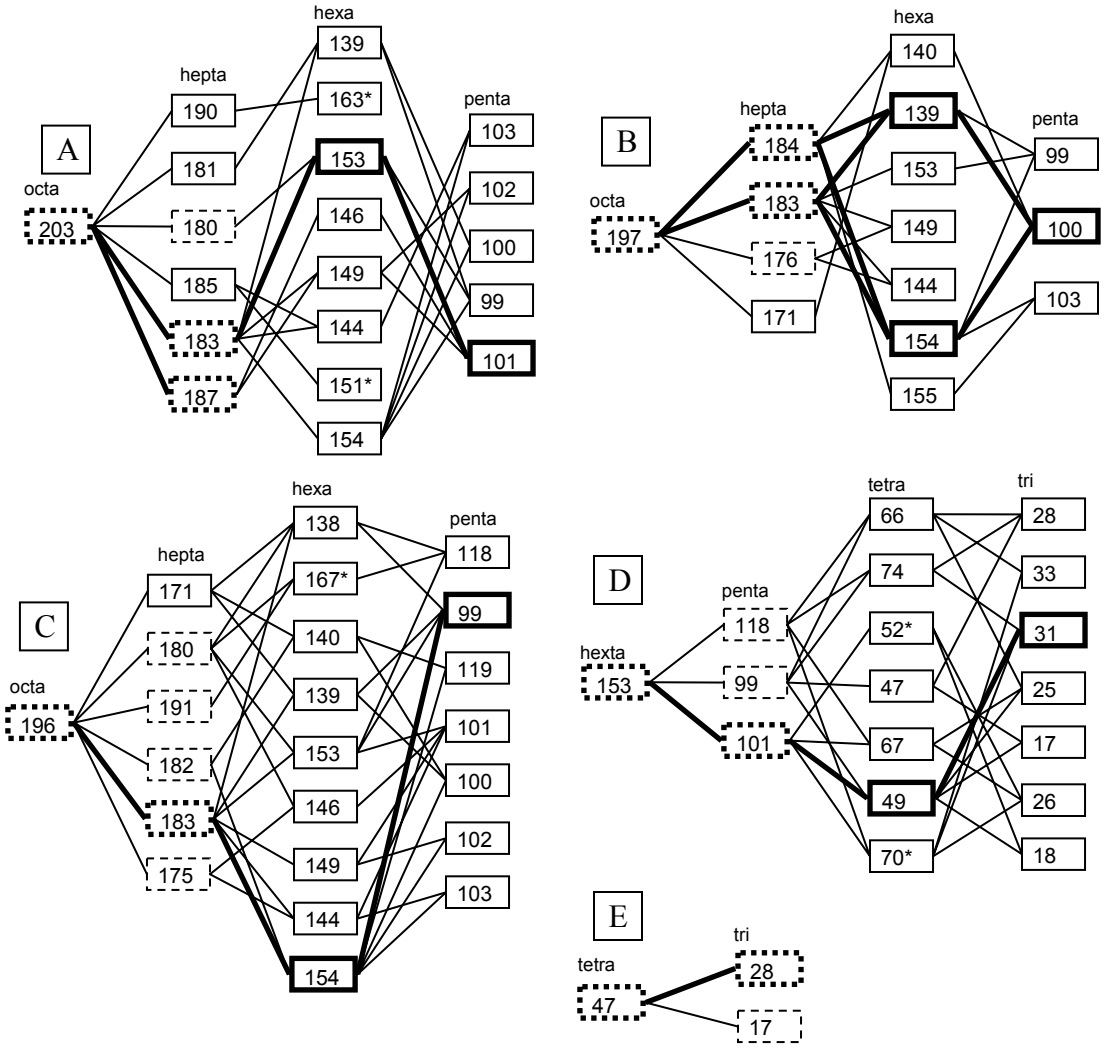

Figure 4.4. Reaction pathways of BDE-203, 197, 196, 153 and 47 photodegradation. Thick lines and boxes represent higher concentration of PBDE congeners in photodegradation. All the boxes represent photodegradation products. Dashed boxes represent products also found in anaerobic biodegradation study.

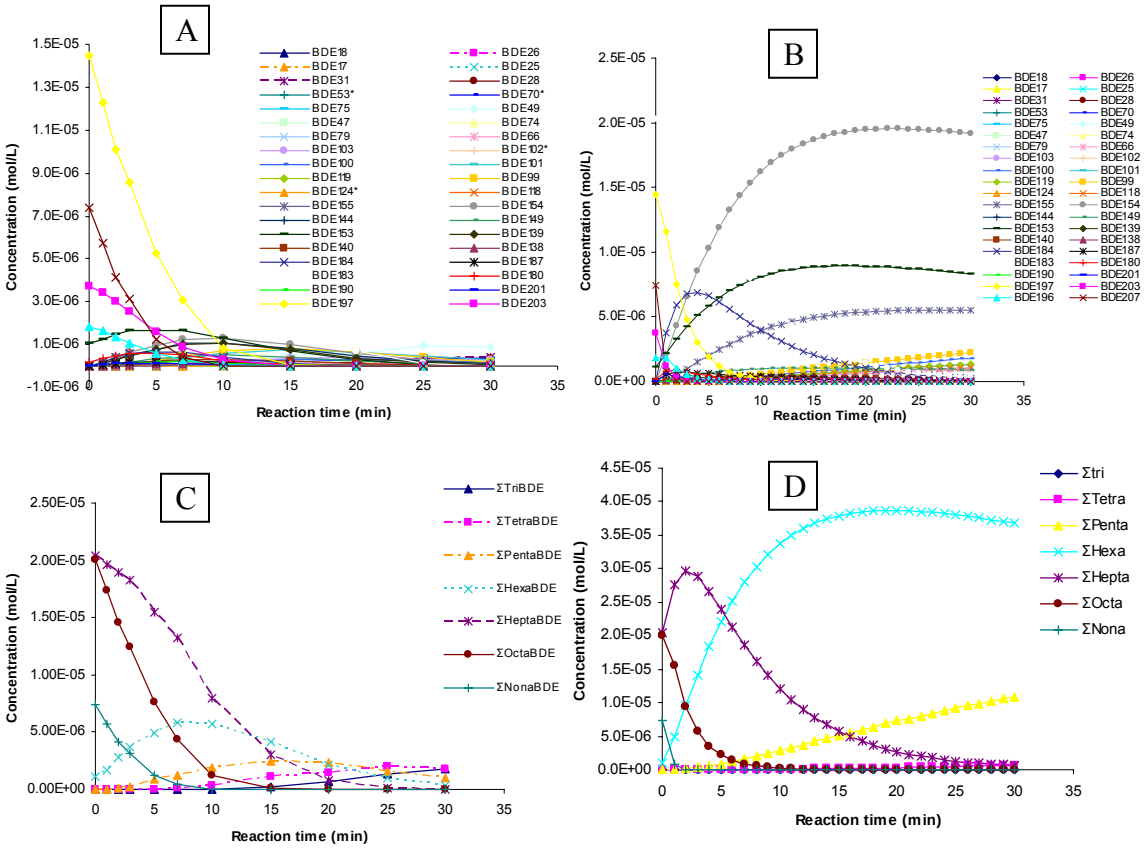

Figure 4.5. Reaction time profile for reactants and products for the octa-BDE technical mixture photodegradation. A and B are experimental results and C and D are model prediction.

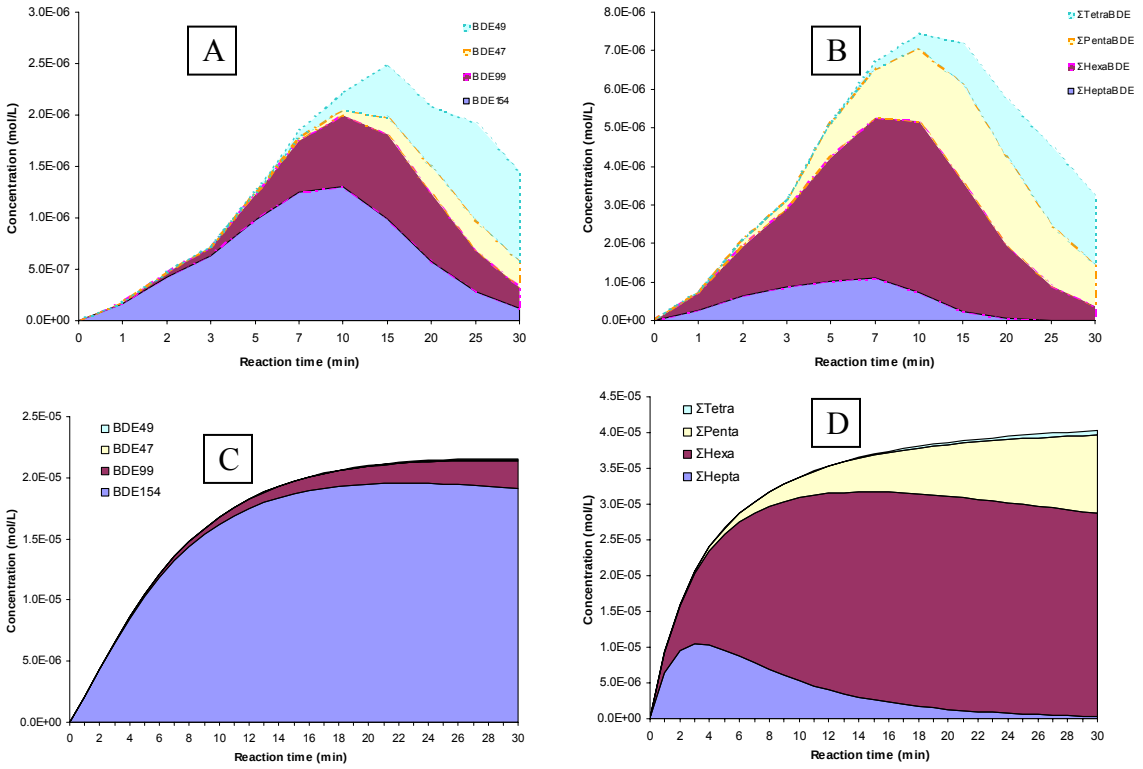

Figure 4.6. Cumulative concentration of the octa-BDE technical mixture photodegradation products. A and B are the experimental results and C and D are model simulation

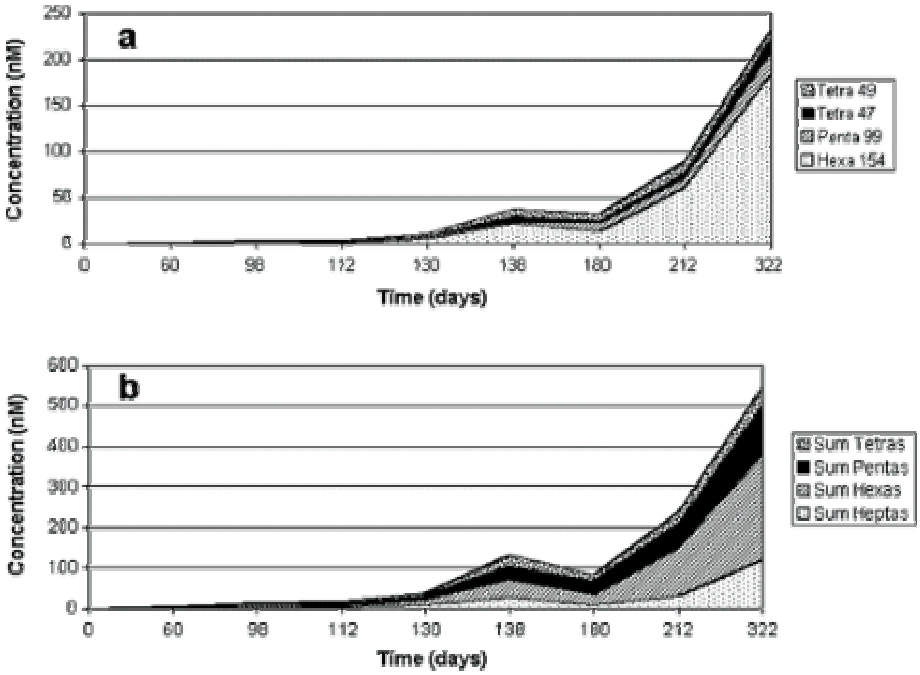

Figure 4.7. Average cumulative concentrations of the octa-BDE technical mixture anaerobic biodegradation products generated by *ANAS195* over 12 months from previous study (*13*). (a) only positively identified products; (b) summed product concentrations for each homologous group. Taken from *Environ Sci Technol* **2006**, *40* with permission.

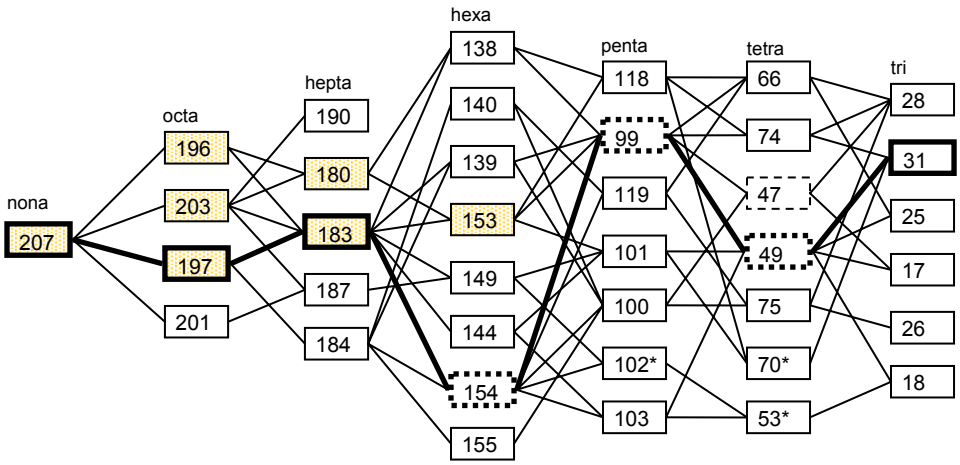

Figure 4.8. Reaction pathways for octa-BDE technical mixture photodegradation and anaerobic biodegradation. Thick lines and boxes represent higher concentrations of PBDE congeners in photodegradation. Shaded boxes represent the components of the octa-BDE technical mixture. All the boxes represent photodegradation products. Dashed boxes represent products also measured in anaerobic biodegradation study (*13*).

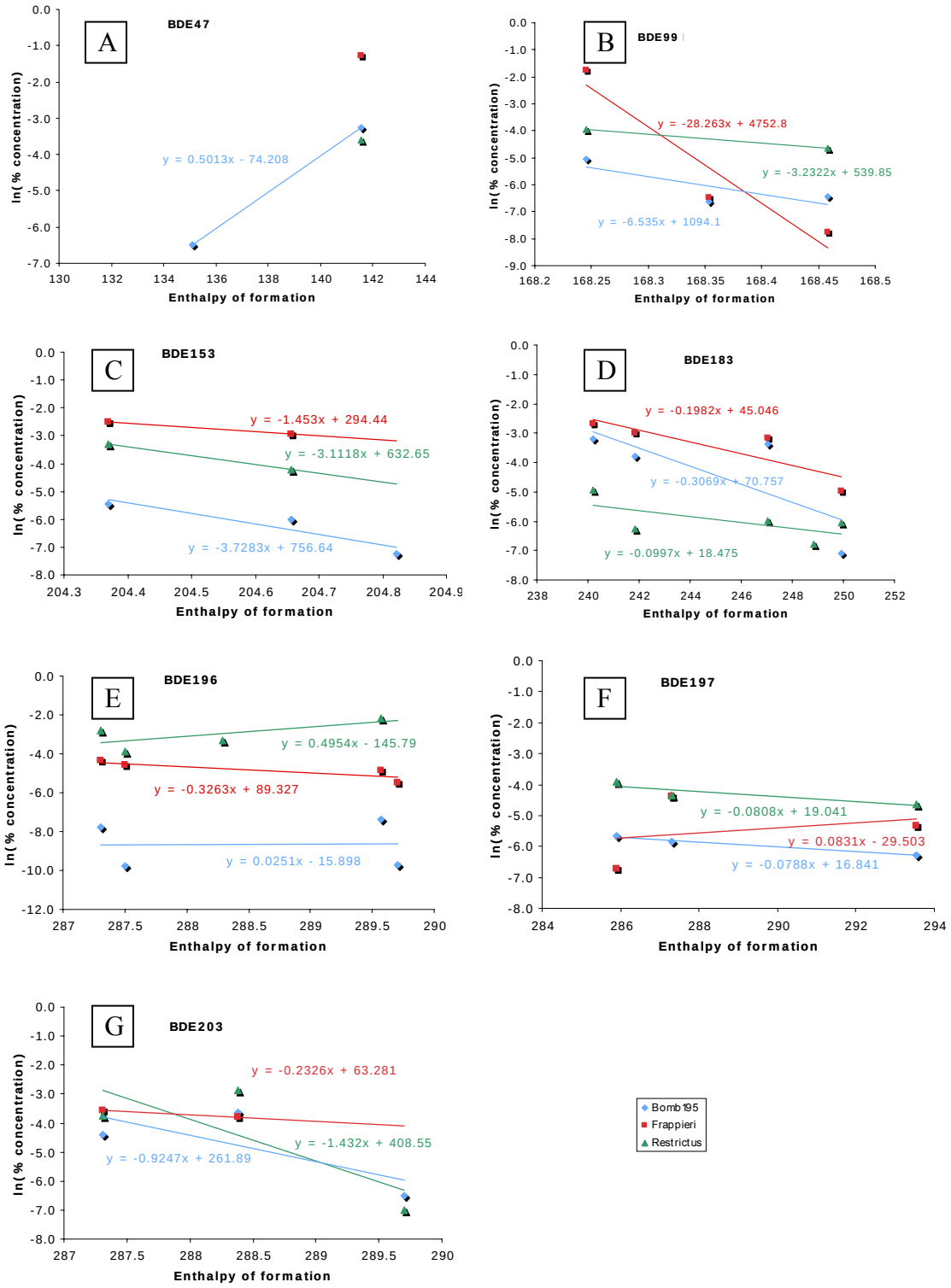

Figure 4.9. Correlation between natural logarithm of the first step anaerobic biodegradation products concentration/(number of reaction pathways) at 30 days and the corresponding enthalpy of formation.

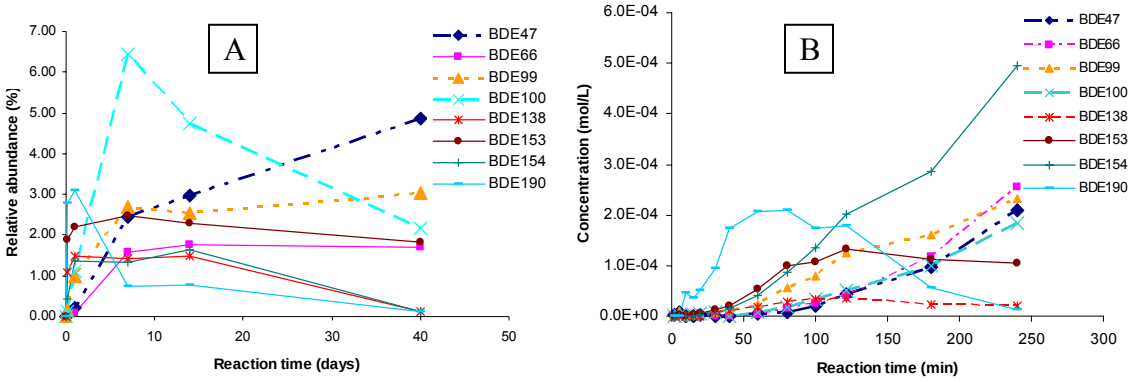

Figure 4.10. Reaction time profile for Fe^0 degradation (A) and photodegradation of BDE-209 (B). Data of Fe^0 degradation were obtained from previous study (*17*) and the photodegradation data were obtained from Chapter Three.

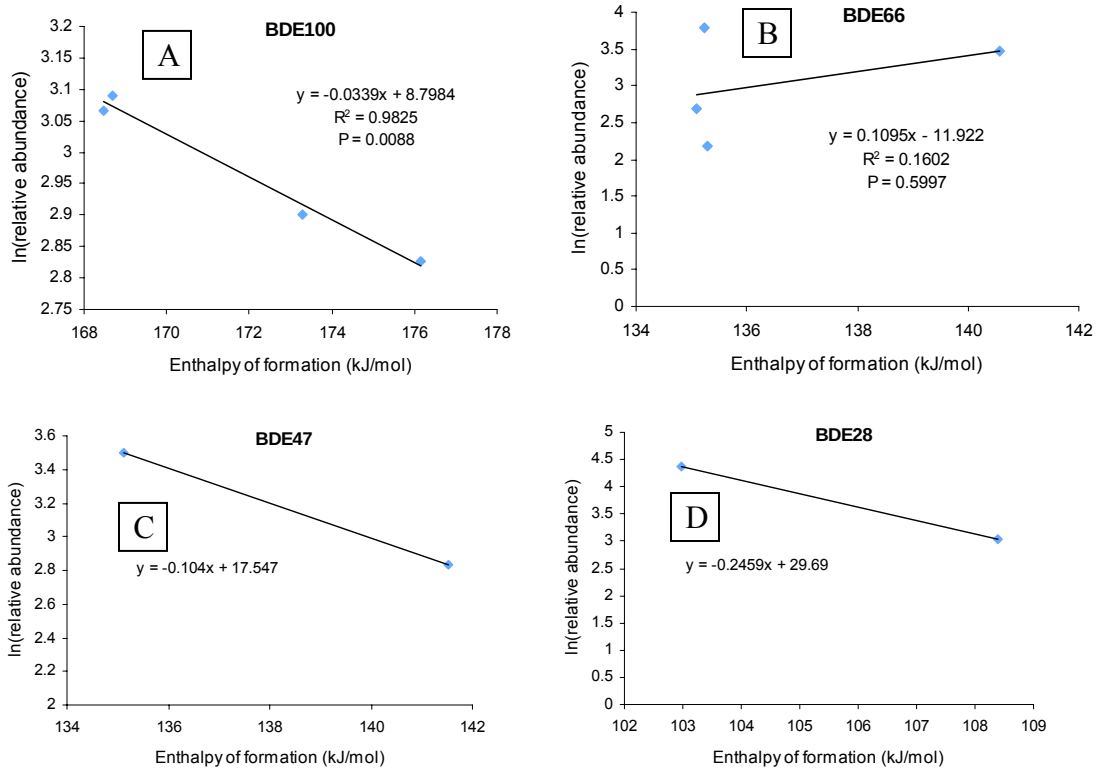

Figure 4.11. Correlation between natural logarithm of the first step Fe^0 reduction products (*17*) relative abundance/(number of reaction pathways) and the corresponding enthalpy of formation.

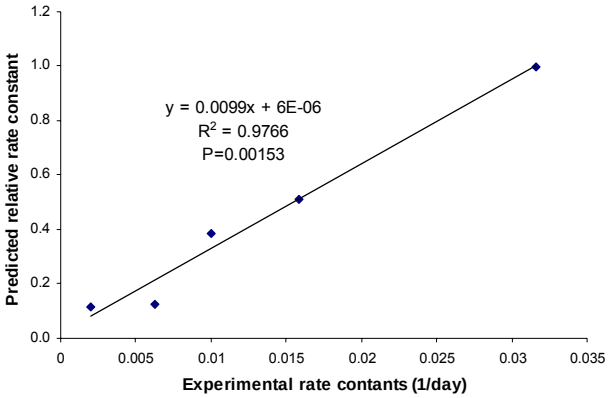

Figure 4.12. Correlation between the model predicted rate constants (relative to BDE-100) and experimental Fe^0 degradation rate constants (*17*) for 5 PBDE congeners.

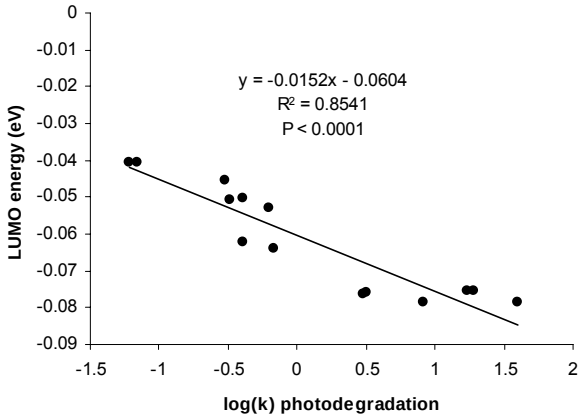

Figure 4.13. Correlation between the calculated LUMO energies and the measured photodegradation rate constants of 15 PBDEs (*4*) in log format.

CHAPTER 5. CONCLUSIONS

The thermodynamic properties of 39 PBDEs have been calculated using Gaussian 03 on the B3LYP/6-31G(d)//B3LYP/6-31G(d) level. The PBDE congeners' enthalpies of formation increase with increasing number of bromines and show a strong dependence on the bromine substitution pattern. The effects of bromine substitution pattern have been quantitatively studied by GAM model based on the output of the theoretical calculations. The results of the GAM were consistent with theoretical calculations, providing a measure of reliability for the theoretical calculations. Furthermore, the GAM model can be used to predict the thermodynamic properties for all of the 209 PBDE congeners.

Use of the isodesmic reaction is a valid method for predicting the enthalpy and Gibbs free energy of formation of PBDEs from the results of DFT calculations and from known experimental values for other compounds. GAM yields results that are consistent with the DFT calculation. The GAM model describes the effect of Br substitution pattern very well and is useful in predicting the thermodynamic properties of all of the 209 PBDE congeners.

Based on the GAM model, the enthalpies of formation of the 209 PBDE congeners were calculated. A photodegradation model was developed and validated to predict the products, and their relative concentrations, from the photodegradation of PBDEs. The relative reaction rate constants for the 209 PBDEs were obtained and these predicted reaction rate constants show linear correlation with previous experimental results. The photodegradation model successfully predicted the products of the photochemical reactions of PBDEs in experimental studies.

A GC retention time model for PBDEs was developed using a multiple linear regression analysis and, for 47 of the PBDEs show good linearity and, in particular, within homologous groups (R^2=0.9939, P<0.0001). With only two exceptions, the predicted GC retention times are within 0.6 min of their corresponding measured retention times, and there is no systematic trend. The photodegradation model, together with the GC retention time model and additional PBDE standards, provided a way to identify unknown products from PBDE photodegradation.

Photodegradation experiments were conducted for BDE-209, BDE-184, BDE-100 and BDE-99. Based on the results of the photodegradation experiments, as well as the model predictions, the photodegradation of PBDEs is a first order reaction and, further, the rate determining step is the stepwise loss of bromine. Our results suggest that, over time, BDE-99 will remain as the most abundant penta-BDE, while BDE-49 and BDE-66 will increase greatly and will be comparable in abundance to BDE-47.

Assuming that most of the BDE-209 in the environment is eventually photodegraded by natural sunlight, the future pattern of the PBDE congeners, caused by BDE-209 degradation in the environment, may be comparable to our results. For example, BDE-99 will remain as the most abundant penta-BDE, while BDE-49 and BDE-66 will increase greatly and will be comparable in abundance to BDE-47. It is also possible that PBDE congeners that have not been used commercially, such as octa BDE-201 and hepta BDE-187, will be present in the environment at significant concentrations among their congener group.

Photodegradation experiments and the photodegradation model were used to study the photodegradation of the octa-BDE technical mixture and its individual components (together with BDE-47). The predicted reaction time profiles of the photodegradation products correlate well with the experimental results. In addition, the photodegradation results were also compared with anaerobic biodegradation. The PBDE products measured in the anaerobic biodegradation were found to be the major products in the photodegradation experiments. The degradation pathways of the technical octa-BDE mixture and its components were summarized. BDE-154, 99, 47 and 31 were found to be the most abundant hexa, penta, tetra and tri-BDE degradation products, respectively. These products may become the most abundant products in their homologous groups when the technical octa-BDE mixture degrades in the environment. The photodegradation experiments and the model predictions were also compared with zero-valent iron reduction of BDE-209, 100 and 47 from a previous study and the same products were found in both photo and Fe^0 degradation. Good correlation between 15 previously reported photodegradation rate constants of PBDE congeners and their calculated LUMO energies was found. This indicates that, similar to the Fe^0 reduction, debromination by UV light is caused by electron transfer. Furthermore, the rate constants for the three different degradation processes are controlled by C-Br bond dissociation energy.

Using the photodegradation model, the degradation profile of PBDEs in the environment can be predicted. Previous studies have shown that mono and di-BDEs react with OH radical in the atmospheric gas phase (with half lives of 2 to 3 days), while the

reactivity of higher brominated diphenyl ethers with OH radical is likely significantly slower because they are mainly found in the particle phase (*1*).

Penta, octa and deca-BDE technical mixtures made up 11.1%, 5.6% and 83.3%, respectively, of the 2001 global market demand of 67309 tons (*2*). The penta and octa-BDE technical mixtures were banned in Europe and voluntarily phased out in the U.S. in 2004. However, there are currently no restrictions on the use of the deca-BDE (BDE-209) technical mixture and its global annual production has not decreased (50000-60000 tons) (*3*).

Assuming that photodegradation is the major degradation process for the PBDEs in the environment, that deca-BDE make up 100% of the 2007 global market demand for PBDEs, and that the half life of BDE-209 is 30 days (*4*), the degradation profile of major PBDE products were predicted using the photodegradation model and are shown in Figure 5.1A for the year 2001 and Figure 5.1B for the year 2007, respectively. After 3000 days of reaction, the 2007 degradation profile was reduced in hexa and hepta-BDEs and BDE-100 by less than 2% compared to 2001, and about 4% for BDE-47 and 99, and increased in the octa and nona-BDEs due to the higher abundance of BDE-209 in 2007. After 30000 days of reaction, the 2007 degradation profile was reduced in hexa and hepta-BDEs and BDE-100 by less than 0.8% compared to 2001, 4.1% for BDE-47, 3.3% for BDE-99, and increased in the octa and nona-BDEs and BDE-154 due to the higher abundance of BDE-209 in 2007. The results showed that there was a very small difference in the hexa, hepta, octa and nona-BDEs degradation profiles between 2001 and 2007 emission scenarios, because they are all degradation products of BDE-209.

However, the 2001 and 2007 degradation profiles of BDE-47 and 99, which are photodegradation products of BDE-209 and the other higher brominated diphenyl ethers as well as major composition of penta and octa-BDE form, were similar. Thus, the ban of the penta and octa-BDE formulations may not affect the degradation profiles of PBDEs in the environment due to the continued use of BDE-209 in large volume.

The PBDE photodegradation model is based on the GAM model, which is an approximation to calculate the ΔH_f of PBDEs. ΔH_f may not be the only factor determining the PBDE photodegradation rate constant. Other factors may include molecular weight, molecular orbital energy, and charge distribution. Furthermore, the model assumes that the solvent effect and light conditions have the same effect on all PBDE congeners. These limitations may cause the observed deviations from the experiment results.

Due to the limited availability of pure PBDE standards, the photodegradation products without available quantification standards were quantified using the average ECNI response of the homologous PBDE group. Therefore, the accuracy of quantification for the PBDE photodegradation products may be limited by the availability of standards.

Future work should include the photodegradation experiments on the penta-BDE technical mixture to get a better understanding of the fate of all of the PBDE products commercially used in the world. Additional PBDE standards are required to identify unknown products and quantify them. Replicate experiments should be performed to obtain higher precision. In addition, the photodegradation experiment should better simulate the conditions in the environment, such as gas and particular phase experiment,

solutions similar to water, and use of natural sunlight instead of artificial UV light. The photodegradation model, which is simply based on the bromine dissociation energy, should be modified according to the experimental results, such as the loss of total mass, to better predict degradation of PBDEs on the environment. In addition, the model can also be applied to calculate the photodegradation of similar compounds such as polychlorinated biphenyls (PCBs) and polybromodibenzo-*p*-dioxins (PBDDs).

References

(1) Raff, J. D.; Hites, R. A., Gas-phase reactions of brominated diphenyl ethers with OH radicals. *J Phys Chem A Mol Spectrosc Kinet Environ Gen Theory* **2006**, *110*, 10783-10792.

(2) La, A. G. M. J.; Hale, R. C.; Harvey, E., Detailed polybrominated diphenyl ether (PBDE) congener composition of the widely used penta-, octa-, and deca-PBDE technical flame-retardant mixtures. *Environ Sci Technol* **2006**, *40*, 6247-6254.

(3) Bergman, Å.; Christiansson, A.; Eriksson, J.; Marsh, G., Polybrominated diphenyl ethers as indicators of environmental DecaBDE exposure *http://www.miljokemi.su.se/forskning/projektdetalj?id=33&lang=eng* **2005-2007**.

(4) Soderstrom, G.; Sellstrom, U.; de Wit, C. A.; Tysklind, M., Photolytic debromination of decabromodiphenyl ether (BDE 209). *Environ Sci Technol* **2004**, *38*, 127-132.

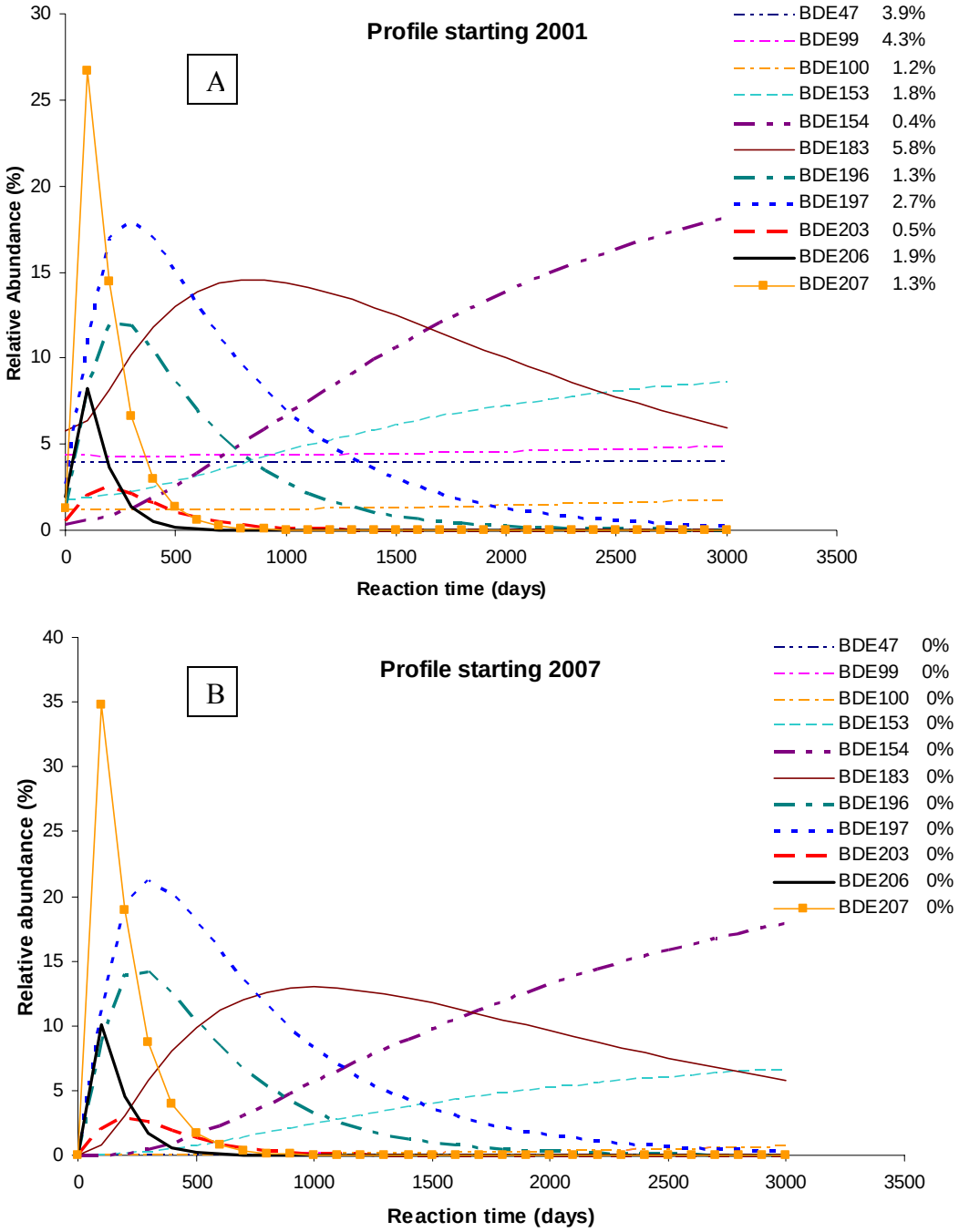

Figure 5.1. Degradation profile of PBDEs starting from 2001 (A) and 2007 (B). The percentages on the right side of the legends are the starting abundance of PBDE congeners.

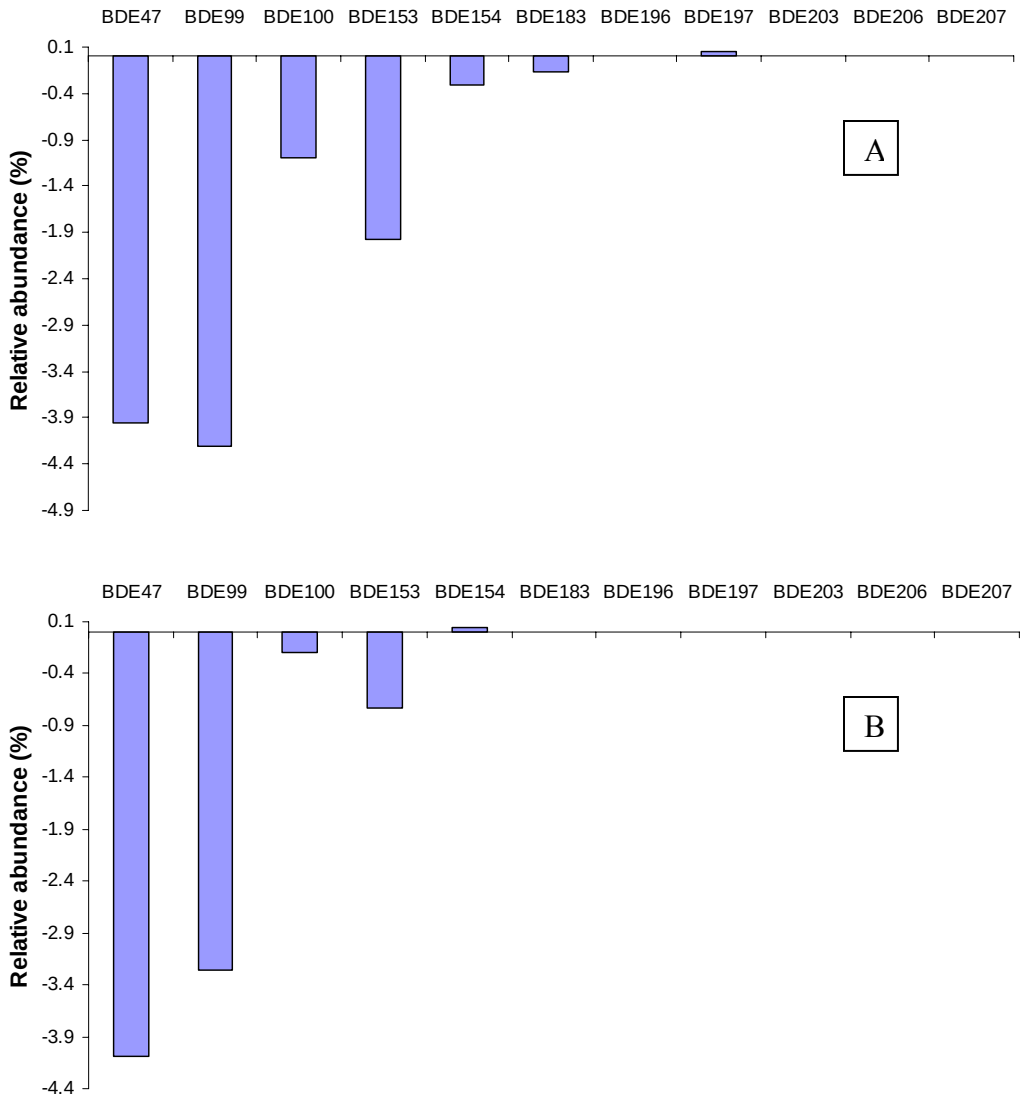

Figure 5.2. Difference between the degradation profile of PBDEs starting from 2001 and 2007 at 3000 days (A) and 30000 days (B).

BIBLIOGRAPHY

"Bromine Science and environmental Forum. Total Market Demand 2003. available at www.bsef.com."

Ackerman, L. K., G. R. Wilson, et al. (2005). "Quantitative analysis of 39 polybrominated diphenyl ethers by isotope dilution GC/low-resolution MS." Analytical Chemistry **77**(7): 1979-1987.

Alaee, M., P. Arias, et al. (2003). "An overview of commercially used brominated flame retardants, their applications, their use patterns in different countries/regions and possible modes of release." Environ Int **29**(6): 683-9.

Alaee, M. and R. J. Wenning (2002). "The significance of brominated flame retardants in the environment: current understanding, issues and challenges." Chemosphere **46**(5): 579-82.

Anon (2002). "CRC Handbook of Chemistry and Physics. 83rd Edition. Edited by David R. Lide (National Institute of Standards and Technology). CRC Press: Boca Raton. 2002. + 2664 pp. $139.95. ISBN 0-8493-0483-0." Journal of the American Chemical Society **124**(47): 14280.

Arias, P. (1992). "Brominated diphenyloxides as flame retardants: bromine based chemicals." Consultant Report to the OECD, Paris.

Ballschmiter, K. and M. Zell (1980). "Analysis of polychlorinated biphenyls (PCB) by glass capillary gas chromatography. Composition of technical Aroclor- and Clophen-PCB mixtures." Fresenius' Zeitschrift fuer Analytische Chemie **302**(1): 20-31.

Barring, H., T. D. Bucheli, et al. (2002). "Soot-water distribution coefficients for polychlorinated dibenzo-p-dioxins, polychlorinated dibenzofurans and polybrominated diphenylethers determined with the soot cosolvency-column method." Chemosphere **49**(6): 515-23.

Benson, S. W. (1976). Thermochemical Kinetics: Methods for the Estimation of Thermochemical Data and Rate Parameters. 2nd Ed. New York, Wiley.

Bezares-Cruz, J., C. T. Jafvert, et al. (2004). "Solar photodecomposition of decabromodiphenyl ether: products and quantum yield." Environ Sci Technol **38**(15): 4149-56.

Braekevelt, E., S. A. Tittlemier, et al. (2003). "Direct measurement of octanol-water partition coefficients of some environmentally relevant brominated diphenyl ether congeners." Chemosphere **51**(7): 563-7.

Darnerud, P. O., G. S. Eriksen, et al. (2001). "Polybrominated diphenyl ethers: Occurrence, dietary exposure, and toxicology." Environmental Health Perspectives Supplements **109**(1): 49-68.

de Wit, C. A. (2002). "An overview of brominated flame retardants in the environment." Chemosphere **46**(5): 583-624.

Dodder, N. G., B. Strandberg, et al. (2002). "Concentrations and Spatial Variations of Polybrominated Diphenyl Ethers and Several Organochlorine Compounds in Fishes from the Northeastern United States." Environ Sci Technol **36**(2): 146-151.

Elliott, J. E., L. K. Wilson, et al. (2005). "Polybrominated diphenyl ether trends in eggs of marine and freshwater birds from British Columbia, Canada, 1979-2002." Environ Sci Technol **39**(15): 5584-91.

Eriksson, J., N. Green, et al. (2004). "Photochemical Decomposition of 15 Polybrominated Diphenyl Ether Congeners in Methanol/Water." Environ Sci Technol **38**(11): 3119-3125.

Føreid, S., L. Knudsen, et al. (2006). "Temporal trends of pollution patterns (chlorinated hydrocarbons and brominated flame retardants) in eggs of seabirds from Northern Norway." Organohalogen Compounds **68** 1462-1465.

Frisch, M. J. (2003). "Gaussian 03, revision B.05." Gaussian Inc. Pittsburg, PA.

Gerecke, A. C., W. Giger, et al. (2006). "Anaerobic degradation of brominated flame retardants in sewage sludge." Chemosphere **64**(2): 311-7.

Gerecke, A. C., P. C. Hartmann, et al. (2005). "Anaerobic degradation of decabromodiphenyl ether." Environ Sci Technol **39**(4): 1078-83.

Gouin, T., S. Bocking, et al. (2005). "Policy by analogy: precautionary principle, science and polybrominated diphenyl ethers." Int. J. Global Environmental Issues **5**: 54-67.

Hageman, H. J., H. L. Louwerse, et al. (1970). "Photoreactions of some diaryl ethers." Tetrahedron **26**(8): 2045-52.

Hale, R. C., M. Alaee, et al. (2003). "Polybrominated diphenyl ether flame retardants in the North American environment." Environ Int **29**(6): 771-9.

Hale, R. C., M. J. La Guardia, et al. (2002). "Potential role of fire retardant-treated polyurethane foam as a source of brominated diphenyl ethers to the US environment." Chemosphere **46**(5): 729-35.

Hale, R. C., M. J. La Guardia, et al. (2001). "Flame retardants: Persistent pollutants in land-applied sludges." Nature (London, United Kingdom) **412**(6843): 140-141.

Harju, M., P. L. Andersson, et al. (2002). "Multivariate physicochemical characterisation and quantitative structure-property relationship modelling of polybrominated diphenyl ethers." Chemosphere **47**(4): 375-84.

He, J., K. R. Robrock, et al. (2006). "Microbial reductive debromination of polybrominated diphenyl ethers (PBDEs)." Environ Sci Technol **40**(14): 4429-34.

Herrmann, T., B. Schilling, et al. (2003). "Photolysis of PBDEs in solvents by exposure to daylight in a routine laboratory." Organohalogen Compounds **63**: 361-364.

Hites, R. A. (2004). "Polybrominated Diphenyl Ethers in the Environment and in People: A Meta-Analysis of Concentrations." Environ Sci Technol **38**(4): 945-956.

Hua, I., N. Kang, et al. (2003). "Heterogeneous photochemical reactions of decabromodiphenyl ether." Environ Toxicol Chem **22**(4): 798-804.

Hundt, K., U. Jonas, et al. (1999). "Transformation of diphenyl ethers by Trametes versicolor and characterization of ring cleavage products." Biodegradation **10**(4): 279-286.

Ikonomou, M. G., M. Fischer, et al. (2000). "Congener patterns, spatial and temporal trends of polybrominated diphenyl ethers in biota samples from the Canadian west coast and the Northwest Territories." Organohalogen Compounds **47**: 77-80.

Ikonomou, M. G., S. Rayne, et al. (2002). "Exponential increases of the brominated flame retardants, polybrominated diphenyl ethers, in the Canadian Arctic from 1981 to 2000." Environ Sci Technol **36**(9): 1886-92.

Irikura, K. K., D. J. Frurip, et al. (1998). Computational Thermochemistry: Prediction and Estimation of Molecular Thermodynamics. (Proceedings of a Symposium at the 212th National Meeting of the American Chemical Society, Orlando, Florida, 25-29 August 1996.) [In: ACS Symp. Ser., 1998; 677].

Jansson, B., L. Asplund, et al. (1987). "Brominated flame retardants - ubiquitous environmental pollutants?" Chemosphere **16**(10-12): 2343-9.

Johnson, T. L., M. M. Scherer, et al. (1996). "Kinetics of Halogenated Organic Compound Degradation by Iron Metal." Environmental Science and Technology **30**(8): 2634-2640.

Keum, Y. S. and Q. X. Li (2005). "Reductive debromination of polybrominated diphenyl ethers by zerovalent iron." Environ Sci Technol **39**(7): 2280-6.

Kieatiwong, S., L. V. Nguyen, et al. (1990). "Photolysis of chlorinated dioxins in organic solvents and on soils." Environmental Science and Technology **24**(10): 1575-80.

Korytar, P., A. Covaci, et al. (2005). "Retention-time database of 126 polybrominated diphenyl ether congeners and two bromkal technical mixtures on seven capillary gas chromatographic columns." J Chromatogr A **1065**(2): 239-49.

Kuriyama, S. N., C. E. Talsness, et al. (2005). "Developmental exposure to low dose PBDE 99: effects on male fertility and neurobehavior in rat offspring." Environ Health Perspect **113**(2): 149-54.

La, A. G. M. J., R. C. Hale, et al. (2006). "Detailed polybrominated diphenyl ether (PBDE) congener composition of the widely used penta-, octa-, and deca-PBDE technical flame-retardant mixtures." Environ Sci Technol **40**(20): 6247-54.

Lee, J. E., W. Choi, et al. (2003). "DFT Calculation on the Thermodynamic Properties of Polychlorinated Dibenzo-p-dioxins: Intramolecular Cl-Cl Repulsion Effects and Their Thermochemical Implications." Journal of Physical Chemistry A **107**(15): 2693-2699.

Lema, S. C., I. R. Schultz, et al. (2007). "Neural defects and cardiac arrhythmia in fish larvae following embryonic exposure to 2,2',4,4'-tetrabromodiphenyl ether (PBDE 47)." Aquat Toxicol **82**(4): 296-307.

Li, X.-W., E. Shibata, et al. (2003). "Theoretical Calculation of Thermodynamic Properties of Polybrominated Dibenzo-p-dioxins." Journal of Chemical and Engineering Data **48**(3): 727-735.

Madia, F., G. Giordano, et al. (2004). "Differential in vitro neurotoxicity of the flame retardant PBDE-99 and of the PCB Aroclor 1254 in human astrocytoma cells." Toxicol Lett **154**(1-2): 11-21.

Meerts, I. A., R. J. Letcher, et al. (2001). "In vitro estrogenicity of polybrominated diphenyl ethers, hydroxylated PDBEs, and polybrominated bisphenol A compounds." Environ Health Perspect **109**(4): 399-407.

Muirhead, E. K., A. D. Skillman, et al. (2006). "Oral exposure of PBDE-47 in fish: toxicokinetics and reproductive effects in Japanese Medaka (Oryzias latipes) and fathead minnows (Pimephales promelas)." Environ Sci Technol **40**(2): 523-8.

Niu, J., Z. Shen, et al. (2006). "Quantitative structure-property relationships on photodegradation of polybrominated diphenyl ethers." Chemosphere **64**(4): 658-665.

Palm, A., I. T. Cousins, et al. (2002). "Assessing the environmental fate of chemicals of emerging concern: a case study of the polybrominated diphenyl ethers." Environmental Pollution (Oxford, United Kingdom) **117**(2): 195-213.

Pedley, J. B., R. D. Naylor, et al. (1986). Thermochemical Data of Organic Compounds. 2nd Ed. New York, Chapman and Hall.

Peterman, P. H., C. E. Orazio, et al. (2003). "Sunlight photolysis of 39 mono-hepta PBDE congeners in lipid." Organohalogen Compounds **63**: 357-360.

Pfeifer, F., H. G. Truper, et al. (1993). "Degradation of diphenylether by Pseudomonas cepacia Et4: enzymatic release of phenol from 2,3-dihydroxydiphenylether." Arch Microbiol **159**(4): 323-9.

Rahman, F., K. H. Langford, et al. (2001). "Polybrominated diphenyl ether (PBDE) flame retardants." Science of the Total Environment **275**(1-3): 1-17.

Rayne, S. and M. G. Ikonomou (2003). "Predicting gas chromatographic retention times for the 209 polybrominated diphenyl ether congeners." J Chromatogr A **1016**(2): 235-48.

Rayne, S., M. G. Ikonomou, et al. (2003). "Anaerobic microbial and photochemical degradation of 4,4'-dibromodiphenyl ether." Water Res **37**(3): 551-60.

Robinson, P. J. and K. A. Holbrook (1972). Unimolecular Reactions.

Safe, S. (1990). "Polychlorinated biphenyls (PCBs), dibenzo-p-dioxins (PCDDs), dibenzofurans (PCDFs), and related compounds: environmental and mechanistic considerations which support the development of toxic equivalency factors (TEFs)." Critical Reviews in Toxicology **21**(1): 51-88.

Sanchez-Prado, L., M. Lores, et al. (2006). "Natural sunlight and sun simulator photolysis studies of tetra- to hexa-brominated diphenyl ethers in water using solid-phase microextraction." J Chromatogr A **1124**(1-2): 157-66.

Scherer, M. M., B. A. Balko, et al. (1998). "Correlation Analysis of Rate Constants for Dechlorination by Zero-Valent Iron." Environmental Science and Technology **32**(19): 3026-3033.

Schmidt, S., R. M. Wittich, et al. (1992). "Biodegradation of diphenyl ether and its monohalogenated derivatives by Sphingomonas sp. strain SS3." Appl Environ Microbiol **58**(9): 2744-50.

Soderstrom, G., U. Sellstrom, et al. (2004). "Photolytic debromination of decabromodiphenyl ether (BDE 209)." Environ Sci Technol **38**(1): 127-32.

Strandberg, B., N. G. Dodder, et al. (2001). "Concentrations and Spatial Variations of Polybrominated Diphenyl Ethers and Other Organohalogen Compounds in Great Lakes Air." Environmental Science and Technology **35**(6): 1078-1083.

van Bavel, B., M. Dam, et al. (2001). "Levels of polybrominated diphenyl ethers in marine mammals." Organohalogen Compounds **52**(Dioxin 2001): 99-103.

Viberg, H., A. Fredriksson, et al. (2003). "Neonatal exposure to polybrominated diphenyl ether (PBDE 153) disrupts spontaneous behaviour, impairs learning and memory,

and decreases hippocampal cholinergic receptors in adult mice." Toxicol Appl Pharmacol **192**(2): 95-106.

Wang, Y., A. Li, et al. (2006). "Development of quantitative structure gas chromatographic relative retention time models on seven stationary phases for 209 polybrominated diphenyl ether congeners." Journal of Chromatography, A **1103**(2): 314-328.

Wania, F., Y. D. Lei, et al. (2002). "Estimating octanol-air partition coefficients of nonpolar semivolatile organic compounds from gas chromatographic retention times." Analytical Chemistry **74**(14): 3476-3483.

Watanabe, I. and S. Sakai (2003). "Environmental release and behavior of brominated flame retardants." Environ Int **29**(6): 665-82.

Wong, A., Y. D. Lei, et al. (2001). "Vapor Pressures of the Polybrominated Diphenyl Ethers." Journal of Chemical and Engineering Data **46**(2): 239-242.

Zeng, X., P. K. Freeman, et al. (2005). "Theoretical Calculation of Thermodynamic Properties of Polybrominated Diphenyl Ethers." Journal of Chemical and Engineering Data **50**(5): 1548-1556.

Zhou, T., D. G. Ross, et al. (2001). "Effects of short-term in vivo exposure to polybrominated diphenyl ethers on thyroid hormones and hepatic enzyme activities in weanling rats." Toxicol Sci **61**(1): 76-82.

Zhou, T., M. M. Taylor, et al. (2002). "Developmental exposure to brominated diphenyl ethers results in thyroid hormone disruption." Toxicol Sci **66**(1): 105-16.

Zhou, Z. and R. G. Parr (1990). "Activation hardness: new index for describing the orientation of electrophilic aromatic substitution." Journal of the American Chemical Society **112**(15): 5720-4.

Zhu, L. and J. W. Bozzelli (2003). "Thermochemical Properties, DfH Deg(298.15 K), S Deg(298.15 K), and Cp Deg(T), of 1,4-Dioxin, 2,3-Benzodioxin, Furan, 2,3-Benzofuran, and Twelve Monochloro and Dichloro Dibenzo-p-dioxins and Dibenzofurans." Journal of Physical and Chemical Reference Data **32**(4): 1713-1735.

APPENDIX A. Nomenclature and structures of 209 PBDE congeners

PBDE Number	structure	PBDE Number	structure	PBDE Number	structure	PBDE Number	structure
BDE1	2-mono	BDE54	2,2',6,6'-tetra	BDE107	2,3,3',4,5'-penta	BDE160	2,3,3',4,5,6-hexa
BDE2	3-mono	BDE55	2,3,3',4-tetra	BDE108	2,3,3',4,6-penta	BDE161	2,3,3',4,5',6-hexa
BDE3	4-mono	BDE56	2,3,3',4'-tetra	BDE109	2,3,3',4',5-penta	BDE162	2,3,3',4',5,5'-hexa
BDE4	2,2'-di	BDE57	2,3,3',5-tetra	BDE110	2,3,3',4',6-penta	BDE163	2,3,3',4',5,6-hexa
BDE5	2,3-di	BDE58	2,3,3',5'-tetra	BDE111	2,3,3',5,5'-penta	BDE164	2,3,3',4',5',6-hexa
BDE6	2,3'-di	BDE59	2,3,3',6-tetra	BDE112	2,3,3',5,6-penta	BDE165	2,3,3',5,5',6-hexa
BDE7	2,4-di	BDE60	2,3,4,4'-tetra	BDE113	2,3,3',5',6-penta	BDE166	2,3,4,4',5,6-hexa
BDE8	2,4'-di	BDE61	2,3,4,5-tetra	BDE114	2,3,4,4',5-penta	BDE167	2,3',4,4',5,5'-hexa
BDE9	2,5-di	BDE62	2,3,4,6-tetra	BDE115	2,3,4,4',6-penta	BDE168	2,3',4,4',5',6-hexa
BDE10	2,6-di	BDE63	2,3,4',5-tetra	BDE116	2,3,4,5,6-penta	BDE169	3,3',4,4',5,5'-hexa
BDE11	3,3'-di	BDE64	2,3,4',6-tetra	BDE117	2,3,4',5,6-penta	BDE170	2,2',3,3',4,4',5-hepta
BDE12	3,4-di	BDE65	2,3,5,6-tetra	BDE118	2,3',4,4',5-penta	BDE171	2,2',3,3',4,4',6-hepta
BDE13	3,4'-di	BDE66	2,3',4,4'-tetra	BDE119	2,3',4,4',6-penta	BDE172	2,2',3,3',4,5,5'-hepta
BDE14	3,5-di	BDE67	2,3',4,5-tetra	BDE120	2,3',4,5,5'-penta	BDE173	2,2',3,3',4,5,6-hepta
BDE15	4,4'-di	BDE68	2,3',4,5'-tetra	BDE121	2,3',4,5',6-penta	BDE174	2,2',3,3',4,5,6'-hepta
BDE16	2,2',3-tri	BDE69	2,3',4,6-tetra	BDE122	2,3,3',4',5'-penta	BDE175	2,2',3,3',4,5',6-hepta
BDE17	2,2',4-tri	BDE70	2,3',4',5-tetra	BDE123	2,3',4,4',5'-penta	BDE176	2,2',3,3',4,6,6'-hepta
BDE18	2,2',5-tri	BDE71	2,3',4',6-tetra	BDE124	2,3',4',5,5'-penta	BDE177	2,2',3,3',4,5',6'-hepta
BDE19	2,2',6-tri	BDE72	2,3',5,5'-tetra	BDE125	2,3',4',5',6-penta	BDE178	2,2',3,3',5,5',6-hepta
BDE20	2,3,3'-tri	BDE73	2,3',5',6-tetra	BDE126	3,3',4,4',5-penta	BDE179	2,2',3,3',5,6,6'-hepta
BDE21	2,3,4-tri	BDE74	2,4,4',5-tetra	BDE127	3,3',4,5,5'-penta	BDE180	2,2',3,4,4',5,5'-hepta
BDE22	2,3,4'-tri	BDE75	2,4,4',6-tetra	BDE128	2,2',3,3',4,4'-hexa	BDE181	2,2',3,4,4',5,6-hepta
BDE23	2,3,5-tri	BDE76	2,3',4',5'-tetra	BDE129	2,2',3,3',4,5-hexa	BDE182	2,2',3,4,4',5,6'-hepta
BDE24	2,3,6-tri	BDE77	3,3',4,4'-tetra	BDE130	2,2',3,3',4,5'-hexa	BDE183	2,2',3,4,4',5',6-hepta
BDE25	2,3',4-tri	BDE78	3,3',4,5-tetra	BDE131	2,2',3,3',4,6-hexa	BDE184	2,2',3,4,4',6,6'-hepta
BDE26	2,3',5-tri	BDE79	3,3',4,5'-tetra	BDE132	2,2',3,3',4,6'-hexa	BDE185	2,2',3,4,5,5',6-hepta
BDE27	2,3',6-tri	BDE80	3,3',5,5'-tetra	BDE133	2,2',3,3',5,5'-hexa	BDE186	2,2',3,4,5,6,6'-hepta
BDE28	2,4,4'-tri	BDE81	3,4,4',5-tetra	BDE134	2,2',3,3',5,6-hexa	BDE187	2,2',3,4',5,5',6-hepta
BDE29	2,4,5-tri	BDE82	2,2',3,3',4-penta	BDE135	2,2',3,3',5,6'-hexa	BDE188	2,2',3,4',5,6,6'-hepta
BDE30	2,4,6-tri	BDE83	2,2',3,3',5-penta	BDE136	2,2',3,3',6,6'-hexa	BDE189	2,3,3',4,4',5,5'-hepta
BDE31	2,4',5-tri	BDE84	2,2',3,3',6-penta	BDE137	2,2',3,4,4',5-hexa	BDE190	2,3,3',4,4',5,6-hepta
BDE32	2,4',6-tri	BDE85	2,2',3,4,4'-penta	BDE138	2,2',3,4,4',5'-hexa	BDE191	2,3,3',4,4',5',6-hepta
BDE33	2,3',4'-tri	BDE86	2,2',3,4,5-penta	BDE139	2,2',3,4,4',6-hexa	BDE192	2,3,3',4,5,5',6-hepta
BDE34	2,3',5'-tri	BDE87	2,2',3,4,5'-penta	BDE140	2,2',3,4,4',6'-hexa	BDE193	2,3,3',4',5,5',6-hepta
BDE35	3,3',4-tri	BDE88	2,2',3,4,6-penta	BDE141	2,2',3,4,5,5'-hexa	BDE194	2,2',3,3',4,4',5,5'-octa
BDE36	3,3',5-tri	BDE89	2,2',3,4,6'-penta	BDE142	2,2',3,4,5,6-hexa	BDE195	2,2',3,3',4,4',5,6-octa
BDE37	3,4,4'-tri	BDE90	2,2',3,4',5-penta	BDE143	2,2',3,4,5,6'-hexa	BDE196	2,2',3,3',4,4',5,6'-octa
BDE38	3,4,5-tri	BDE91	2,2',3,4',6-penta	BDE144	2,2',3,4,5',6-hexa	BDE197	2,2',3,3',4,4',6,6'-octa
BDE39	3,4',5-tri	BDE92	2,2',3,5,5'-penta	BDE145	2,2',3,4,6,6'-hexa	BDE198	2,2',3,3',4,5,5',6-octa
BDE40	2,2',3,3'-tetra	BDE93	2,2',3,5,6-penta	BDE146	2,2',3,4',5,5'-hexa	BDE199	2,2',3,3',4,5,5',6'-octa
BDE41	2,2',3,4-tetra	BDE94	2,2',3,5,6'-penta	BDE147	2,2',3,4',5,6-hexa	BDE200	2,2',3,3',4,5,6,6'-octa
BDE42	2,2',3,4'-tetra	BDE95	2,2',3,5',6-penta	BDE148	2,2',3,4',5,6'-hexa	BDE201	2,2',3,3',4,5',6,6'-octa
BDE43	2,2',3,5-tetra	BDE96	2,2',3,6,6'-penta	BDE149	2,2',3,4',5',6-hexa	BDE202	2,2',3,3',5,5',6,6'-octa
BDE44	2,2',3,5'-tetra	BDE97	2,2',3,4',5'-penta	BDE150	2,2',3,4',6,6'-hexa	BDE203	2,2',3,4,4',5,5',6-octa
BDE45	2,2',3,6-tetra	BDE98	2,2',3,4',6'-penta	BDE151	2,2',3,5,5',6-hexa	BDE204	2,2',3,4,4',5,6,6'-octa
BDE46	2,2',3,6'-tetra	BDE99	2,2',4,4',5-penta	BDE152	2,2',3,5,6,6'-hexa	BDE205	2,3,3',4,4',5,5',6-octa
BDE47	2,2',4,4'-tetra	BDE100	2,2',4,4',6-penta	BDE153	2,2',4,4',5,5'-hexa	BDE206	2,2',3,3',4,4',5,5',6-nona
BDE48	2,2',4,5-tetra	BDE101	2,2',4,5,5'-penta	BDE154	2,2',4,4',5,6'-hexa	BDE207	2,2',3,3',4,4',5,6,6'-nona
BDE49	2,2',4,5'-tetra	BDE102	2,2',4,5,6'-penta	BDE155	2,2',4,4',6,6'-hexa	BDE208	2,2',3,3',4,5,5',6,6'-nona
BDE50	2,2',4,6-tetra	BDE103	2,2',4,5',6-penta	BDE156	2,3,3',4,4',5-hexa	BDE209	2,2',3,3',4,4',5,5',6,6'-deca
BDE51	2,2',4,6'-tetra	BDE104	2,2',4,6,6'-penta	BDE157	2,3,3',4,4',5'-hexa		
BDE52	2,2',5,5'-tetra	BDE105	2,3,3',4,4'-penta	BDE158	2,3,3',4,4',6-hexa		
BDE53	2,2',5,6'-tetra	BDE106	2,3,3',4,5-penta	BDE159	2,3,3',4,5,5'-hexa		

Appendix B. Visual BSAIC source code of the photodegradation model

```
Private Sub btn_Exit_Click()
   End
End Sub

Private Sub btnExcelFile_Click()
   CDlogout.FileName = ""
   CDlogout.InitDir = Path
   CDlogout.Filter = "Excel files (*.xls)|*.XLS|All files (*.*)|*.*"
   CDlogout.FilterIndex = 1
   CDlogout.Flags = cdlOFNFileMustExist Or cdlOFNPathMustExist
   CDlogout.Action = 2
   If CDlogout.FileName = "" Then
      MsgBox "NO File selected"
      Exit Sub
   End If
   lblOutputFile.Caption = CDlogout.FileName
End Sub


Private Sub btnInputFile_Click()
   CDLogin.InitDir = Path
   CDLogin.Filter = "TXT files (*.TXT)|*.TXT|All files (*.*)|*.*"
   CDLogin.FilterIndex = 1
   CDLogin.Flags = cdlOFNFileMustExist Or cdlOFNPathMustExist
   CDLogin.Action = 1
   If CDLogin.FileName = "" Then
      MsgBox "NO File selected"
      Exit Sub
   End If
   lblInputFile.Caption = CDLogin.FileName

End Sub

Private Sub btnListName_Click()
   Dim b, i, j, k, l, m, x, y, z, BrNum(300) As Integer
   Dim str, linehead, testchar, BDEName(209) As String
   Dim NumDH2(6) As Integer
   Dim Xrray(5), Yrray(5), var As Integer
   Dim DH1(5), SumH1(300), DH2(6), SumH2(300), DH3(6), SumH3(300), DHF(300),
         TotalKK(209), CreatK(300, 10) As Double
```

```
Const FactorofK As Double = 2.13315E+49

Dim Xring(209, 5), Yring(209, 5) As Integer
Dim Xforward, Xbackward, Yforward, Ybackward As Integer
Dim Sublist, a, Subnum(209), h, StartinExcel(209) As Integer
Dim XringSub(209, 10, 5), YringSub(209, 10, 5) As Integer
Dim Product(209, 10) As Integer
Dim Reactnum(300), Reactant(300, 10) As Integer

Dim TotalTime, DispTimeInt, CalcTimeInt, InitialConc, Conc(300), KxConc(300) As
      Double
Dim InterV, StartBDE, LowerBDE As Long

Dim xlApp As excel.Application      'initiate excel file. Need add excel library as
      reference
Dim wb As excel.Workbook
Dim ws As excel.Worksheet
Set xlApp = New excel.Application
Set wb = xlApp.Workbooks.Add
wb.SaveAs lblOutputFile.Caption
Set ws = wb.Worksheets("Sheet1") 'Specify your worksheet name
str = ""
k = 1
DH1(1) = 0.002614 * 627.5 * 4.184   'DH1 ortho position
DH1(2) = 0                          'DH1 meta position
DH1(3) = 0.000301 * 627.5 * 4.184   'DH1 para position
DH1(4) = 0                          'DH1 meta position
DH1(5) = 0.002614 * 627.5 * 4.184   'DH1 ortho position

DH2(1) = 9.6354382                 'DH2(2,3)
DH2(2) = 3.063911821               'DH2(2,4)
DH2(3) = 2.66746736                'DH2(2,5)
DH2(4) = 1.47288306                'DH2(2,6)
DH2(5) = 9.19698638                'DH2(3,4)
DH2(6) = 3.415723461               'DH2(3,5)

DH3(1) = 1.22608982                'DH3(2,2')
DH3(2) = 1.005551181               'DH3(2,3')
DH3(3) = 0.21791318                'DH3(2,4')
DH3(4) = 1.562148701               'DH3(3,3')
DH3(5) = 1.063311302               'DH3(3,4')
DH3(6) = 0.876903641               'DH3(4,4')
```

```
Open lblInputFile.Caption For Input As #1
Do While Not EOF(1)                         ' Loop until end of file.
   Line Input #1, str
   If str =
      "============================================================
      ======================" Then
      Line Input #1, str                    ' Find the IUPAC name
      If Right(str, 5) <> "IUPAC" Then
         Do Until Right(str, 5) = "IUPAC"
            Line Input #1, str
         Loop
      End If

      linehead = Left(str, 41)              ' Get characters before pattern
      BDEName(k) = Mid(linehead, 8, 32)     ' get PBDE name of sub pattern
      b = 32
      testchar = Mid(BDEName(k), b, 1)
      Do While testchar <> "C"
         b = b - 1
         testchar = Mid(BDEName(k), b, 1)
      Loop
      BDEName(k) = Mid(BDEName(k), 1, b - 1) + "BDE"
      For i = 1 To 5
         Xrray(i) = Val(Mid(str, 42 + (i - 1) * 2, 1))
         Xring(k, i) = Xrray(i)
         If Xrray(i) = 1 Then
            SumH1(k) = SumH1(k) + DH1(i)        'DH1 for ring 1
            BrNum(k) = BrNum(k) + 1
         End If
      Next
      For j = 1 To 5
         Yrray(j) = Val(Mid(str, 60 - (j - 1) * 2, 1))
         Yring(k, j) = Yrray(j)
         If Yrray(j) = 1 Then
            SumH1(k) = SumH1(k) + DH1(j)        'DH1 for ring 2
            BrNum(k) = BrNum(k) + 1
         End If
      Next

      For x = 1 To 5                        'DH2 for ring 1
         If Xrray(x) = 1 Then
            For y = x + 1 To 5
               If Xrray(y) = 1 Then
                  i = x + 1
```

```
            j = y + 1
            If i + j > 8 Then              'change i,j value to 1 to 5
               j = 8 - j
               i = 8 - i
               l = j
               j = i
               i = l
            End If
            SumH2(k) = SumH2(k) + DH2((j - i) + 4 * (i - 2))
            NumDH2((j - i) + 4 * (i - 2)) = NumDH2((j - i) + 4 * (i - 2)) + 1
         End If
      Next
   End If
Next


For x = 1 To 5                         'DH2 for ring 2
   If Yrray(x) = 1 Then
      For y = x + 1 To 5
         If Yrray(y) = 1 Then
            i = x + 1
            j = y + 1
            If i + j > 8 Then          'change i,j value to 1 to 5
               j = 8 - j
               i = 8 - i
               l = j
               j = i
               i = l
            End If
            SumH2(k) = SumH2(k) + DH2((j - i) + 4 * (i - 2))
            NumDH2((j - i) + 4 * (i - 2)) = NumDH2((j - i) + 4 * (i - 2)) + 1
         End If
      Next
   End If
Next

For x = 1 To 5                         'DH3
   If Xrray(x) = 1 Then
      For y = 1 To 5
         If Yrray(y) = 1 Then
            i = x + 1
            j = y + 1
            If i > 4 Then
               i = 8 - i
```

```
            End If
            If j > 4 Then
               j = 8 - j
            End If
            If i > j Then
               l = j
               j = i
               i = l
            End If
            m = i + j - 3
            If i > 2 Then
               m = m + 1
            End If
            SumH3(k) = SumH3(k) + DH3(m)
         End If
      Next
   End If
Next

Sublist = 0
For i = 1 To 5                          ' Try each positions with Br in Xring
   If Xring(k, i) = 1 Then
      Sublist = Sublist + 1
      For a = 1 To 5
         XringSub(k, Sublist, a) = Xring(k, a)
         YringSub(k, Sublist, a) = Yring(k, a)
      Next a
      XringSub(k, Sublist, i) = 0
      Xforward = 0
      Xbackward = 0
      Yforward = 0
      Ybackward = 0
      For j = 1 To 5
         x = 1
         For m = 1 To 5 - j
            x = x * 2
         Next
         Xforward = XringSub(k, Sublist, j) * x + Xforward
         Yforward = YringSub(k, Sublist, j) * x + Yforward
         Xbackward = XringSub(k, Sublist, 6 - j) * x + Xbackward
      Next
      If Xbackward > Xforward Then
         x = Xforward                   ' Swap Xforward and Xbackward
         Xforward = Xbackward
```

```
            Xbackward = x
            x = XringSub(k, Sublist, 1)            ' Swap the array of Xringsub
backwards
            XringSub(k, Sublist, 1) = XringSub(k, Sublist, 5)
            XringSub(k, Sublist, 5) = x
            x = XringSub(k, Sublist, 2)
            XringSub(k, Sublist, 2) = XringSub(k, Sublist, 4)
            XringSub(k, Sublist, 4) = x
        End If
        If Yforward > Xforward Then                ' Swap the array of Xringsub and
YringSub
            For a = 1 To 5
               x = XringSub(k, Sublist, a)
               XringSub(k, Sublist, a) = YringSub(k, Sublist, a)
               YringSub(k, Sublist, a) = x
            Next a
        End If
    End If
Next i

For i = 1 To 5                                 ' Try each positions with Br in Yring
    If Yring(k, i) = 1 Then
        Sublist = Sublist + 1
        For a = 1 To 5
            XringSub(k, Sublist, a) = Xring(k, a)
            YringSub(k, Sublist, a) = Yring(k, a)
        Next a
        YringSub(k, Sublist, i) = 0
        Xforward = 0
        Xbackward = 0
        Yforward = 0
        Ybackward = 0
        For j = 1 To 5
            x = 1
            For m = 1 To 5 - j
               x = x * 2
            Next
            Xforward = XringSub(k, Sublist, j) * x + Xforward
            Yforward = YringSub(k, Sublist, j) * x + Yforward
            Ybackward = YringSub(k, Sublist, 6 - j) * x + Ybackward
        Next
        If Ybackward > Yforward Then
            x = Yforward                           ' Swap Xforward and Xbackward
            Yforward = Ybackward
```

```
            Ybackward = x
            x = YringSub(k, Sublist, 1)          ' Swap the array of Xringsub
      backwards
            YringSub(k, Sublist, 1) = YringSub(k, Sublist, 5)
            YringSub(k, Sublist, 5) = x
            x = YringSub(k, Sublist, 2)
            YringSub(k, Sublist, 2) = YringSub(k, Sublist, 4)
            YringSub(k, Sublist, 4) = x
          End If
          If Yforward > Xforward Then              ' Swap the array of Xringsub and
      YringSub
            For a = 1 To 5
              x = XringSub(k, Sublist, a)
              XringSub(k, Sublist, a) = YringSub(k, Sublist, a)
              YringSub(k, Sublist, a) = x
            Next a
          End If
        End If
      Next i
      Subnum(k) = Sublist

      k = k + 1
      For z = 1 To 6
        NumDH2(z) = 0
      Next
    End If
Loop
Close #1

StartinExcel(1) = 1                                'calculate where they start in excel
For h = 2 To 209
  'StartinExcel(h) = StartinExcel(h - 1) + Subnum(h - 1) + 1
  StartinExcel(h) = StartinExcel(h - 1) + 10
Next h

For h = 1 To 300                                   ' have to consider DE which is 0
  DHF(h) = 21.979 * BrNum(h - 1) + 56.569 + SumH1(h - 1) + SumH2(h - 1) +
    SumH3(h - 1) 'calc DHF of each congener
Next h

For k = 1 To 209
  ws.Cells(StartinExcel(k) + 1, 10).Value = Subnum(k)          ' list how many
    products
  For m = 1 To Subnum(k)
```

```
i = 1                                          ' find the congener which fits the pattern
of product
x = 0
Do While x = 0 And i <= 209
   If Xring(i, 1) = XringSub(k, m, 1) And Xring(i, 2) = XringSub(k, m, 2) And
Xring(i, 3) = XringSub(k, m, 3) And Xring(i, 4) = XringSub(k, m, 4) And Xring(i,
5) = XringSub(k, m, 5) And Yring(i, 1) = YringSub(k, m, 1) And Yring(i, 2) =
YringSub(k, m, 2) And Yring(i, 3) = YringSub(k, m, 3) And Yring(i, 4) =
YringSub(k, m, 4) And Yring(i, 5) = YringSub(k, m, 5) Then
      x = i
   End If
   i = i + 1
Loop
ws.Cells(StartinExcel(k) + m + 1, 10).Value = x                    ' List the names of
products
ws.Cells(StartinExcel(k) + m + 1, 11).Value = DHF(x + 1)           ' have to
consider DE which is 0
ws.Cells(StartinExcel(k) + m + 1, 12).Value = DHF(k + 1) - DHF(x + 1) '
calculate Delta(DHf)
ws.Cells(StartinExcel(k) + m + 1, 13).Value = 353.9489 - (DHF(k + 1) - DHF(x +
1) - 21.979)    ' Activation Energy Ea 353.9489 kJ/mol is the C-Br bond energy
ws.Cells(StartinExcel(k) + m + 1, 14).Value = Exp((DHF(k + 1) - DHF(x + 1) -
21.979 - 353.9489) * 1000 / 8.3145 / 298.15) ' exp(-Ea/RT)
TotalKK(k) = TotalKK(k) + Exp((DHF(k + 1) - DHF(x + 1) - 21.979 - 353.9489)
* 1000 / 8.3145 / 298.15) ' total k/A for all the 209 congeners
Product(k, m) = x

'***************  Below for reactant *************
If x > 0 Then                                  'avoid displaying DiphenylEther which has
x=0
   Reactnum(x) = Reactnum(x) + 1
   Reactant(x, Reactnum(x)) = k
   CreatK(x, Reactnum(x)) = Exp((DHF(k + 1) - DHF(x + 1) - 21.979 - 353.9489)
* 1000 / 8.3145 / 298.15)
   ws.Cells(StartinExcel(x) + 1, 17).Value = Reactnum(x)
   ws.Cells(StartinExcel(x) + Reactnum(x) + 1, 17).Value = k
   ws.Cells(StartinExcel(x) + Reactnum(x) + 1, 18).Value = DHF(k + 1)
   ws.Cells(StartinExcel(x) + Reactnum(x) + 1, 19).Value = DHF(k + 1) - DHF(x
+ 1)
   ws.Cells(StartinExcel(x) + Reactnum(x) + 1, 20).Value = 353.9489 - (DHF(k +
1) - DHF(x + 1) - 21.979)
   ws.Cells(StartinExcel(x) + Reactnum(x) + 1, 21).Value = Exp((DHF(k + 1) -
DHF(x + 1) - 21.979 - 353.9489) * 1000 / 8.3145 / 298.15)
```

```
            ws.Cells(StartinExcel(x) + Reactnum(x) + 1, 22).Value = FactorofK *
        Exp((DHF(k + 1) - DHF(x + 1) - 21.979 - 353.9489) * 1000 / 8.3145 / 298.15)
        End If
    Next m
    ws.Cells(StartinExcel(k) + 1, 15).Value = TotalKK(k)
    ws.Cells(StartinExcel(k) + 1, 16).Value = TotalKK(k) * FactorofK
Next k

'********************** start output excel file
        ***************************
ws.Cells(1, 1).Value = "PBDE Name"
ws.Cells(1, 2).Value = "PBDE name"
ws.Cells(1, 3).Value = "Br Number"
ws.Cells(1, 4).Value = "DH1"
ws.Cells(1, 5).Value = "DH2"
ws.Cells(1, 6).Value = "DH3"
ws.Cells(1, 7).Value = "Sum of DH"
ws.Cells(1, 8).Value = "Linear Eq"
ws.Cells(1, 9).Value = "DHf"
ws.Cells(1, 10).Value = "Number of products"
ws.Cells(1, 11).Value = "DHf of each product"
ws.Cells(1, 12).Value = "Difference of DHf"
ws.Cells(1, 13).Value = "Activation Energy"
ws.Cells(1, 14).Value = "individual k/A"
ws.Cells(1, 15).Value = "Total k/A"
ws.Cells(1, 16).Value = "Modified Total k as reactant"
ws.Cells(1, 17).Value = "Number of reactant"
ws.Cells(1, 18).Value = "DHf of each reactant"
ws.Cells(1, 19).Value = "Difference of DHf"
ws.Cells(1, 20).Value = "Activation Energy"
ws.Cells(1, 21).Value = "individual k/A"
ws.Cells(1, 22).Value = "Modified k as product"

Range(Cells(1, 1), Cells(1, 25)).Interior.Color = RGB(256, 256, 200)
For k = 1 To 209
    Range(Cells(StartinExcel(k) + 1, 1), Cells(StartinExcel(k) + 1, 9)).Interior.Color =
        RGB(200, 200, 256)
    Range(Cells(StartinExcel(k) + 1, 10), Cells(StartinExcel(k) + 1, 16)).Interior.Color
        = RGB(200, 256, 200)
    Range(Cells(StartinExcel(k) + 1, 17), Cells(StartinExcel(k) + 1, 25)).Interior.Color
        = RGB(256, 200, 200)
    ws.Cells(StartinExcel(k) + 1, 1).Value = "PBDE" & k
    ws.Cells(StartinExcel(k) + 1, 2).Value = BDEName(k)
    ws.Cells(StartinExcel(k) + 1, 3).Value = BrNum(k)
```

```
    ws.Cells(StartinExcel(k) + 1, 4).Value = SumH1(k)
    ws.Cells(StartinExcel(k) + 1, 5).Value = SumH2(k)
    ws.Cells(StartinExcel(k) + 1, 6).Value = SumH3(k)
    ws.Cells(StartinExcel(k) + 1, 7).Value = SumH1(k) + SumH2(k) + SumH3(k)
    ws.Cells(StartinExcel(k) + 1, 8).Value = 21.979 * BrNum(k) + 56.569
    ws.Cells(StartinExcel(k) + 1, 9).Value = 21.979 * BrNum(k) + 56.569 + SumH1(k)
       + SumH2(k) + SumH3(k)

Next

'********************************** Sheet 2 for displaying the real time
       concentrations ***************
TotalTime = txtTotalTime.Text
CalcTimeInt = txtCalcTimeInterv.Text
DispTimeInt = txtDispTimeInterv.Text
InitialConc = txtInitConc.Text
StartBDE = txtStartBDE.Text
Set ws2 = wb.Worksheets("Sheet2") 'Specify your worksheet name
ws2.Cells(1, 1).Value = "BDE Number"
ws2.Cells(1, 2).Value = "Br Number"
ws2.Cells(1, 3).Value = "DHf"
For k = 1 To 209
    ws2.Cells(k + 1, 1).Value = k
    ws2.Cells(k + 1, 2).Value = BrNum(k)
    ws2.Cells(k + 1, 3).Value = DHF(k + 1)
Next k

Conc(StartBDE) = InitialConc
InterV = DispTimeInt / CalcTimeInt

LowerBDE = StartBDE - 1
Do While LowerBDE >= 1 And BrNum(LowerBDE) = BrNum(StartBDE)
       ' Find the BDEs one less Br than StartBDE
    LowerBDE = LowerBDE - 1
Loop

For m = 1 To TotalTime / CalcTimeInt
    If m Mod InterV = 0 Then
       ws2.Cells(1, m / InterV + 3).Value = CalcTimeInt * m
    End If
    For n = StartBDE To 1 Step -1
       For o = 1 To Reactnum(n)
          KxConc(n) = KxConc(n) + FactorofK * CreatK(n, o) * Conc(Reactant(n, o))
       'calc the creating rate from up PBDEs
```

```
            Next o
            Conc(n) = Conc(n) - (Conc(n) * FactorofK * TotalKK(n) - KxConc(n)) *
            CalcTimeInt
            If m Mod InterV = 0 And Conc(n) <> 0 Then
               ws2.Cells(n + 1, m / InterV + 3).Value = Conc(n)
            End If
            KxConc(n) = 0
         Next n
      Next m

      wb.Save
      wb.Close
      xlApp.Quit
      Set ws = Nothing
      Set ws2 = Nothing
      Set wb = Nothing
      Set xlApp = Nothing

End Sub
```